TUM

Crosstalk communication between skeletal muscle and intermuscular adipose tissue (IMAT) in progressive insulin resistance.

Amare Desalegn Wolide

Acknowledgement

I want to express my heartfelt gratitude to Dr Dominik Lutter for offering me the opportunity to pursue my PhD in his lab and serving as my direct supervisor throughout the journey. I am genuinely grateful for his exceptional guidance, unwavering support, and thought-provoking discussions during the project. His continuous challenges, both personally and professionally, have played a crucial role in shaping me into a better researcher.

I sincerely thank Prof. Dr Paul.T. Pflueger and Prof. Dr Henriette Uhlenhaut for their willingness to act as my university advisers and for our fruitful discussions regarding my PhD project during the thesis annual committee (TAC) meetings. I am grateful for their valuable insights and agreeing to examine this thesis. Additionally, I would like to express my deep appreciation to Prof. Dr Med. Susanna Hofmann for her insightful ideas and discussions during the TAC meetings and symposium, which have contributed significantly to the development of my research.

Special gratitude goes to Dr Manuel Monroy Kuhn, who has always been there for me, supporting me through both good and bad times. His patience, encouragement, and extensive knowledge of computational algorithms and tools have been instrumental in my growth as a researcher.

I would also like to thank Dr Victorian Miok, Dr Ekta Pathak, Dr Konstantinos Makris, and Dr Mariana Ponce for their valuable discussions, collaborations, and the enjoyable moments we shared in the lab. Their contributions have fostered a productive working environment and made our coffee breaks and lunchtime delightful.

A heartfelt thank you goes to Philipp Melander and Marion Konheiser for warmly welcoming me and providing invaluable support during my time at the IDO. Their assistance handling my contracts and visa matters every year and season is deeply appreciated.

Above all, I am profoundly grateful to my family, especially my parents, for their unwavering love and kindness throughout this journey. Their support has been a constant source of strength and motivation for me.

Lastly, I attribute all the glory to the almighty God for all the blessing I received and for helping me overcome challenges and succeed.

Index of Contents

Index of Figures

Index of Tables

1. Summary

Skeletal muscle plays a critical role in regulating glucose metabolism, and factors like environmental influences or genetic predispositions can lead to excess fat accumulation within the muscle, resulting in insulin resistance and diabetes. Intermuscular Adipose Tissue (IMAT), a type of fat found within muscle, has been linked to the regulation of insulin sensitivity in obese individuals. However, the factors secreted by IMAT that influence insulin resistance in skeletal muscle are not well understood. It is possible that due to their physical proximity, IMAT and skeletal muscle may have a direct impact on the development of metabolic diseases. In this study, we used transcriptomics data to explore the communication between IMAT and skeletal muscle in the context of progressive insulin resistance. Our study included 54 participants from different groups: 19 individuals with obesity (OB), eight patients with type 2 diabetes (T2D), 14 endurance athletes (ATH), and 13 lean controls (LC). To conduct the RNAseq experiment, we obtained skeletal muscle biopsies from the *vastus lateralis* of the *quadriceps femoris* after a 12-hour fast. IMAT samples were carefully dissected from the muscle biopsies using a dissection microscope. We collected various metabolic parameters such as Glucose Infusion Rate (GIR), Fasting Glucose (FG), Postprandial Glucose (glucose 2 hours after a meal), fat mass(FM), Fat-Free Mass (FFM), as well as height, weight, and Body Mass Index (BMI) from all study participants who gave their consent. To better understand the communication between IMAT and skeletal muscle, we constructed a sender-receiver interaction network. This network was developed through an extensive search of databases and existing literature. We integrated this network with the gene expression data from both muscle and IMAT, focusing on genes whose expression correlated with GIR, which serves as a measure of insulin sensitivity. This allowed us to assess the role of each gene in the communication network. The genes identified in the network were associated with functions like extracellular matrix (ECM) remodeling, cytokine-cytokine receptor interactions, and TGF-beta signaling. These findings suggest an enrichment of inflammatory processes within the network. Furthermore, by applying a rewiring analysis, we observed changes in IMAT genes during communication with skeletal muscle under insulin-sensitive and insulin-resistant conditions. This indicates that IMAT is a dynamic tissue that responds to changes in insulin sensitivity within the muscle. After applying different criteria, we identified a cluster of genes in IMAT, including laminins, collagens, bone morphogenic, and calmodulins, which are implicated as drivers of insulin resistance in skeletal muscle. Furthermore, our analysis revealed that muscle signaling, mainly through semaphorins and laminins, may play a role in interacting with rewired IMAT signal-receiving genes, such as Plexins and Integrins. In conclusion, our data suggest that the communication between IMAT and muscle is regulated by interactions involving extracellular matrix (ECM) components and inflammatory cytokine proteins. This conclusion is based on a bioinformatics approach, and further experimental validation may be necessary to establish the findings conclusively.

1. Zusammenfassung

Der Skelettmuskel spielt eine entscheidende Rolle bei der Regulierung des Glukosestoffwechsels, und Faktoren wie Umwelteinflüsse oder genetische Veranlagungen können zu einer übermäßigen Fettansammlung im Muskel führen, was wiederum Insulinresistenz und Diabetes zur Folge hat. Intermuskuläres Fettgewebe (IMAT), eine Art von Fett im Muskel, wird mit der Regulierung der Insulinempfindlichkeit bei fettleibigen Personen in Verbindung gebracht. Die von IMAT ausgeschiedenen Faktoren, die die Insulinresistenz in der Skelettmuskulatur beeinflussen, sind jedoch nicht gut bekannt. Es ist möglich, dass IMAT und Skelettmuskel aufgrund ihrer räumlichen Nähe einen direkten Einfluss auf die Entwicklung von Stoffwechselkrankheiten haben. In dieser Studie untersuchten wir anhand von Transkriptomikdaten die Kommunikation zwischen IMAT und Skelettmuskulatur im Zusammenhang mit einer fortschreitenden Insulinresistenz. Unsere Studie umfasste 54 Teilnehmer aus verschiedenen Gruppen: 19 Personen mit Fettleibigkeit (OB), acht Patienten mit Typ-2-Diabetes (T2D), 14 Ausdauersportler (ATH) und 13 magere Kontrollpersonen (LC). Zur Durchführung des RNAseq-Experiments wurden Skelettmuskelbiopsien aus dem Vastus lateralis des Quadriceps femoris nach einem 12-stündigen Fasten entnommen. Die IMAT-Proben wurden mit einem Präparationsmikroskop sorgfältig aus den Muskelbiopsien herauspräpariert. Wir erfassten verschiedene Stoffwechselparameter wie Glukose-Infusionsrate (GIR), Nüchtern-Glukose (FG), postprandiale Glukose (Glukose 2 Stunden nach einer Mahlzeit), Fettmasse (FM), fettfreie Masse (FFM) sowie Größe, Gewicht und Body-Mass-Index (BMI) von allen Studienteilnehmern. Dieses Netzwerk wurde durch eine umfangreiche Suche in Datenbanken und bestehender Literatur entwickelt. Wir integrierten dieses Netzwerk in die Genexpressionsdaten von Muskeln und IMAT und konzentrierten uns dabei auf Gene, deren Expression mit der GIR korrelierte, die als Maß für die Insulinempfindlichkeit dient. Auf diese Weise konnten wir die Rolle jedes Gens in dem Kommunikationsnetzwerk bewerten. Die im Netzwerk identifizierten Gene wurden mit Funktionen wie dem Umbau der extrazellulären Matrix (ECM), Zytokin-Cytokin-Rezeptor-Interaktionen und TGF-beta-Signalen in Verbindung gebracht. Diese Ergebnisse deuten auf eine Anreicherung von Entzündungsprozessen innerhalb des Netzwerks hin. Darüber hinaus haben wir mit Hilfe einer Neuverdrahtungsanalyse Veränderungen in IMAT-Genen während der Kommunikation mit dem Skelettmuskel unter insulinempfindlichen und insulinresistenten Bedingungen beobachtet. Dies deutet darauf hin, dass IMAT ein dynamisches Gewebe ist, das auf Veränderungen der Insulinempfindlichkeit im Muskel reagiert. Nach Anwendung verschiedener Kriterien identifizierten wir eine Gruppe von Genen im IMAT, darunter Laminine, Kollagene, Knochenmorphogene und Calmoduline, die als Triebkräfte der Insulinresistenz im Skelettmuskel gelten. Darüber hinaus ergab unsere Analyse, dass die Muskelsignalübertragung, hauptsächlich über Semaphorine und Laminine, eine Rolle bei der Interaktion mit neu verdrahteten IMAT-Signalempfangsgenen wie Plexinen und Integrinen spielen kann. Zusammenfassend deuten unsere Daten darauf hin, dass die Kommunikation zwischen IMAT und Muskeln durch Interaktionen zwischen Komponenten der extrazellulären Matrix (ECM) und Entzündungen reguliert wird. Diese Schlussfolgerung basiert auf einem bioinformatischen Ansatz und eine weitere experimentelle Validierung kann erforderlich sein, um die Ergebnisse endgültig zu ermitteln.

2. Introduction

2.1. Diabetes mellitus

Diabetes mellitus (DM) is a chronic metabolic disorder characterized by high blood glucose levels resulting from defects in insulin production, insulin action, or both(1). Insulin is a peptide hormone produced by the β cells of the pancreatic islets of Langerhans that helps regulate blood sugar levels by facilitating cellular glucose uptake, regulating carbohydrate, lipid and protein metabolism, and promoting cell division and growth through its mitogenic effects (2). The disruption in metabolic regulation caused by diabetes mellitus (DM) leads to additional physiological changes in various organ systems, placing a significant burden on individuals living with diabetes and the healthcare system(3). According to the International Diabetes Federation (IDF) in 2021, Diabetes is a global health problem that affects 537 million adults between the ages of 20 and 79 which accounts for approximately 1 in 10 individuals(4). Shockingly, this number is projected to rise to 643 million by 2030 and 783 million by 2045(5). In 2021 alone, diabetes was responsible for 6.7 million deaths, equating to one life lost every 5 seconds(6). The economic impact is also substantial, for example healthcare expenditures related to diabetes reached to 966 billion USD(6). In Europe, the prevalence of diabetes is a significant concern. Approximately 1 in 11 adults, which translates to 61 million individuals, are living with diabetes. Projections indicate that the number of adults with diabetes is anticipated to rise to 67 million by 2030 and further increase to 69 million by 2045.The economic burden of diabetes in Europe is substantial, with an estimated expenditure of 189 billion USD(4).

2.1.1. Type of DM

There are different types of diabetes, with the most common ones being type 1 DM, type 2 DM, and gestational diabetes(1, 3). Type 1 DM usually develops in childhood or adolescence and is caused by an autoimmune response where the immune system mistakenly attacks and destroys the insulin-producing beta cells in the pancreas(7, 8). People with type 1 DM require lifelong insulin therapy(9). Type 2 DM, on the other hand, is the most prevalent form and typically occurs in adulthood(10). It is often associated with lifestyle factors such as obesity, sedentary behavior, and poor dietary choices(11). In type 2 DM, the body becomes resistant to the effects of insulin, leading to elevated blood sugar levels(12). Gestational diabetes develops during pregnancy and usually resolves after childbirth. It occurs when hormonal changes during pregnancy cause insulin resistance(13, 14). Gestational diabetes requires careful monitoring and management to avoid complications for both the mother and the baby(14). Uncontrolled diabetes can have significant health implications. Persistently high blood sugar levels can damage blood vessels and organs, leading to complications such as heart disease, stroke, kidney disease,

nerve damage, and eye problems(15, 16, 17, 18, 19). Diabetic individuals may also be at higher risk for infections, slow wound healing, and foot ulcers(20, 21, 22).

2.1.2. Diagnosis of DM

The diagnosis of diabetes can be determined through different criteria, such as the glucose tolerance test using hemoglobin A1c (HbA1c) or plasma glucose levels (fasting plasma glucose (FPG) or the 2-hour plasma glucose (2-h PG) after a 75-g oral glucose tolerance test (OGTT)) (1, 3). According to American Diabetes Association (ADA) report 2014, normal glucose tolerance is defined as an FPG of less than 5.6 mmol/L (100 mg/dL), a plasma glucose level of less than 140 mg/dL (11.1 mmol/L) after an oral glucose challenge, or an HbA1c level of less than 5.7%. On the other hand, a diagnosis of DM is defined when the FPG is equal to or greater than 7.0 mmol/L (126 mg/dL), the glucose levels are equal to or greater than 11.1 mmol/L (200 mg/dL) 2 hours after an oral glucose challenge, or the HbA1c level is equal to or greater than 6.5%(Figure 1) (23, 24).

Stages Types	Normoglycemia	Hyperglycemia		
	Normal Glucose Regulation	Impaired Glucose Tolerance or Impaired Fasting Glucose (Prediabetes)	Diabetes Mellitus	
			Not insulin requiring / Insulin requiring for control / Insulin requiring for survival	
Type 1*				
Type 2				
Other Specific Types**				
Gestational Diabetes**				

Figure 1. Diagnosis and Classification of DM. The range from normal glucose tolerance to diabetes in type 1 DM, type 2 DM, other specific types of diabetes, and gestational DM is shown from left to right. Arrows indicate that changes in glucose tolerance may be bidirectional in some types of diabetes. The figure was taken from Diabetes Care. 2013;37: S81-S90. doi:10.2337/dc14-S081.

2.1.3. Symptoms and management of DM

Common symptoms of diabetes include frequent urination, excessive thirst, unexplained weight loss, increased hunger, fatigue, and blurred vision(25). If left uncontrolled, diabetes can lead to severe complications affecting multiple organ systems, including the cardiovascular system (heart disease, stroke), kidneys (diabetic nephropathy), eyes (diabetic retinopathy), nervous system (neuropathy), and feet (diabetic foot ulcers)(26). The management of diabetes revolves around maintaining blood sugar levels within a target range. This involves a combination of healthy eating, regular physical activity, monitoring blood sugar levels, and, when necessary, taking medication or insulin(27). Monitoring blood

sugar levels is vital for individuals with diabetes as it helps to make informed decisions about food choices, physical activity, and medication.

2.1.4. Obesity as the major risk factor for development of type 2 DM

Obesity is a state of excess adipose tissue(lipid-storing adipose cell) accumulation in the body resulting from multiple factors, including genetic predisposition, environmental influences, socio-cultural factors, and individual behaviors, with a complex molecular mechanism(28, 29, 30). Although genetic factors can influence a person's susceptibility to weight gain through various mechanisms, environmental factors such as sedentary lifestyles and excessive calorie intake contribute to obesity by disturbing the physiological regulation of energy balance(31). Obesity is now a public health issue worldwide(32), affecting over 2 billion people across all age groups(33, 34) and contributes to numerous chronic diseases, including cancers, insulin resistance, diabetes, metabolic syndrome, respiratory disorders, musculoskeletal problems, cardiovascular diseases, and mental health issues(29, 30, 32, 35). Body mass index (BMI) is the most employed method to assess obesity. It is calculated by dividing a person's weight by the square of the height (in kg/m^2)(36). The World Health Organization (WHO) classification on BMI is widely utilized as a screening tool to evaluate the prevalence of obesity at the population level. In this classification, BMI higher than 30 is considered as an indication of obesity for men and women(32). While BMI is widely used, it is not a direct measure of body fat. Other techniques for quantifying obesity include anthropometry, which involves measuring skin-fold thickness, densitometry using underwater weighing, and imaging methods such as computed tomography (CT), magnetic resonance imaging (MRI) or electrical impedance can also be utilized as an approach to measure body composition and estimate obesity levels (37, 38, 39). The way adipose tissue distributed in different parts of the body has significant implications for health risks(40, 41). Specifically, fat located in the abdomen and around the organs (intraabdominal) and just beneath the skin in the abdominal area called abdominal subcutaneous has more impact on health than fat in the buttocks and lower extremities(42, 43), although the exact mechanism behind this association is not known(37, 42). However, intraabdominal fat cells are more active in releasing fatty acids (FAs) than other fat deposits meaning the lipolytic rate of such fat depot is high, yet the exact mechanism is unknown(44, 45, 46, 47). When these fatty acids enter the circulation, they can have harmful effects on the peripheral organs. Additionally, different types of fat cells in various depots may release specific substances called adipokines and cytokines, which could contribute to the systemic complications associated with obesity(28, 34). For example, obesity-associated insulin resistance (the decreased ability of insulin to act effectively on insulin sensitive target tissues, leading to impaired glucose utilization and increases hepatic glucose output, contributing to elevated blood sugar levels know as

hyperglycemia) is a prominent feature of type 2 DM(34, 48). The molecular causes of insulin resistance due to the increase of FAs and several other metabolites including acyl-CoAs, ceramides, and diacylglycerol(DAG)is through the activation of intracellular metabolites that activate protein kinases such as Protein Kinase C (PKC), Jun kinase (JNK), and the inhibitor of nuclear factor-κB (NFκB) kinase-β (IKKβ) which provides a molecular mechanism for inflammation(34, 49, 50, 51). These kinases and the inflammatory mediators can then activate serine/threonine kinases that inhibit insulin signaling by increasing the inhibitory serine phosphorylation of insulin receptor substrates (IRS)(52, 53).
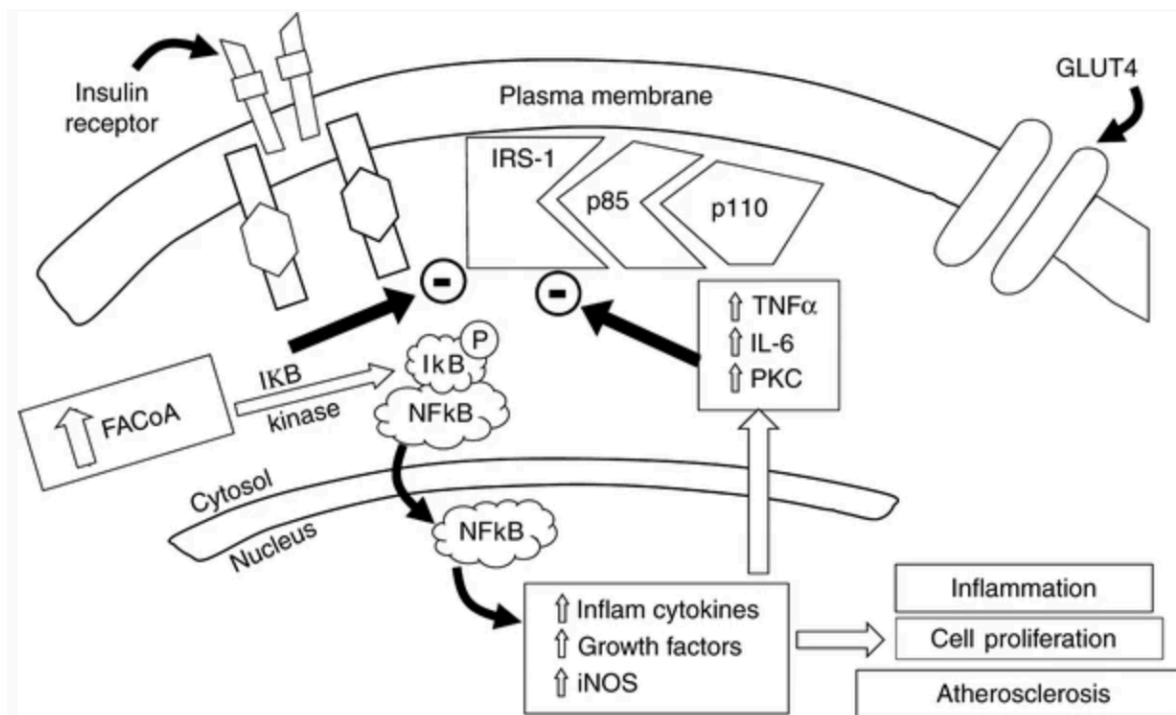
Figure 2.Molecular mechanism on the relationship between intracellular fatty acyl CoA levels (FACoA), IkB/NFkB and the insulin signal transduction pathway. Figure was taken from Diabetologia. 2010; 53:1270–1287. https://doi.org/10.1007/s00125-010-1684-1).

The build-up of lipids in insulin-sensitive tissues can disrupt mitochondrial oxidative phosphorylation, leading to decreased Adenosine Triphosphate (ATP) production. Additionally, the impaired oxidation of fatty acids and the accumulation of lipids in these tissues can generate reactive oxygen species, including lipid peroxides, which can affect insulin signaling adversely(54, 55, 56, 57). Moreover, in individuals with obesity, the adipose tissue experiences infiltration by mononuclear cells, including lymphocytes and monocytes, resulting in a state of persistent inflammation(51, 58). This inflammatory state is marked by the release of proinflammatory and prothrombotic cytokines (such as tumor necrosis factor alpha(TNF-a), resistin, Interleukin-6 (IL-6), plasminogen activator inhibitor-1(PAI-1), and retinol binding protein-4(RBP4)) from the adipocytes and macrophages(58) and they play a significant role in the development and progression of insulin resistance(51, 52, 53, 58, 59). Therefore, addressing the obesity epidemic is a key to stop the development of type 2 DM and requires a multi-faceted approach involving individuals, communities, healthcare

professionals, scientists, policymakers, and other stakeholders. Encouraging healthy eating habits and promoting physical activity are essential factors to stop the progress of obesity and diabetes.

2.2. Physiological regulation of energy balance

The regulation of energy balance depends on a complex interplay of hormonal and neural signals between the brain and various peripheral tissues(60, 61, 62). This complex regulatory system is necessary because even slight imbalances between energy intake and expenditure will significantly affect body weight. Arcuate nuclei in the hypothalamus are one of the most critical places where multiple hormones released from the gastrointestinal tract and adipose tissue assemble to regulate food intake and energy expenditure(63). These hypothalamic nuclei could also influence the secretion of several hormones that regulate energy balance and metabolism, including those from the thyroid and adrenal glands and the pancreatic islet cells(64). A central regulator is the adipocyte-derived hormone leptin, which acts predominantly in the hypothalamus to influence appetite, energy expenditure, and neuroendocrine function(65, 66). Leptin acts as a satiety hormone. An increased fat mass may lead to a higher leptin level in the circulation and induce leptin resistance, potentially may cause appetite disruption and overeating (66, 67). Furthermore, insulin, cortisol, and gut peptides such as peptide YY (PYY) and cholecystokinin (CCK) signals to the hypothalamus to regulate feeding behavior. However, the hormones ghrelin, secreted by the stomach, especially during fasting, stimulate appetite and food intake(33, 65, 66, 67). In addition, neural input through the vagus nerve from the viscera is vital to bringing sensory information to the hypothalamus about stomach emptiness and filling to control feeding(68, 69). Other areas of the brain such as brain steam and neural centers above the hypothalamus especially the amygdala and the prefrontal cortex are involved in the regulation of feeding behaviors and energy balance(64).
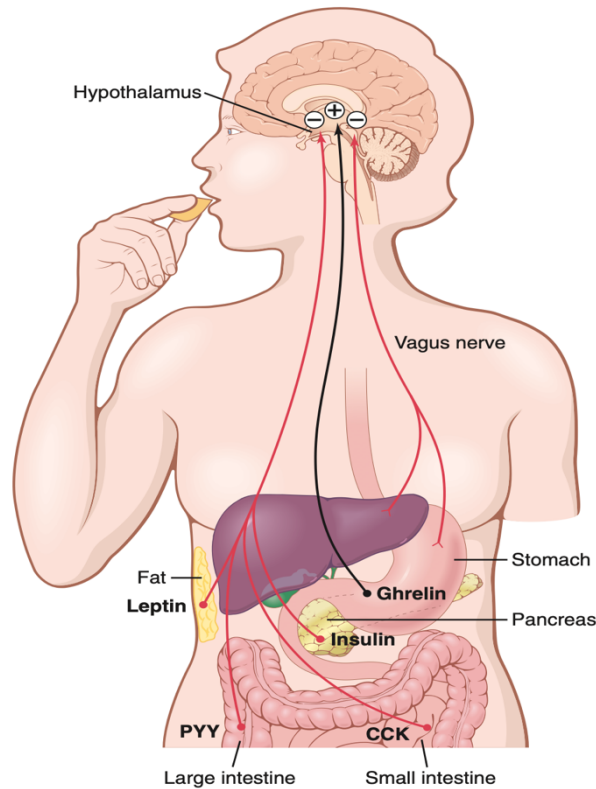
Figure 3.The role of peripheral hormones and vagal input in the control of energy balance. The vagal nerve takes sensory information from visceral part to brain especially to hypothalamus about stomach filing and destination. Additionally, gut hormones such as leptin, PYY, CKK, Insulin, and Ghrelin communicate the hypothalamus about nutrient availability (taken from Guyton and Hall Textbook of Medical Physiology 2015, 13 editions, page 889).

2.3. Insulin and its role in the regulation of glucose homeostasis

Metabolic equilibrium between hepatic glucose production and peripheral glucose uptake and utilization could be referred as glucose homeostasis (70, 71). Neural input, metabolic signals, and hormones, such as insulin, glucagon, cortisol, thyroid, and growth hormones, are essential in glucose supply and utilization(62, 63, 65, 68, 69). Insulin is secreted by the pancreatic beta cells response to glucose abundance and it circulates almost entirely in an unbound form, has a 6-minute plasma half-life, and is cleared from circulation within 10 to 15 minutes(52, 64, 72, 73). Except for the portion of the insulin that combines with receptors in the target cells, the rest is degraded by the enzyme insulinase, mainly in the liver, to a lesser extent in the kidneys and muscles(64, 73, 74). The primary role of insulin is facilitating glucose uptake into target cells, primarily muscle, adipose, and liver cells(70, 71, 72, 74). It does this by binding to specific insulin receptors present on the surface of these cells(75). The insulin-receptor interaction triggers a signaling cascade that promotes the translocation of glucose transporters, particularly Glucose transporter (GLUT) 4, to the cell membrane(73, 76). These transporters act as channels, allowing glucose to enter the cells from the bloodstream. Once inside the cells, glucose undergoes various metabolic processes, including glycolysis, the citric acid cycle (also known as the Krebs cycle), and oxidative

phosphorylation, to generate energy through ATP which is essential for the proper functioning of cells and enables various physiological processes(48, 64).
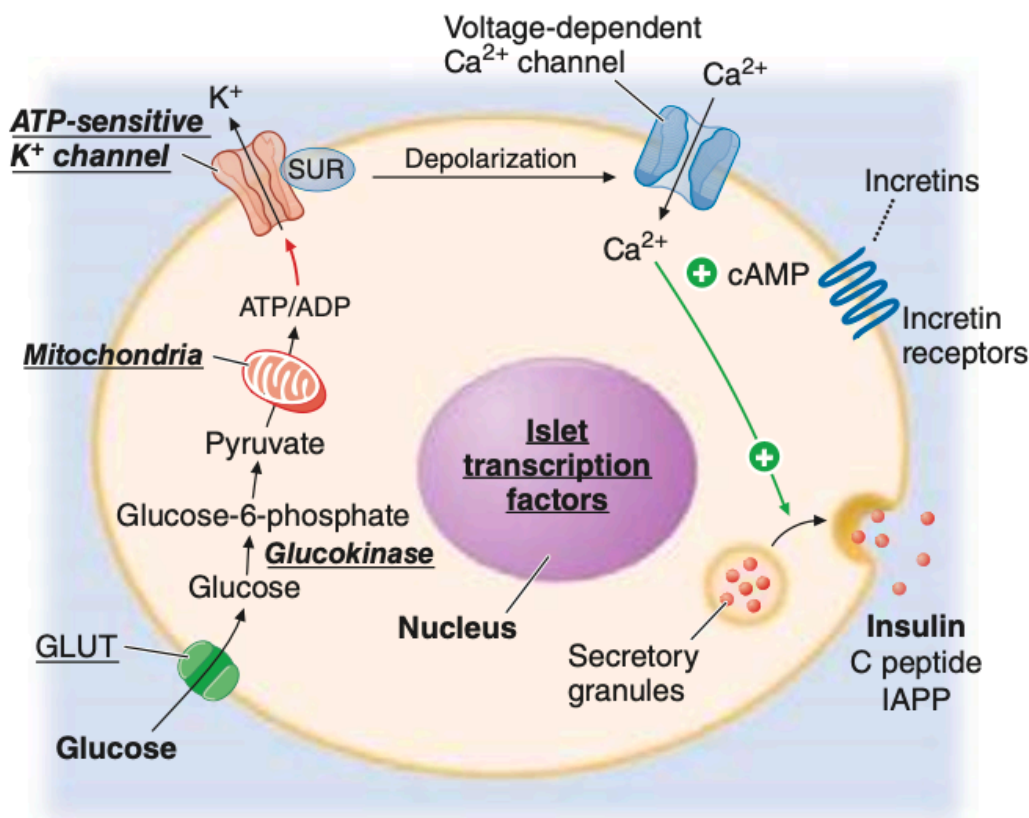
Figure 4.Glucose induced insulin secretion in the pancreatic beta cell. Glucose transporter protein 1 and 2 (GLUT1 and/or GLUT2 in humans, GLUT2 in rodents); The SUR receptor is the binding site for some drugs that act as insulin secretagogues. ADP, adenosine diphosphate; ATP, adenosine triphosphate; cAMP, cyclic adenosine monophosphate (taken from Harrison's principles of internal medicine, 2015, 19 editions, page 2402).

Insulin enhances glucose uptake and influences the metabolism of carbohydrates, lipids, and proteins(77). It promotes glycogen synthesis in the liver and muscle cells immediately after a meal. This glycogen can be readily broken down into glucose when energy demands increase, such as during physical activity or fasting, helping to maintain blood glucose levels within a normal range(70, 78). Insulin also regulate glucose homeostasis by suppresses glucose production in the liver (decreasing gluconeogenesis activity) through stimulating the conversion of excess glucose into fatty acids (77, 79). In addition to its effects on glucose metabolism, insulin influences lipid metabolism by storing excess amount glucose as fatty acid in the liver cell and used to form triglycerides, the usually form of storage fat(78, 80). Then, triglycerides are released from liver cell to the blood stream where insulin activated lipoprotein lipase enzyme degrade them into fatty acids again. Then, the adipose cells would absorb the fatty acids and stored them as triglycerides(81). Insulin inhibits the action of hormone sensitive lipase enzyme on stored triglycerides in adipose cells, thus preventing the release of excessive fatty acids into the bloodstream from adipose cells(70, 74, 78, 80,

82, 83). This mechanism helps in maintaining appropriate lipid levels and prevents the accumulation of lipids in tissues other than adipose tissue. However, insulin deficiency can promote fat utilization as an energy source, accelerating the breakdown of stored fat in adipose tissue. This can lead to elevated plasma cholesterol levels, phospholipids, ketosis, and acidosis(2, 24, 27). Additionally, insulin deficiency stimulates production of glucose from none-carbohydrate sources in the liver to increase plasma glucose level. Insulin also plays an important role in protein metabolism as well. It enhances amino acid uptake into cells by increasing the activity of amino acid transporters on the cell membrane and incorporation into proteins(48, 64). Additionally, insulin stimulates ribosomal activity and enhances the translation of messenger RNA (mRNA) into proteins(84, 85), and it inhibits the activity of proteolytic enzymes, such as proteasomes, which are responsible for degrading proteins. Also, insulin activates the mechanistic target of the rapamycin (mTOR) pathway that promotes protein anabolism by increasing the availability of cellular energy and activating protein synthesis machinery(86, 87). This effect is significant in muscle cells, contributing to muscle growth and repair. Insulin also inhibits protein degradation, ensuring that proteins are preserved and not broken down excessively.

2.4. Intermuscular adipose tissue (IMAT)

2.4.1. IMAT definition, location and its role in health and disease.

IMAT refers to the ectopic adipose tissue located in the muscle bed and interspersed among the muscle fibers in humans (88, 89, 90, 91). IMAT is a component of overall muscle lipid content, also termed as myosteatosis(88). However, IMAT should not be confused with the storage of lipids in adipocytes located within a single muscle group called intramuscular fat (IMATA)(92, 93, 94). In addition, there exist a smaller group lipids accumulation within the muscle cells called intramyocellular lipids (IMCL), which are non-adipocyte lipids specifically refers to triglyceride implicated in insulin resistance in obesity, type 2 DM, and HIV-associated lipodystrophy(88, 91, 92, 95). Initially, the quantification of adipose content within muscle was achieved through computed tomography (CT) imaging and, subsequently, magnetic resonance imaging (MRI) in older individuals, obese individuals, and those with type 2 diabetes mellitus(92, 93, 96, 97, 98). However, these techniques could not accurately measure microscopic IMAT distinct from other adipocytes or intramyocellular lipids in muscle cells(92). Nevertheless, recent advancements in molecular assay and sequencing technologies from biopsy samples have made it possible to differentiate the molecular profiles of various muscle adipocytes and lipids (88, 91). The presence, quantity and distribution of IMAT can vary among individuals and can be influenced by factors such as age, sex, genetics, and lifestyle(92, 94, 99, 100, 101, 102). IMAT, which constitutes approximately 5% of the overall fat content in the thigh, is thought

to play a vital role in providing cushioning, insulation and energy source for adjacent muscles (90, 91, 92, 102, 103). This hypothesis suggests that IMAT serves as a protective layer and helps maintain the structural and integrity of the muscles. However, it is important to note that currently, there is a lack of empirical data available to confirm this hypothesis definitively. Further research is needed to gather evidence and investigate the specific functions and contributions of IMAT in cushioning and insulating the surrounding muscle tissues. Moreover, excessive IMAT deposition is associated with adverse health effects, including metabolic disorders, cardiovascular diseases, and insulin resistance(88, 91, 92, 94, 96, 97, 100, 101, 102, 104, 105). Extensive investigations have been carried out on IMAT among individuals affected by a range of metabolic, orthopaedic, and neurologic conditions typically observed in rehabilitative environments. These studies aim to comprehend the impact of IMAT on health in different diseases and search into the cellular and molecular mechanisms that underlie its effects, aiming to identify potential therapeutic interventions. The study has revealed that elevated levels of IMAT are closely linked to various negative health outcomes, including insulin resistance, diminished muscular strength, and impaired mobility(88, 90, 91, 92, 94, 96, 97, 101, 102, 105, 106, 107). This association has been observed in diverse patient populations as well such as in chronic back pain, HIV infection, and spinal cord injury patients, cerebrovascular accidents (CVAs), diabetes, and chronic obstructive pulmonary disease (COPD)(88, 89, 90, 92, 94, 99, 102, 106, 108, 109). Moreover, it has been observed that older adults who exhibit higher levels of IMAT in their locomotor muscles tend to experience muscle weakness, reduced functionality in terms of mobility, and an increased vulnerability to future limitations in mobility(107, 110, 111, 112, 113). This suggests that IMAT accumulation plays a critical role in age-related declines in musculoskeletal health and overall physical function(89, 93, 94, 96, 106). Therefore, IMAT could be considered an important marker of body composition and an independent risk factor for various chronic diseases.
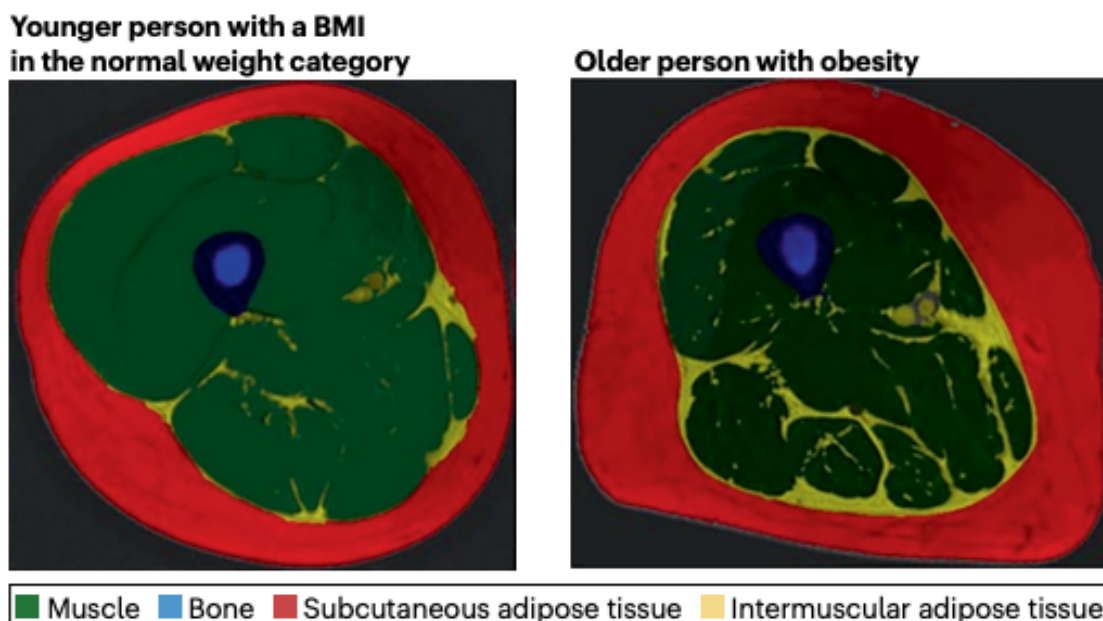
Figure 5.Magnetic resonance images that illustrate human IMAT. In left panel, a younger (32 years of age) person with a body weight in the normal BMI category. In the right panel, an older (62 years of age) person with obesity. Figure was taken from Nat Rev Endocrinol 2023;19(5):285-298. doi: 10.1038/s41574-022-00784-2.

2.4.2. Cellular origins of IMAT in humans

Adipogenesis refers to the differentiation and maturation of precursor cells, known as adipose stem cells (ASCs), into adipocytes, the primary cells composing adipose tissue (49). These ASCs are primarily found in the perivascular stroma of conventional adipose tissues, such as visceral fat, abdominal subcutaneous fat, and gluteal subcutaneous fat(88). Yet, the precise origin of adipocyte precursors remains unclear and need to be determined whether these precursors exclusively arise from resident cells within the adipose tissue or if cells from other tissues can migrate into an adipose depot and undergo adipogenic differentiation(88, 92, 102). Although categorized as ectopic, IMAT is a type of adipose depot and likely originates from multiple distinct cell types such as muscle satellite stem cells (MSCs) and fibro-adipogenic progenitor cells (FAPs) present within the muscle, and adipose-derived stem cells that migrate from other adipose depots into the muscle tissue itself(88, 114). MSCs are a committed stem cell population derived primarily from humans and mouse myoblasts(115), expressing classic myogenic markers, such as paired box proteins (PAX7), and muscle regulatory factors(MYF5, MYOD, MYOG, and MRF4)(116) and can differentiate into adipocytes when treated with adipogenic factors in vitro(88, 117, 118). When skeletal muscles experience pathological alterations due to aging and/or muscle injury, myoblasts, and muscle progenitor cells (MPCs) exhibit adipogenic differentiation and give rise to adipogenic cells (ACs) within the muscle tissue(117, 118, 119, 120).
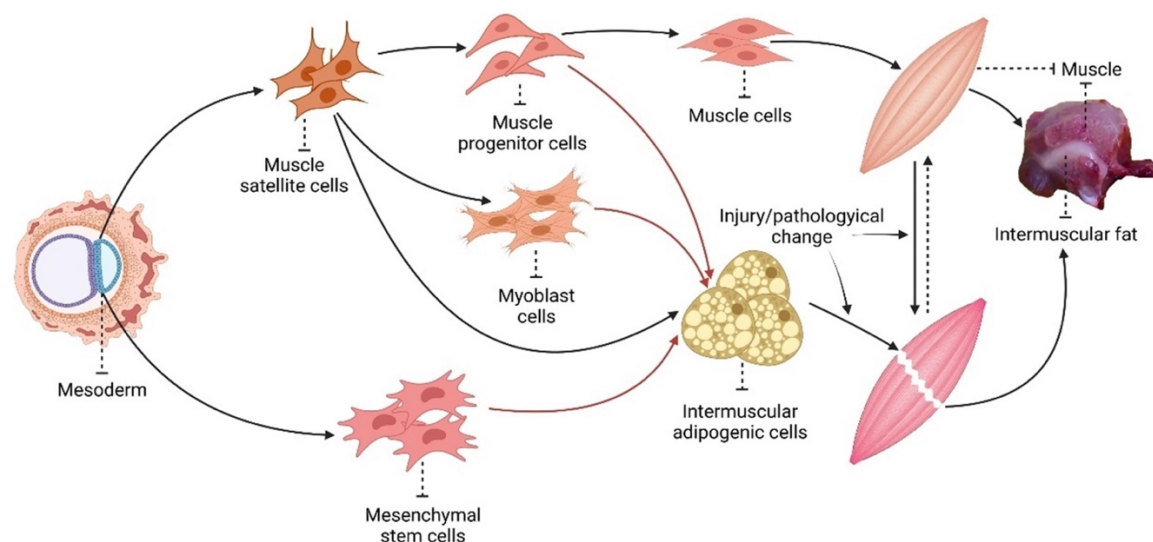
Figure 6.Schematic presentation on the origin of IMAT. Muscle stem cells and MSCs have similar activation and proliferation processes. When there is muscle injury, myopenia, oxidative stress, aging, or glucocorticoid therapy, mesenchymal stem cells can differentiate into large ACs and eventually lead to the formation and accumulation of IMAT as indicated by the red arrows. Inhibitory processes are indicated by the broken dot lines. Figure is taken from Diabetes Research and Clinical Practice 2022 187DOI: (10.1016/j.diabres.2022.109881)

In addition, FAPs are a unique group of cells found in muscle tissue that can differentiate into various cell types, including muscle cells and are distinguished by specific markers such as SCA1, CD34, PDGFRα, CD15, and CD90(88, 121, 122). When tissue damage or injury occurs, inflammatory signals prompt FAPs to change their fate, potentially diverting them from becoming muscle cells. However, in the case of healthy muscle, FAPs do not integrate or transform into adipocytes, indicating that the infiltration of fibro-adipogenic cells primarily occurs during ageing or disease when the muscle's ability to regenerate is compromised(88, 102, 123). Furthermore, recent findings in mice provide compelling evidence that ASCs are released into the bloodstream from subcutaneous adipose tissue (SAT) in the abdominal region. This release is primarily regulated by the interaction between a chemokine called CXCL12 and its receptor CXCR4, and it may play a role in the genesis and deposition of IMAT within the muscle(124). On top of these findings, another study has shown that when mice consume excessive nutrient intake or are exposed to some pharmacological treatments for the release of a specific subset of ASCs from the SAT depot in the abdomen induces the formation of adipocytes within skeletal muscle, leading to IMAT(125).

2.4.3. Molecular profiles of IMAT

Genomic investigations of IMAT in livestock animals have unveiled numerous genes and signaling pathways associated with adipogenesis, lipogenesis, glucose metabolism, cholesterol, and bile acid homeostasis(126, 127, 128). Analyses conducted in beef cattle and pigs have revealed distinct mRNA expression patterns among the visceral, subcutaneous, and intermuscular adipose depots, indicating that each depot is subject to

unique regulatory mechanisms and notably, IMAT displayed low transcript levels of genes related to oxidative metabolism while exhibiting high transcript levels of genes associated with inflammatory cytokines, suggesting a propensity for storage and inflammation (128, 129, 130). Furthermore, epigenomics of adipose tissue in pigs demonstrated that IMAT and VAT exhibit similar DNA methylation patterns to those observed in SAT(91). Likewise, from Sachs et al work (90), IMAT and VAT demonstrate statistically similar basal lipolysis rates compared to SAT in obese humans. This suggests that IMAT is an adipose tissue depot with distinct regulatory characteristics, sharing a molecular profile like VAT. Additionally, human IMAT gene expression among diverse insulin sensitivity groups in both sex is associated with insulin, MAPK and JAK-STAT signaling pathways. The same study has shown that negative relationships between insulin sensitivity measured by hyperinsulinaemic-euglycemic clamp and IMAT gene expression of macrophage, inflammatory cytokines, and oxidative phosphorylation markers. Moreover, the study found that extracellular matrix genes like COL24A1, DDR1, and CTGF are associated with insulin sensitivity in IMAT. These genes may play a role in the secretion of extracellular matrix proteins. Furthermore, the expression of lipolytic genes in IMAT, notably PLIN5 and peroxisome genes, exhibited a positive correlation with insulin sensitivity (90). This gene may regulate lipid metabolisms such as beta-oxidation or triglyceride reesterification, but no data have been obtained to confirm this hypothesis in humans. Additionally, the study has shown that IMAT has unique transcriptome, signaling and secretory properties and can be a potent inflammatory mediator compared to other adipose tissue depots among obese humans (90, 131).

2.4.4. Relationship between IMAT and total body adiposity

There is a positive association between IMAT and overall adiposity(88, 92, 105, 132). For instance in the Look AHEAD (Action for Health in Diabetes)Trial, type 2DM patients showed a positive correlation between IMAT and total adipose tissue level in the body(133). However, the ability of IMAT to independently predict metabolic risk factors remains uncertain and requires further investigation. When statistical models are adjusted to account for BMI or total adiposity, it has been found that IMAT remains a significant predictor of insulin sensitivity. Nevertheless, the same association is not observed for dyslipidemia markers (105, 134, 135, 136, 137). This suggests that the relationship between IMAT and metabolic risk factors may vary independently of overall adiposity, depending on the specific risk factor being considered(88). Although the size of IMAT is small compared to other adipose, studies have shown that it is positively correlated with other adipose depots, particularly abdominal adipose tissue, which is known to have a stronger association with cardiometabolic risk factors(92, 105). However, it remains uncertain gain whether IMAT can independently predict metabolic risk when considering abdominal adipose tissue,

specifically VAT. For example, a comprehensive study that included individuals from African American and Caucasian backgrounds showed that IMAT independently predicts plasma glucose and total cholesterol levels but not triglycerides, HDL-cholesterol, or insulin levels(138). This may imply that IMAT could strongly predict glucose metabolism and insulin sensitivity, even after adjusting for other ectopic adipose depots such as VAT(135, 136, 138, 139, 140), but its power of predicting cardiometabolic risk markers(dyslipidemia) needs more investigation.

2.4.5. Metabolic role of IMAT as evidenced from lower animal.

Studies from lower animal provide evidence that IMAT may play a crucial role in maintaining overall metabolic balance in the body. For instance, when observing nibbling and gorging mice, it was found that IMAT converted glucose into fatty acids at a quicker pace than muscle tissue. This indicates that IMAT potentially contributes to the creation of fat from dietary carbohydrates through de novo synthesis (141). Furthermore, a three-month exercise follow-up study on guinea pigs revealed that IMAT exhibited greater glucose utilization than other fat storage areas. Moreover, during this period, the lipid (fat) ratio decreased while the protein proportion increased, indicating that IMAT might serve as a nearby energy source for neighboring muscles (142). Likewise, exercise for an hour in a hamster ball increased the rate of fatty acid/triacylglycerol cycling in the IMAT and correlated with hexokinase and phosphofructokinase activity at specific sites(143). Another evidence documented again in the guinea pigs is that, simultaneously administration of noradrenaline and insulin to the isolated IMAT depot demonstrate an essential role of IMAT in neutralizing lipids locally to the nearby muscle (144).

2.4.6. Secretory and signaling effect of IMAT.

Adipose tissue's secretory and signaling capabilities are critical in regulating metabolic processes. Adipose tissue functions as a hub for communication, with more than 300 proteins being secreted to interact with other tissues through endocrine or paracrine signaling pathways and to engage in self-regulation through autocrine mechanisms(145). This extensive protein secretion allows adipose tissue to actively communicate and coordinate metabolic activities with various organs and tissues in the body(106). As an illustration, when adipocytes derived from SAT were co-cultured with muscle cells, it reduced insulin signaling and impacted the accumulation of triacylglycerol and diacylglycerol in the muscle(132, 146, 147). Moreover, the media conditioned by VAT led to insulin resistance in myotubes compared to condition media by SAT, and it also triggered inflammation and atrophy in primary muscle cell cultures(148, 149). Likewise, adipogenic progenitor cells isolated from human skeletal muscle decreased insulin signalling and insulin sensitivity in primary myotubes(150). These studies offer crucial evidence indicating that the paracrine signalling of adipose tissue influences the metabolic function of muscle

and provides a foundation for understanding the mechanistic relationships between IMAT and muscle metabolic function in vivo(88, 90, 103). Basing the above findings, a recent and exciting study has revealed that in cases of obesity, human IMAT exhibited a higher release of various pro-inflammatory cytokines, such as IL2, IL18, IL27, FGF23, and CSF1. Additionally, IMAT was found to release homeostatic chemokines like CCL25 and CCL27 and inflammatory chemokines, including CCL11 and IL8. Furthermore, adipokines like Resistin and HGF, and eicosanoids such as thromboxane B2 (TXB2), 5-hydroxyeicosatetraenoic acid (5-HETE), and 12-hydroxyeicosatetraenoic acid (12-HETE) were released at higher levels in IMAT compared to SAT and VAT(131). Furthermore, in the same study, when human primary muscle cell cultures were exposed to conditioned media derived from IMAT and VAT, there was a notable reduction in muscle insulin sensitivity, which was not observed with SAT(90).
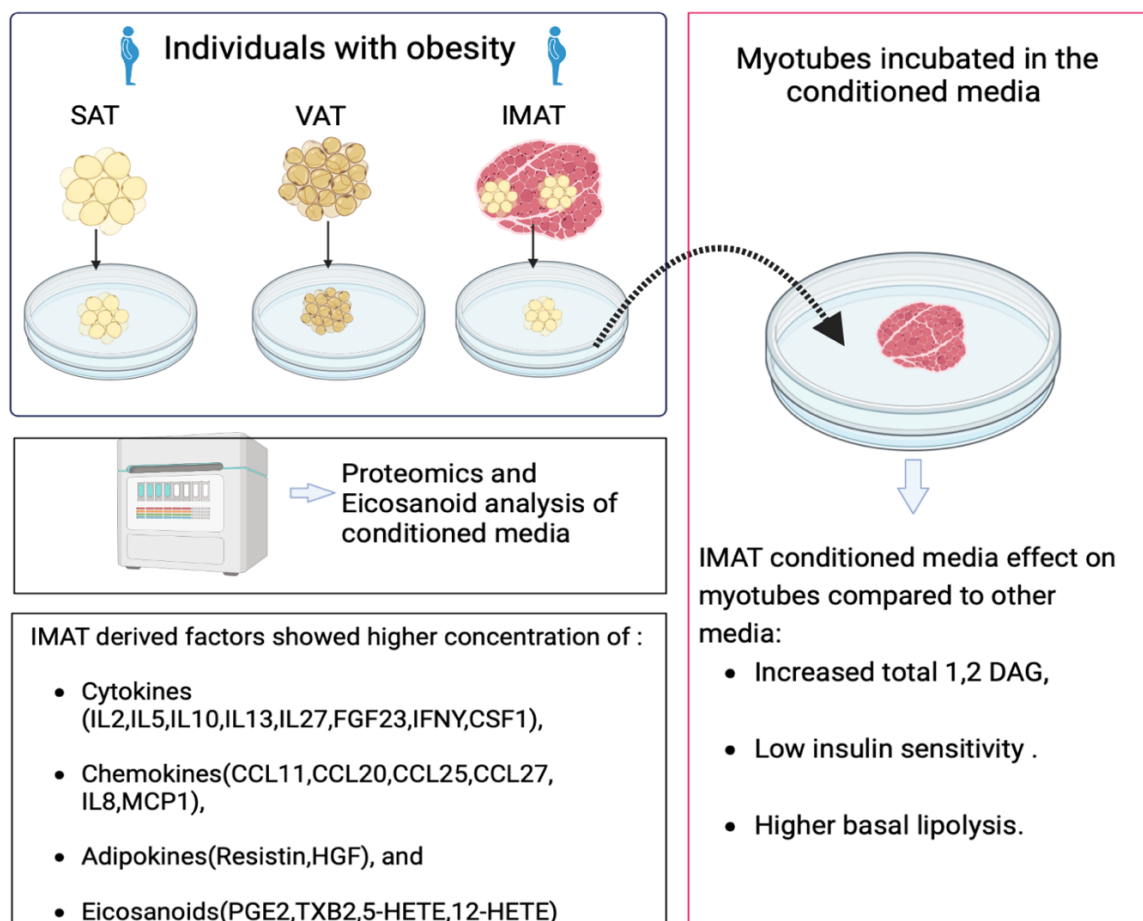
Figure 7.Inflammatory secretome of different adipose tissue depot. How condition media of IMAT regulate insulin sensitivity of the skeletal muscle (adapted from Physiol Rep. 2022;10(16): e15424. doi: 10.14814/phy2.15424 and Am J Physiol Endocrinol Metab. 2019;316(5): E866-E879. doi: 10.1152/ajpendo.00243.2018).

Combining the data, IMAT plays a significant role in the secretion of inflammatory cytokines, chemokines, and lipids that promotes inflammation and the infiltration of macrophage and other immune cells that can contribute to muscle inflammation and insulin resistance. Therefore, due to its physical closeness to the muscle, IMAT can alter muscle metabolic

function through the secretion of proteins. This suggests that IMAT-secreted proteins have the potential to be targeted in therapeutic interventions aimed at addressing muscle-related health issues, specifically focusing on muscle insulin resistance(88, 90, 91, 92).
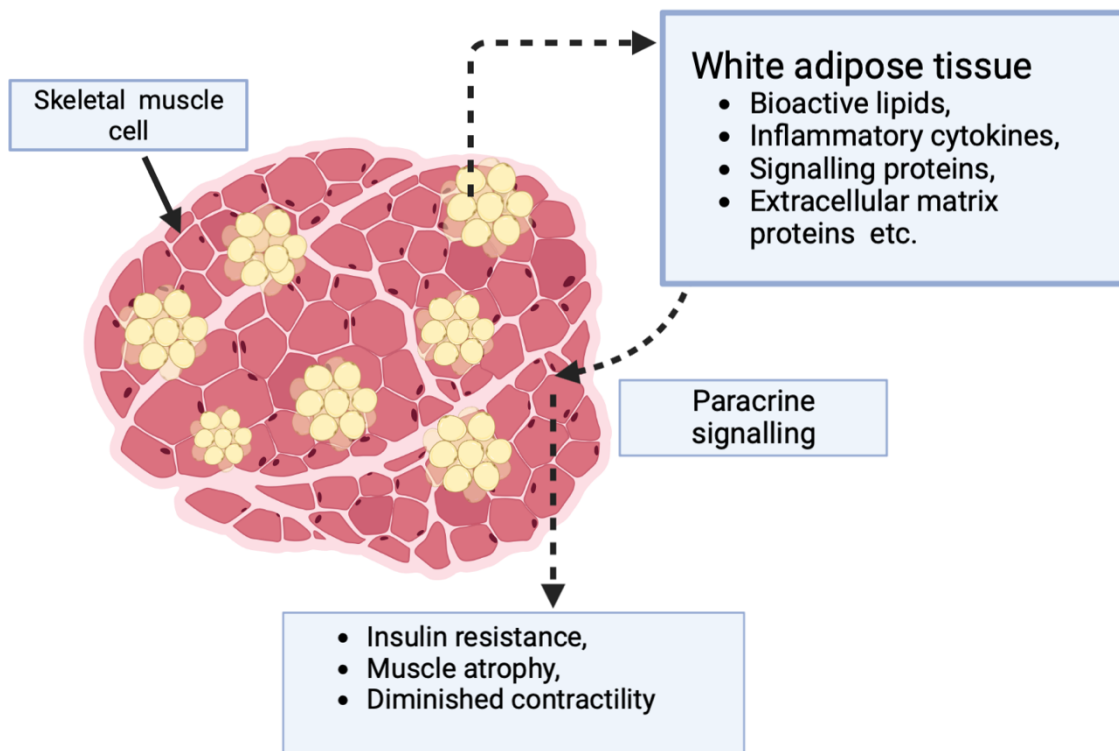
Figure 8.Graphic demonstration how IMAT secretion and paracrine signaling affect skeletal muscle insulin sensitivity. IMAT factors are locally regulating skeletal muscle insulin signaling and may induce the development of skeletal muscle insulin resistance, atrophy and could diminished muscular contractility.

While the paracrine effects of IMAT on muscle function are evident(90), further investigation into its endocrine roles is crucial. Because adipose tissue secretions primarily from VAT, like adiponectin and leptin, influence the insulin sensitivity of various tissues and predict cardiovascular disease risk by endocrine signaling(100, 104, 140). Considering the similar content of IMAT and VAT in humans, it is intriguing to hypothesize that IMATs endocrine action may influence remote tissues and provide insights into the association between IMAT content and cardiovascular disease risk(88).

2.5. Tissue cross talk: why, how, and when?

Multicellular organisms depend on sophisticated yet coordinated cellular activities, which rely on crosstalk between different cell types to orchestrate various biological phenomena (151, 152, 153). Crosstalk communication generally involves the physical interactions of multiple molecules through paracrine, endocrine, autocrine and Juxtacrine fashion (154). Eventually, these interactions are organized into a sequence of signaling pathways that may activate or inhibit downstream signaling and alter gene expression in the target cell to shape organismal homeostasis(155, 156, 157). For example, cells may produce and release

signaling proteins (e.g., ligand) that could be detected in the same or different cells through the membrane or intracellular proteins (e.g., receptor), triggering signaling pathways that control other processes (156, 157). The totality of these processes determines the function and development of diseases in the tissue. Thus, to comprehend physiological and pathological processes at the tissue level, one needs to consider molecular interactions of proteins within each cell type and between cell types (158). Direct measurement of proteins from single cell could be the best and preferable way to explore the role of interacting cells, as protein mediate most of the signaling cascade(156). However, proteomic technologies have shown significant difficulties in reproducibility and require specialized biochemical assays and extensive domain knowledge(156). Hence, RNA sequencing technology has become more popular and states forward to predict cell-cell communication and interactions from gene expression measurements through cross-referencing to prior understanding of sender protein-receiver protein interactions(156, 159, 160, 161, 162, 163, 164, 165, 166, 167, 168). However, transcriptomics data must be carefully analyzed and validated to prevent misleading conclusions since transcriptomics may not represent a fully accurate view of intercellular communication, as post-transcriptional and post-translational processes can uncouple transcript and protein abundances(156). Computational methods are the cornerstone in analyzing big omics data and building databases to understanding systems biology. In this regard, Kyoto Encyclopedia of Genes and Genomes(KEGG) (169), Gene ontology(GO) (170), and string(171) databases are the most powerful databases computationally curated to retrieve several protein-protein interactions and signaling pathways.

3. Aims of the thesis

This thesis aims to delve into the intricate interplay between IMAT and skeletal muscle, focusing on insulin resistance development. Skeletal muscle is responsible for a significant portion (80%) of glucose utilization after meals, and its insulin sensitivity can be affected by various factors. In conditions such as obesity and related diseases, an excessive buildup of fatty acid intermediates (diacylglycerol, triacylglycerol, and ceramides) impedes insulin signaling by reducing the presence of GLUT4 transporters on the surface of myocyte membranes. This disruption is considered a pivotal contributor to skeletal muscle insulin resistance. Furthermore, the accumulation of lipid deposits within muscle fibers or a direct infusion of fatty acids can also impact skeletal muscle insulin sensitivity. For instance, studies have shown that exposing primary skeletal muscle cells to IMAT condition media during obesity in humans leads to an increase in 1,2-diacylglycerol (1,2 DAG) levels within skeletal muscle myotubes. Although the exact mechanism by which IMAT-conditioned media elevates 1,2 DAG and induces insulin resistance in skeletal muscle remains unclear, it is hypothesized that the release of proinflammatory cytokines, chemokines, and lipids from IMAT plays a significant role. Consequently, unravelling the molecular mechanisms underlying skeletal muscle adiposity holds great promise for identifying novel therapeutic targets to address the escalating health concerns associated with muscle dysfunction, including insulin resistance, diabetes, and myopathy. Hence, the primary objective of this study is to comprehensively understand the molecular crosstalk between IMAT and skeletal muscle during insulin resistance progression, ultimately paving the way for the discovery of innovative therapeutic approaches to treat muscle-related disorders.

The specific aims of this thesis are as follows:

1. Understand transcriptomics regulation of IMAT and muscle.
2. Explore differentially regulated genes between groups in each tissue.
3. Gain a comprehensive understanding of the biological role differentially expressed genes or genes correlated to insulin sensitivity.
4. Build a reference network based on prior knowledge to illustrate potential interactions between sender and receiver coding genes described in various research articles, textbooks, and databases.
5. Investigate the communication network between IMAT and muscle by correlating the expression level of senders or/and receiver coding genes in both tissues with insulin sensitivity.
6. Identify distinct clusters or communities within the communication network, which may suggest unique or specific biological functions. This analysis will help uncover modules of genes that work together to regulate insulin sensitivity and provide insights into the overall network structure.

7. Highlight the most rewired genes within the communication network. Specifically, focus on identifying genes that interact with a diverse range of genes exhibiting various degrees of insulin sensitivity. This approach will offer valuable insights into understanding the alterations occurring in the molecular interaction network between IMAT and muscle during the development of insulin resistance.

By addressing these specific aims, this thesis aims to unravel the molecular mechanisms and communication patterns between IMAT and skeletal muscle, contributing to a better understanding of insulin resistance development and potentially identifying novel therapeutic targets for muscle-related disorders.

4. Material and Methods

4.1. Materials

Table 1.List of R packages used in the analysis.

Package	Version
AnnotationDbi	1.60.2
BiocParallel	1.32.6
broom	1.0.5
corrplot	1.03
circlize	0.4.16
clusterProfiler	4.7.1.003
ComplexHeatmap	2.15.4
cowplot	1.1.1
data.table	1.14.8
DESeq2	1.38.3
doParallel	1.0.17
dplyr	1.1.2
EnhancedVolcano	1.16.0
forcats	1.0.0
ggcorrplot	0.1.4
ggplot2	3.4.2
ggplotify	0.1.1
ggpubr	0.6.0
ggthemes	4.2.4
ggraph	2.1.0
grid	4.2.3
gridExtra	2.3
gridtext	0.1.5
igraph	1.5.0.1
kableExtra	1.3.4.9
magick	2.7.4
magrittr	2.0.3
moderndive	0.5.5
org.Hs.eg.db	3.16.0
patchwork	1.1.2
pheatmap	1.0.12
proustr	4.4.0
plotly	4.10.2
psycho	0.6.1
RColorBrewer	1.1.3

RCy3	2.18.0
readr	2.1.4
rstatix	1.3
Reshape2	1.4.4.9
Stringr	1.5.0
tibble	3.2.1
tidyverse	2.0.02.9
VennDiagram	1.7.3
viridis	0.6.4
Cytoscape Software	3.10.0

4.2. Methods

4.2.1. Study subjects, sampling, and measurements

Data collection, study design, and sampling procedures employed in this study are based on the methodology described by Sachs et al. (90). In the following section, a brief overview of the key aspects of the method is provided. Therefore, this study involved a total of 54 participants who were categorized into four groups: 19 individuals who were Obese (OB), 8 patients diagnosed with type 2 DM, 14 endurance athletes who were training for cycling and triathlon competitions (ATH), and 13 lean controls (LC). Various clinical variables were collected for all participants who provided their written informed consent, including the Glucose Infusion Rate (GIR), Fasting Glucose (FG), Postprandial Glucose (glucose 2 hours (PPG)), fat mass, Fat-Free Mass (FFM), as well as height, weight, and Body Mass Index (BMI). GIR was measured using hyperinsulinemic-euglycemic clamp, which is the most widely used procedure, also regarded as the gold standard to evaluate insulin sensitivity and glucose metabolism in research and clinical settings(172, 173). During a hyperinsulinemic-euglycemic clamp study, insulin is consistently administered at a physiologically relevant rate (40mU/min.m2) into the bloodstream to increase insulin levels to suppress hepatic glucose production while ensuring that blood glucose levels remain stable (euglycemia (100mg/dl)) by infusing glucose at a variable rate(174, 175, 176, 177). Therefore, among insulin-sensitive individuals, the rate of glucose appearance in the bloodstream, which includes both endogenous glucose (hepatic glucose production) and exogenous glucose (infused glucose), becomes equal to the glucose disappearance rate where a significant portion of glucose uptake (approximately 80%) occurs in the skeletal muscle. In this study, the antecubital vein of one arm was cannulated to facilitate the administration of insulin, [6,6-2H2] glucose, and dextrose infusions. In addition, a catheter was inserted into the contralateral arm in the retrograde dorsal hand vein for blood sampling. An ongoing infusion of [6,6-2H2]glucose, with an initial priming dose of 0.04 mg·kg−1·min−1, was initiated and maintained throughout a 2-hour equilibrium period, followed by a subsequent 3-hour insulin clamp phase and the rate of glucose disappearance was calculated as previously described for similar study(177, 178). After allowing a 2-hour duration for the tracer to achieve equilibrium, a percutaneous needle biopsy was performed in the *vastus lateralis* of the *quadriceps femoris* at a specific location between the greater trochanter of the femur and the patella for the RNA-seq experiment. Then, the muscle samples were rapidly frozen in liquid nitrogen and stored at -80°C until IMAT dissection is performed. IMAT samples were carefully dissected from the muscle biopsy with the help of a dissection microscope on ice to maintain the temperature(90).Additionally, demographic variables age and sex are obtained from all participants. As inclusion and

exclusion criteria, it is worth noting that individuals with a BMI below 20 kg/m2 or above 25 kg/m2 were excluded from the lean and athlete groups, while those with a BMI below 30 kg/m2 were excluded from the obese and T2D groups. Moreover, individuals with fasting triglyceride levels exceeding 150 mg/dl, and those with liver, kidney, thyroid, or lung diseases were also excluded from the study. Individuals with type 2 DM who used insulin or thiazolidinediones were not included in the study. Finally, this study was approved by the Colorado Multiple Institution Review (CMR) board at the University of Colorado.

4.2.2. RNA isolation and analysis

In this study, total RNA was extracted from both IMAT and skeletal muscle biopsies using the RNeasy Lipid Tissue Kit (QIAGEN). An Agilent 2100 Bioanalyzer and Agilent 6000 Nano Kit (Agilent) were used to assess the quality of isolated RNA. Samples with RNA integrity numbers (RINs) greater than 7 selected for the RNA sequencing or gene expression experiment. For library preparation, 300 μg of total RNA per sample was utilized. RNA molecules were subjected to poly(A) selection, fragmentation, and reverse transcription using the Elute, Prime, Fragment Mix (Illumina, San Diego, CA). Subsequent steps, including end-repair, A-tailing, adaptor ligation, and library enrichment, were carried out following the Low-Throughput Protocol of the TruSeq RNA Sample Prep Guide (Illumina), employing the Bravo Automated Liquid Handling Platform (Agilent Technologies, Santa Clara, CA). The quality and quantity of the RNA libraries were assessed using the Agilent 2100 Bioanalyzer and the Quant-iT PicoGreen dsDNA Assay Kit (Thermo Fisher, Waltham, MA). Sequencing of the RNA libraries was performed on an Illumina HiSeq2500 platform with 100-bp paired-end runs. Primary analysis, including base calling and quality scoring, was conducted using the Real-Time Analysis software (Illumina). Alignment of the sequences against the hg19 genome and UCSC (University of California Santa Cruz) known gene annotation assembly (GTF file) was performed using Genome Multitool (GEM) mapper (version 1.7.1) with standard parameters (except mismatches = 0.04 and min-decoded-strata = 2). Read counts were determined using HTSeq-count (version 0.6.0)

4.2.3. Statistical and Bioinformatic Analysis

4.2.3.1. Demographic and clinical variable data

Differences in clinical variables between groups and sex were analyzed using ANOVA and t-test using base R functions (such as **anova** and **t.test** respectively). The anova function compute analysis of variance table for the fitted model (linear regression) between a factor variable group and a numeric clinical variable. Whereas the t-test function compares the mean of a clinical data between two groups. Furthermore, pairwise correlation analysis (using **cor** function in base R) was performed to explore potential relationships between the

clinical variables across all groups. The mathematical description about the function mentioned here will be discuss the following sections.

4.2.3.2. RNAseq data preprocessing and cleaning

A total of 21185 protein coding mRNA genes detected from IMAT and skeletal muscle among 50 participating individuals. The data obtained from RNA sequencing is typically in the form of raw read counts, representing the number of times each RNA transcript in the samples is detected. Therefore, the read count of those genes was generated as data table where genes were arranged as rows (21185 genes) and samples (IMAT and muscle) as column. Then, imported to the R pregaming language(179) for data preprocessing. Lowly expressed genes are genes with low transcription or expression levels in a biological sample and removing them is a common practice in analyzing RNA-seq data. Often those genes may not show differences in expression between conditions as well. Here a gene is defined as lowly expressed when the row sum counts among the smallest group is below 50 read count. Thus, genes containing 50 or more raw counts among the smallest sample group (T2D samples) were kept (total of 11828 genes) for downstream analysis.

4.2.3.3. Gene normalization

The R package DESeq2 used for raw counts normalization, transformation, and differential expression (DE) analysis (180). Read count normalization is necessary for any DE analysis to compare gene expression between samples accurately. Various factors, including sequencing depth, gene length, RNA composition, and the actual RNA expression, can influence the counts of mapped reads for each gene. Normalization involves scaling the raw count values to account for these factors, enabling more meaningful comparisons of gene expression levels within and between samples. DESeq2 employs size factors to address variations in sequencing depth across samples. These factors act as scaling coefficients, adjusting the raw read counts for each sample to ensure comparability between them. To estimate these size factors, DESeq2 utilizes the median-of-ratios method(181), involving the following steps:

1. It constructs a pseudo-reference sample for each gene, potentially equating to the geometric mean across all samples (i.e., averages calculated from the log values of the reads). Scaling the reads on logs eliminate genes that are only transcribed in one sample type and helps to smooth over outlier read counts.

2. A log ratio is calculated for each gene in a sample using the sample count and the corresponding pseudo-reference sample count. Alternatively, we can calculate it by subtracting the average log value from the log count of the gene in each sample. This will allow us to identify genes within each sample that are expressed at levels significantly higher than the average or close to the average or significantly less than the average.

3. Then, it calculates a size factor (normalization factor) for each sample, determined as the median value of all ratios specific to that sample. However, these median values are in natural log values, thus transformed into regular numbers by inverse logarithm operation that is raising exponents to the median value. Using the median is another way to avoid extreme genes from influencing the value too much in one direction. Mathematically the above three step could be expressed as follows:

$$s_j = \ median_i \ \frac{k_{ij}}{\left(\prod_{i=1}^{m} k_i\right)^{1/m}} \tag{1}$$

Where:

-   s_j is sample size factors, k_{ij} is a $n \ x \ m$ read count matrix where i = 1,…, n indexes the genes, and j = 1,…, m indexes the samples; the $\prod$ and the whole denominator refer pseudo reference sample(181).

4. Finally, each raw count value in each sample k_{ij} is divided by its corresponding normalization factor (size factor) s_j to generate the normalized count q_{ij} values. This normalization ensures in identifying of differentially expressed genes between conditions or treatments.

$$q_{ij} = \frac{k_{ij}}{s_j} \tag{2}$$

5. However, for each experimental condition ρ, mean normalized count q_{ip} calculated as the average of the counts from the samples j corresponding to condition ρ. This again expressed mathematically as below as indicated in the Anders and Huber publications in 2010(181).

$$q_{ip} = \frac{1}{m_p} \sum_{j:p(j)=p} \frac{k_{ij}}{s_j} \tag{3}$$

Where:

-   q_{ip} is the mean estimate of gene count *i* in condition ρ, m_p is the number of replicates in condition ρ and the sum runs over the replicates, k_{ij} the raw count value assigned to gene *i* in sample j and s_j is size factors described in the equation 1 above.

Table 2.Standard normalization methods in gene expression analysis adapted from (182)

Normalization Method	Description	Accounted factors	When to use
Median ratios as described in DESeq2(180)	Counts divided by sample-specific size factors determined by median ratio of gene counts relative to geometric mean per gene.	Sequencing depth and RNA composition.	Gene count comparisons between samples and for DE analysis but not recommended for within sample comparisons.
TMM as depicted in EdgeR(183)	Uses a weighted trimmed mean of the log expression ratios between samples.	Sequencing depth, RNA composition, and gene length	Gene count comparisons between and within samples and for DE analysis.
CPM(184)	Counts scaled by total number of reads that is the relative abundance of a gene is the ratio between raw count of gene to the total number of reads in the sample multiplying by a million	Sequencing depth.	Gene count comparisons between replicates of the same sample group; not recommended for within sample comparison or DE analysis.
TPM(185, 186)	Counts per length of transcript (kb) per million reads mapped. The relative abundance of a gene is the ratio of the raw count of a gene to the effective length of the gene adjusted for its length and the library size and then multiplying by a million.	Sequencing depth and gene length.	Gene count comparisons within a sample or between samples of the same sample group; and not recommended for DE analysis.

TPM-Transcripts per kilobase Million, **CPM** -Counts per Million, **TMM**-Trimmed mean of M values. **DESeq2**- Differential Expression analysis of RNA-Seq version 2, **EdgeR**- Empirical analysis of Digital Gene Expression in R,

4.2.3.4. Differential expression analysis

Differential expression analysis is a powerful method used to compare the expression levels of genes between two different conditions or groups, providing valuable insights into the molecular basis of various diseases and physiological processes. The gene expression level determines the amount of protein produced that carries out vital functions within an organism. Before conducting the analysis, the data must be preprocessed and normalized to account for differences in sequencing depth and other technical factors, as explained above. We use a statistical method called generalized linear model (GLM) in DESeq2 to

understand differential expression between IMAT and muscle or between different groups within the same tissue. The model uses a negative binomial (NB) distribution suitable for RNA sequencing count data because it accommodates the overdispersion often observed in such data, where the variance is higher than the mean(181, 187). The method efficiently models the relationship between the dispersion and the average expression of a gene across all samples. As a result, it can detect and adjust the dispersion estimates for each gene and using this information it calculates statistical significance(p-values and adjusted p-values) and fold changes between conditions(180). Matmatmticaly the model calculate the following:

1. First, the mean parameter, denoted μ_{ij}, is calculated as a product of a normalized gene count $q_{i\rho}$ as stated in equation 2 and a size factor s_j as described in equation 1.

$$\mu_{ij} = q_{i,\rho(j)}s_j \tag{4}$$

2. Second, add the mean parameter μ_{ij} with the raw count variance parameter α_i to calculate variance σ^2_{ij}. The variance calculation is motivated by assuming that the actual concentration of fragments from gene *i* in sample j is proportional to a random variable R_{ij}, such that the rate that fragments from gene *i* are sequenced is the product of the size factor in the sample and the read count of the fragments.

$$\sigma^2_{ij} = \mu_{ij} + \alpha_i \mu^2_{ij} \tag{5}$$

3. Next, NB distribution of the mean μ_{ij} and variance σ^2_{ij} are computed to understand how the observed count of each gene *i* in all samples *j* likely to vary around the mean. Therefore, for each gene *i* and all samples *j* of condition ρ, the R_{ij} are with mean $q_{i\rho}$ and variance $\alpha_{i\rho}$. In other words, the count value K_{ij}, conditioned on $R_{ij} = r_{ij}$, is the NB distribution with mean μ_{ij} and variance σ^2_{ij} .

$$K_{ij} = NB(\mu_{ij}, \sigma^2_{ij}) \tag{6}$$

4. Then, it performs statistical tests using logarithm of the likelihood to assess the significance of DE for each gene between two conditions (e.g., A and B) using the NB distribution information. In the statistical tests, the null hypothesis H_0 assumes no expression difference between conditions, and the alternative H_1 assumes that there is a difference. The detail of the method is stated in DESeq (181) and DESeq2 (180)work flow.

4.2.3.5. Principal components analysis

Principal components analysis (PCA) is one of the most used dimensional reduction techniques in genomics to pinpoint the most important information in the dataset. Principal components (PCs) are calculated using **prcomp** function in R and involves three main steps. It starts by generating a covariance matrix through pairs wise correlation between variables. The covariance matrix denoted here as **Cov** is a square (n x n) matrix, where n is the number of rows and columns that describes the relationships and variances between different variables in the dataset. The element **Cov** (i, j) represents the covariance between the ith and j^{th} variables.

$$Cov(x, y) = \frac{\sum_{i=0}^{n}(x_i - \overline{X})(y_i - \overline{Y})}{n - 1} \tag{7}$$

Where:
- xi and yi are individual data points from the samples of X and Y, respectively.
- $\overline{X}$ and $\overline{Y}$ are the sample means of X and Y, respectively.
- x_i and y_i the values of the x-variable and y-variable in a sample
- n is the number of data points in the sample

In the second step, it calculates the eigenvalues (λ_1, λ_2, ..., λn) and corresponding eigenvectors (v_1, v_2, ..., vn) of the covariance matrix. Eigenvalues (λ) of the **Cov** matrix are calculated by solving the characteristic equation of:

$$\det(Cov - \lambda I) = 0 \tag{8}$$

Where:
- **det** denotes the determinant, a scalar value computed from a square matrix **Cov** as the product of the elements along the main diagonal (from top-left to bottom-right) minus the product of the elements along the opposite diagonal (from top-right to bottom-left) and can be defined in several equivalent ways such as Leibniz formula, Laplace expansion or Gaussian elimination. If the determinant is zero (**det (Cov) = 0**), the matrix is said to be singular, and it does not have an inverse and may have multiple or no solutions. However, If the determinant is non-zero (**det (Cov) ≠ 0**), the matrix is considered non-singular, has an inverse and a unique solution.
- **I** is the identity matrix of the same size as **Cov** matrix, with ones on the main diagonal (from the top-left to the bottom-right) and zeros elsewhere. The identity matrix acts as the multiplicative identity for matrices, much like how the number 1 is the multiplicative identity for real numbers.

Then, next step is calculating the eigenvectors for each eigenvalue. When a non-zero vector is multiplied by a matrix and results in another vector parallel to the first or equal to **0**, this vector is called an eigenvector of the matrix, and this could be done by solving the linear equations of:

$$(Cov - \lambda I) * v = 0 \tag{9}$$

Where:

- **Cov** is the square matrix, **v** is the eigenvector corresponding to eigenvalue(**λ**) and **I** is the identity matrix.

Lastly, eigenvectors are assigned into a new variable know as PC and would be sorted by their eigenvalues from highest to lowest to tell how much information or variance can be attributed to each PCs. Thus, PCs form a new orthogonal basis for the data.

4.2.3.6. Clustering analysis

Clustering analysis using distance or correlation as a measure of sample or future dis(similar) could be the alternative way to learn the presence or absence pattern within groups or between groups. R built-in functions **dist** used to calculate the Euclidean distance between two data points in a Euclidean space. This distance can be derived from the Cartesian coordinates of the points, employing the Pythagorean theorem, commonly referred to as Pythagorean distance.

$$d(x,y) = \sqrt{\sum_{i=1}^{n}(x_i - y_i)2} \tag{10}$$

Where:

- **x** and **y** are two data points in the Euclidean n-space,
- x_i and y_j are Euclidean vectors, starting from the origin of the space (initial point),
- **n** represent n-space.

In addition, correlation of two data points is examined using R built in function **cor.test** and mathematically correlation of two data point could be expressed as below.

$$r(x,y) = \quad (x,y) = \frac{\Sigma(x_i - \overline{X})(y_i - \overline{Y})}{\sqrt{(x_i - \overline{X})2}\sqrt{(y_i - \overline{Y})2}} \tag{11}$$

Where:
- **r (x, y)**, is the correlation coefficient of the linear relationship between the variables x and y
- $\overline{X}$ and $\overline{Y}$ are the sample means of X and Y**,** respectively.
- x_i **and** y_i the values of the x-variable and y-variable in a sample

After computing the dis(similarity) matrix based on either distance or correlation, hierarchical clustering with the complete linkage method is employed using the R built-in function called **hclust**. This specific clustering technique establishes the distance between two clusters as the maximum separation observed among their individual elements. In each step of the clustering procedure, the two closest clusters are combined to create a new cluster. This sequence of actions is iterated until the entire dataset consolidates into a single, unified cluster. This approach enables us to cluster similar features or variables together(188). Mathematically, the complete linkage function could be described by the following expression:

$$D(X,Y) = \frac{max}{x \in X, y \in Y} d(x,y) \tag{12}$$

Where:

- D (x, y) is the distance between elements $x \in X$ and $y \in Y$
- X and Y are two sets of clusters

4.2.3.7. Correlation and linear regression analysis

Correlation and regression analysis were used to see the association between insulin sensitive/Glucose Infusion Rate/ and gene expression in the whole sample of muscle and IMAT respectively. Correlation is a standardized measure that tells you whether two variables change together and the strength and direction of their relationship. In addition, it could help to identify connections, patterns, or dependencies between variables. However, correlation doesn't imply causation – a strong correlation doesn't mean that changes in one variable cause changes in the other (Other factors might be at play). Thus, correlation is sensitive to linear relationships; it might not capture more complex associations and does not support confounding variable adjustment. The correlation coefficient ranges between -1 and 1. A value close to 1 signifies a strong positive correlation, meaning that as one variable increases, the other also tends to increase. Conversely, a value near -1 indicates a strong negative correlation where when one variable goes up, the other typically goes down. A correlation of 0 means there's no linear relationship between the variables. The mathematically notation of correlation is described in the equation 8. Furthermore, we used the linear regression function **lm** in base R to correlate gene expression in the muscle and IMAT respectively with whole-body insulin sensitivity after adjusting for body mass index. The general formula for linear regression is expressed as:

$$\hat{Y} = \widehat{\beta_0} + \widehat{\beta_1 X} + \epsilon \tag{13}$$

Where:

- $\hat{Y},$ is the response variable to be predicted (represent here the insulin sensitivity here) and X is the predictor variable (represent here as gene expression).
- $\beta_1,$ is the slop, also known as the coefficient of the predictor variable, telling the expected change in insulin sensitivity for a one-unit change in the gene expression level. In another word it is the correlation (Cor) between the insulin sensitive and gene expression level multiply by the ratio of standard deviation (SD) of the insulin sensitive and gene expression level.

$$\widehat{\beta_1} = Cor(Y, X) * \frac{SD(Y)}{SD(X)} \tag{14}$$

- $\beta_0,$ is the intercept representing the expected value of insulin sensitivity when the expression level of a gene is zero, and often, this is less interesting because studying gene expression levels closer to zero may not correlate with insulin sensitivity or anything biologically interesting.

$$\widehat{\beta_0} = mean(Y) - \hat{\beta}_1 * mean(X) \tag{15}$$

- The error term ϵ in equation 9 describes variability in the insulin sensitivity not explained by the linear relationship.

Furthermore, we expanded the formula to multivariate with covariates adjustment feature as below.

$$\widehat{Y} = \widehat{\beta_0} + \widehat{\beta_1}\, X_1 \; + \; \widehat{\beta_2}\, X_2 + \cdots + \; \widehat{\beta_n}\, X_n \; + \; \widehat{\beta_{bmi}}\, bmi \; + \epsilon \tag{16}$$

4.2.3.8. Pathway enrichment analysis

Pathway enrichment analysis was used to understand the underlying biological processes that differentially expressed genes between tissues or within the same tissue of different groups, genes associated with insulin sensitivity via regression and correlation analysis is overrepresented in biological pathways. The statistical approach, Over Representation Analysis (ORA), is used to identify significantly enriched genes in the pathway through a hypergeometric distribution test also called fisher exact test[189]. Pathways used in this analysis were from the molecular signatures database(MSigDB)[190] collation C2 and H. Pathways are predefined based on the gene sets involved in the same biological processes. Mathematically hypergeometric distribution test was expressed as follows[189]:

$$p \; = \; 1 - \sum_{i=0}^{k-1} \frac{\binom{M}{i}\binom{N-M}{n-i}}{\binom{N}{n}} \tag{17}$$

Where:

- **N** is the total number of genes in the background distribution could be all gene detected in the experiment or all genes annotated in the pathways,
- **M** is the number of genes within that distribution that are annotated to the gene set of interest (how many of the differently expressed genes or genes correlated to our phenotype-insulin sensitivity are overlapping to the background genes),
- **n** is the size of the list of genes of interest and **k** is the number of genes within that list which are annotated to the gene set.

One major caveat of the ORA approach is that it finds the enrichment of genes in the pathways when the size of genes we want to enrich in the pathway is large and fails when the size is small. Thus, gene set enrichment analysis (GSEA) was used when necessary to complement the ORA approach[191]. In GSEA, all genes were ranked by a numeric parameter (log fold change or by regression or correlation coefficient) to identify if pathway genes(S) overlap among sorted gene lists(L) when walking from the top to the bottom. In the GSEA, there are two major statistical tests should be performed. First, determine the enrichment score by a running sum statistic to increase when a gene in **S** is enriched in **L** while walking down from the top in **L** and decreases otherwise. The magnitude of the increase or decrease in the enrichment score depends on the gene ranking parameter, such as fold change or regression coefficients, as stated in the Kolmogorov-Smirnov statistic.

(192). Second, estimating the significance level of the enrichment score using an empirical phenotype-based permutation test that preserves the complex correlation structure of the gene expression data(191). The R package clusterProfiler(193) was used for all kind of pathway enrichment analysis, which is widely utilized for exploring functional characteristics of genomic data across various species. The tool is known for its comprehensive gene annotation, making it a popular choice for this type of analysis.

4.2.3.10. Cross tissue communication analysis

To analyze cross-tissue communication between IMAT and muscle with the aim that signaling proteins putatively interact with the signal-receiving proteins to trigger intracellular signaling and influence gene expression in the target tissue was based on a manually curated list of interacting proteins. First, we manually curate a comprehensive sender-receiver database that considers the known putative interactions of ligand-receptor, extracellular matrix proteins, and adhesion interactions. Then, we did statistical tests between IMAT and muscle gene expression, described in the follow-up sections. Then, we integrated them with the sender-receiver database to filter the possible sender-receiver pairs that derive the communication between the tissues.

4.2.3.10.1. Sender-receiver reference network

We curated a comprehensive sender-receiver database to infer the physical interaction between 1201 unique protein-coding sender genes and 1261 protein-coding receiver genes through extensive databases search at NCBI(194), KEGG(195), GO(196), Uniport(197), Guide to Pharmacology(198), Cell-Cell interaction database(199), CellChat(200), CellPhoneDB(163),CellTalkDB(164),iTalk(201),OmniPath(202),Omniextra(162),NicheNet(155),Adhesome(203),Cellinker(204),ICELLNET(205),Liana(206),LRdb (168), NATMI(207), Ramilowski-pairs (208) and text mining. IntACT(209),BioGRID(210) and String(211) databases were used to verify the sender-receiver interaction network. Interaction data base is essential to appreciate mechanistic models driving pathway and transcriptional activity from transcriptomics and graph-based analysis methods(162). Then a consensus annotation score was calculated by assigning a score of either 0 or 1 to each pair to indicate whether two or more databases support the interaction evidence between sender and receiver. As a result, 4,769 pairs of genes involving 974 sender genes and 881 receiver genes supported by 25% of the database were identified. Protein coding genes with the potential function of secretion and transmission of information such as growth factor, cytokine, immune checkpoint, neuropeptides, secreted extracellular matrix, adhesion proteins, endocrine glycoproteins, and secreted surface proteins to the target cell defined as sender genes. In addition, receiver genes were defined as protein-coding genes such as G protein-coupled receptors (GPCRs), nuclear receptors, surface proteins, catalytic proteins, transporter proteins, and adhesion proteins with the function of receiving and

transducing the incoming stimuli. Finally, we summarize the class and superclass of each sender gene and receiver gene after their function and chemical nature using KEEG(195), GO(196), Uniport(197) and NCBI(194) literatures. Therefore, senders were labeled into six class as cytokines, growth factors, neuropeptides, Junctional, secreted, and predicted-ligand (for proteins we could not find literature reference or have more than one functional annotation) proteins. Class for receivers were GPCRs, Enzyme-linked receptors (receptor for insulin, various growth factors, and immune responses), Adhesion and other receptors (ion channels, nuclear hormone receptors, and intracellular enzyme linked receptors) proteins.
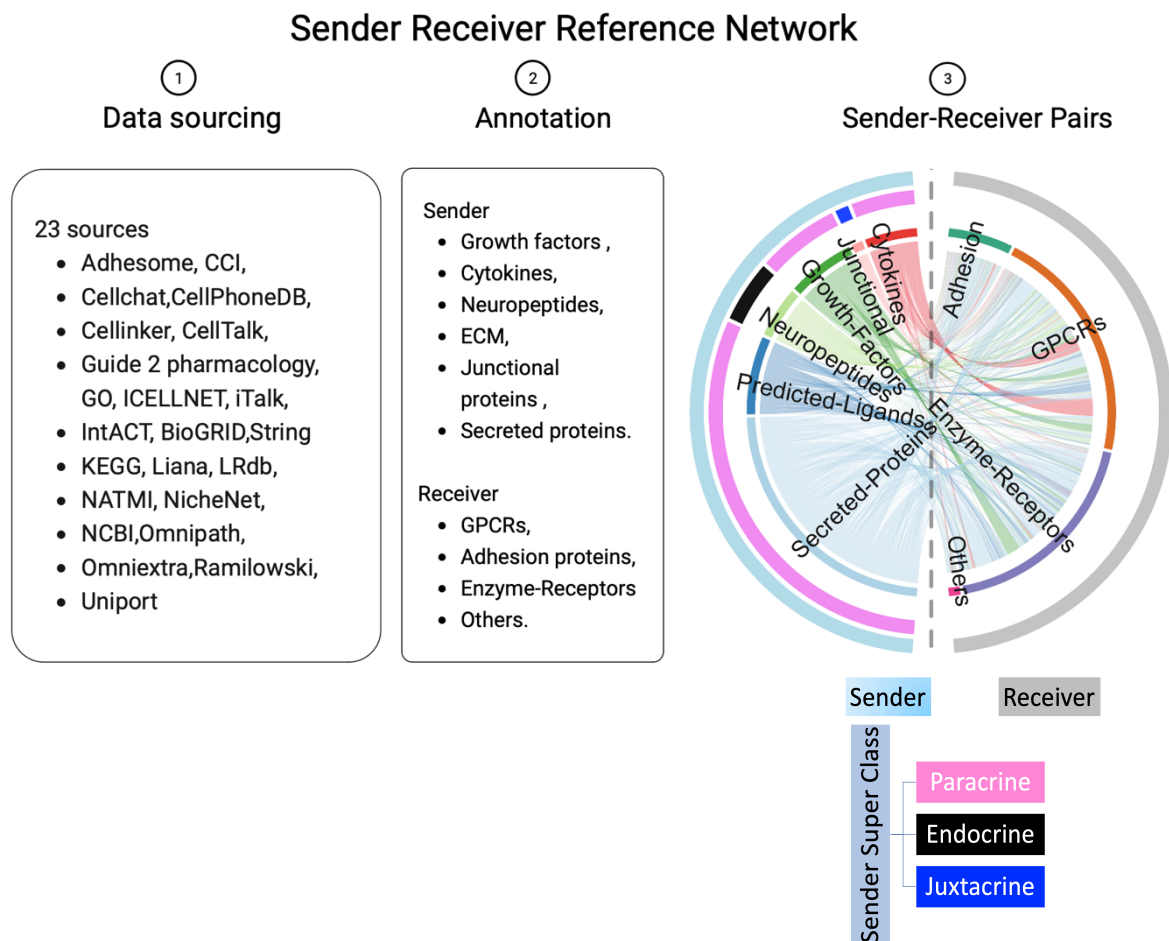
Figure 9.Sender receiver data base (intercellular communication reference network) made based on prior knowledge from published literatures and publicly available database. Sender coding genes here represent a signaling molecules and classified in to six main class and 3 super class based on their function and chemical nature. Whereas receiver coding genes representing molecules potentially responds for the incoming stimulus and able to transduces to others. Although not indicated here, GPCRs, Enzyme-linked receptors, and Ion channels could be mapped to a superclass called cell surface receptors. Nuclear and intracellular enzyme-linked receptors as intracellular receptors, and adhesion receptors as Junctional.

4.2.3.10.2. Crosstalk between IMAT and muscle scored by cross-tissue correlation.

IMAT and muscle expression levels are used as input to infer the cross-communication between the tissues. First, we applied cross-tissue gene correlation approach to understand the communication between the tissues. Cross-tissue gene correlation analysis is a method used to examine the relationships between gene expression patterns across different tissues or cell types within an organism. This approach helps identify co-expressed genes (i.e., their expression levels change similarly) across multiple tissues, providing insights into potential functional relationships and shared regulatory mechanisms (212, 213, 214). Furthermore, this analysis was motivated by the hypothesis that co-expressed (cross-correlated) sender-receiver pairs could regulate tissue communication(156). Cross tissue gene correlation was computed using a function **cor.test** in base R where x and y parameter takes the expression matrix of IMAT and muscle respectively. Mathematically expression for this analysis is described in equation 11. Then, significantly correlated gene pairs were integrated with the sender-receiver database to filter sender-receiver pairs systematically and analyzed logically from network biology and insulin sensitivity/insulin resistance perspective. Thus, the analysis was done to each group where the total number of samples (combined IMAT and muscle) used in LC was 16, and for ATH, OB, and T2D were 12, 20 and 12, respectively. Also, since each IMAT and muscle sample are taken from the same patient, both expression data tables had similar sample IDs and size. We used R packages igraph(215), RCyt3(216) and Cytoscape software (217) to analyze network statistics and visualizing it. To further characterize the talk, the communication network was classified as IMAT to muscle network (IMCN) when IMAT acts as signaling and muscle as target tissue, and muscle to IMAT network (MICN) when the other way round is happening. Thus, we were able to determine the overall edges (connectivity between genes), nodes (all genes), influential out-degree nodes (nodes that disseminate information to many recipient nodes), and influential in-degree nodes (nodes that absorb information from many source nodes) in the network. We compared these network statistics in all groups to understand shared and unique nodes as insulin resistance advances from an active-sedentary lifestyle to an Obese-T2D state. Furthermore, all individual communication networks, encompassing ATH, LC, OB, and T2D networks, were integrated to explore inter-tissue communication dynamics within the landscape of progressive insulin resistance (to detect alterations or rewiring rates). The detailed explanation of this method will be provided in subsequent sections of this thesis. Lastly, based on all the above analysis, a list of candidate genes was generated and summarized in a table with information about their function, mean normalized expression levels across groups, correlation to insulin sensitivity (GIR), degree and rewiring rate.

4.2.3.10.3. Crosstalk between IMAT and muscle scored by differential combination.

In this approach, we employed DEA, as described in equation 7, to understand crosstalk communications between IMAT and muscle samples. The primary objective of this approach was to identify genes acting as "DE-senders" and "DE-receivers" (differentially expressed sender and receiver genes). The rationale behind this model rests on the premise that if a sender gene in the signaling tissue (IMAT) is DE and its corresponding receiver gene in the receiving tissue (muscle) is also DE, it strongly suggests a likelihood of communication occurring through their protein products (156). To establish these sender-receiver pairs, we combined the DE-sender genes identified in IMAT with the DE-receiver genes identified in muscle, using the curated reference database. This allowed us to infer the putative signaling process from IMAT to muscle tissue. Conversely, when investigating the signaling process from muscle to IMAT, we combined the DE-sender genes identified in muscle with the DE-receiver genes in IMAT to unravel the sender-receiver relationships for this direction of communication. It's worth noting that the concept of DE-based cell-cell communication scoring has become increasingly prevalent with the advent of single-cell sequencing technologies. For example, the most popular tools, CellChat(218) and Nichenet(155) utilize DEA and other statistical methodologies to dissect cell communication networks. Therefore, we conducted this analysis for all groups and subsequently, a comprehensive comparison of the edges and nodes was carried out across these groups. This comparative analysis aimed to reveal the shared, lost, gained, hub, and rewired nodes and edges as the progression of insulin resistance unfolds.

4.2.3.10.4. Rewiring analysis via DyNet

To explore the dynamics of the integrated networks, a rewiring analysis using DyNet(219) was used. Rewiring in graph theory generally refers to a change in the connectivity of a node in different networks(219, 220). The rewiring process could involve adding new connections, removing existing connections or modifying the strengths of existing connections(221), thus impacting the overall structure and function of a network, and can be used to study how changes to a network's connectivity can affect its behaviour(222). This could be an excellent model to answer questions like how condition difference changes the molecular composition and connectivity between interacting proteins to gain insights into the underlying mechanisms of complex biological systems(222, 223, 224, 225). In the DyNet application(219), two or more network files representing different conditions or time points could be imported to describe a dynamic network. Then, it makes a pairwise comparison and produces a summary statistic of node/edge rewiring when the networks are only two; otherwise, for more than two networks, it applies a distance-based rewiring score to compute the variance between each node's connectivity between networks. A dynamic network is modeled as a weighted node adjacency matrix. This representation is

extended into a third dimension, denoted as S, to encompass the state space, thus forming the framework M (P, Q, S) commonly known as three-dimensional Euclidean space. M stands for adjacency matrix, P and Q for rows and columns of the matrix, respectively, whereas S stands for state or condition. For every node (xi) present in each network (si), the Euclidean distance between that node and a centroid (c) was calculated. The centroid is determined as the geometric mean of a node computed across all networks. Subsequently, the sum of the calculated distances for each node in the various networks is divided by the total number of networks (N). This division by (N - 1) serves to normalize the results. The mathematical expression could be summarized as below(219).

$$D_n - score = \frac{\sum_{i=1}^{N} d(x_i, c)}{N - 1} \tag{18}$$

Therefore, the node gets a higher rewiring score when most of its neighborhoods are different i.e., when the neighborhoods of the given node are representing the different networks state. Dynet assigns a zero value when a node has no connection and 1 when it does. Consequently, group-specific nodes in the combined network become group-specific networks; however, in the other groups(networks), as edgeless nodes. Therefore, a group-specific node exhibiting a high centrality (degree centrality) may receive a higher rewiring score. In this senior, the score should indicate group-specific rewiring, as a rewired node should no longer be considered group-specific.

4.2.3.10.5. Crosstalk between IMAT and muscle weighted by insulin sensitivity.

In this approach, we employed a novel method using correlation analysis, as elucidated in equation 11, to discern communication between IMAT and muscle by assigning an insulin sensitivity attribute to every node in the crosstalk communication network. This allows us to represent a dynamic network (network reflects insulin sensitivity and resistance) in a continuous measure. This would enable us to catch the dynamic changes between IMAT and muscle crosstalk communication during insulin resistance progression. First, additional filtering was done from the processed transcriptome (11828 genes) to remove genes showing similar expression patterns across samples. The filtering was performed tissue-wise by taking the 10th percentile values from the quantile distribution. Subsequently, only genes with expression levels above the 10th percentile in each sample were retained for crosstalk communication analysis. Next, we correlate each gene within the IMAT and muscle with the clinical variable GIR respectively. This initial step allowed us to establish the strength and directionality of the relationship between gene expression and insulin sensitivity for IMAT and muscle tissues respectively. Third, the IMAT and muscle insulin sensitivity correlation vectors were integrated with the curated reference database. This enabled us to identify specific sender-receiver pairs for the IMAT-to-muscle (IM) and muscle-to-IMAT(MI) communication networks. This selective filtering process ensured that

only relevant signaling relationships were included in our analysis. In the fourth step, edge information connecting the sender and receiver gene was investigated to explore condition-specific networks and their functions. Therefore, the edge was weighted by adding the correlation coefficient obtained for each sender and receiver gene and could classify the network as a positive network when the insulin sensitivity attributes of both nodes were positive. A negative network was defined when the interacting nodes had negative insulin sensitivity attributes. Based on the above information, when the edge is positive, that specific network is referred to as insulin sensitive network, and when it is negative referred to as an insulin resistance network. Lastly, for each network, the number of nodes(genes), edges(connectivity) and associated network statistics was quantified. Moreover, pathway enrichment analysis was done to link the genes with their biological functions.

4.2.3.10.6. Network clustering and community detection

Network clustering or community detection was performed to identify functionally different modules for IMCN and MICN respectively. A Cytoscape application called GLay was used for both community analysis and the layout of graphs(226). It automatically transforms the input network into a simplified model by eliminating edge direction information, redundant connections, and self-referential loops. The interconnected cluster within the network is recognized by calculating edge betweenness score, a concept introduced in a notable paper by Newman and Girvan in 2004(227). Edge betweenness score involves calculating the shortest paths passing through each edge and identifying the edge with the highest betweenness score. This edge is crucial for maintaining network connectivity and is likely to be a bridge between different communities. Then, it removes the identified edge from the network and re-computes the edge betweenness scores for the remaining edges. The process repeats until the edges' removal leads to the network being split into distinct communities or until a predefined number of communities is reached. For each network cluster, the number of genes tissue-wise was summarized, and pathway enrichment analysis was done to link cluster genes to function.

4.2.3.10.7. Rewiring analysis based on the variance of neighborhoods.

Here we employed a new method to understand the rewiring rate of a gene in the IMAT muscle cross talk communication network. This model aims to identify a gene of interest, often referred to as the central gene (CG) in the network. This gene plays a fundamental role in communicating(interacting) with its neighbouring genes (NG), which can exhibit a diverse range of insulin sensitivity attributes. The analysis first calculates the variance of a node also referred to as the central node (CN) from the numeric attributes of neighborhood nodes (NNs). The variability of the NNs provides information about the variation among the NNs in terms of insulin sensitivity and how much this variation would imply for the CN to differ from its NNs. Higher variance of a CN could indicate higher variability in the

neighbourhoods and may tell that the neighbourhoods have higher impact on the variance/change of the CN. Variance of the CN could be expressed mathematically as below.

$$V_i = \frac{\sum_{i=1}^{n}(x_i - \overline{X})}{N - 1} \tag{19}$$

Where:

- V_i is the variance of a node (CN),
- x_i is NN insulin sensitivity attribute value,
- X-bar is arithmetic mean of all neighborhood node insulin sensitivity attribute value.
- N stands for the total number of nodes in the network

However, an additional metric called the node rewiring score (R-score) was devised by multiplying the variance of the node (as per equation 19) by its degree and then dividing it by the absolute insulin sensitivity value of the node. The rewiring score takes two critical factors into consideration. First and foremost, degree of the node. because we want to highlight Hub nodes in our scoring due to their potential roles in regulating a wide range of biological processes or propagating the effect of a perturbation. This emphasis is set on identifying hub nodes in our scoring process, as they have a crucial role in regulating various biological processes or spreading the effects of perturbations(means the rewiring of a hub gene can result in concurrent rewiring of numerous edges and, probabilistically, can impact various cellular processes) (222, 228). Secondly, we include the absolute insulin sensitivity value of the node in the calculation. This inclusion ensures that our rewiring scoring remains unbiased by adjusting the relationship between the neighboring nodes and the central node. Subsequently, the top rewired nodes were identified by taking those at the 90th percentile within the quantile distribution.

This score is calculated using the formula:

$$R_{i-score} = V_i * \left(\frac{deg\left(c_{i-degree}\right)}{|c_{i-gir} + 1|} \right) \tag{20}$$

Where:

- $R_{i-score}$ is the rewiring score,
- V_i is the variance of a node determined from its neighborhood nodes,
- $c_{i-degree}$ is degree of the node.
- $|c_{i-gir} + 1|$ is represents the absolute insulin sensitivity attribute value of the node.

4.2.3.10.8. Jaccard similarity index identify strongly connected rewiring nodes.

The Jaccard similarity index (JSI) is a widely used method to quantify the similarity between two sets by measuring the ratio of the size of their intersection to the size of their union. In the context of networks, it is employed to identify strongly connected nodes or nodes that share common neighbors and exhibit similar connectivity patterns. For example, it helps identify functionally related genes or proteins that participate in similar pathways or processes in biological networks. The index ranges from 0 to 1, with 0 indicating no common elements between sets and 1 indicating complete overlap. A function called **similarity** in R package(igraph) was used to calculate the JSI of the subnetwork created based on the top rewired nodes along their NNs. Then, the relationship between rewired nodes in the network was examined, and nodes that showed similar scores were filtered for further characterization of their insulin sensitivity, interaction, and pathways they involved.

4.2.3.11. Data visualization

The data visualization methods employed in this study were crucial for comprehending complex biological data, such as gene expression profiles and network interactions. Therefore, R packages ComplexHeatmap and pheatmap were used for gene expression data visualization. For network visualization, both Cytoscape and igraph were used. R packages such as ggplot2, ggpubr, ggplotify, plotly, and Base R graphics (see table 4.1) were used to generate various plot types like histograms, scatter plots, and bar charts.

5. Results

5.1. Decreased insulin sensitivity observed among T2D and OB study subjects.

The clinical profiles of the study subjects were reviewed to gain insights into the insulin sensitivity and metabolic parameters across different groups. As presented in Figure 10, the results reveal a significant trend: insulin sensitivity, as quantified by the GIR, exhibited a linear decrease from the ATH group to the T2D group. This pattern, confirmed by ANOVA testing, emphasizes significant variability in insulin sensitivity among these groups. Notably, when comparing the mean GIR values of ATH, OB, and T2D groups to the LC group, statistically significant differences ($p < 0.05$) were observed. This finding suggests the presence of insulin resistance in metabolically active organs, particularly skeletal muscle, within the OB and T2D groups. The reduced GIR values in these groups indicate a diminished response to insulin, signifying an impairment in glucose uptake and utilization. Moreover, our analysis revealed distinct differences in FPG and PPG levels, particularly in the T2D group, where these levels were significantly different ($p < 0.0001$) compared to LC. Additionally, the OB and ATH groups did not exhibit significant differences in FPG and PPG levels compared to LC. These findings indicate T2D group had liver insulin resistance. Liver insulin resistance often leads to increased hepatic glucose production and elevated fasting glucose levels. In terms of body composition, BMI and body FM were significantly different ($p < 0.0001$) in the T2D and OB groups compared to LC. In contrast, the ATH group did not exhibit significant differences in BMI and body FM compared to LC. These differences highlight the impact of adiposity on insulin sensitivity, with elevated BMI and body FM associated with decreased insulin sensitivity (Figure 11). Besides, we observed sex-related differences in body composition, with significant variations in body FM and FFM between males and females. These distinctions highlight the role of gender in influencing body composition. However, there were no differences in FPG, PPG, BMI, and age.
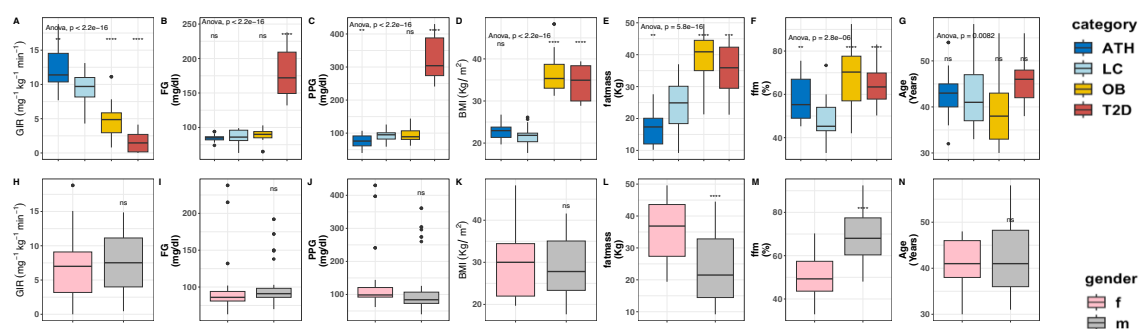
Figure 10.Boxplot for comparing each clinical variable distribution between participants' categories and sexes. One-way ANOVA to see differences across groups, t-test for difference between each group against LC. Key *: p <= 0.05, **: p, <0.01, ***: p <0.001

Pairwise correlation analysis between clinical variables found a negative correlation between the GIR and key metabolic parameters, FG, PPG, BMI, FM, and FFM. This negative correlation suggests that these variables tend to increase as GIR decreases, indicating a strong association between low GIR and insulin resistance (Figure 11). This finding aligns with the widely accepted notion that reduced insulin sensitivity is a fundamental characteristic of insulin resistance. Importantly, our study highlights GIR as a robust measure for predicting insulin resistance, emphasizing its clinical significance in assessing metabolic health. Furthermore, our correlation analysis revealed positive associations among key anthropometric variables, specifically FM, FFM, and BMI. This positive correlation suggests that individuals with higher FM tend to have higher FFM and BMI and highlights the intricate relationship between body composition and metabolic outcomes.
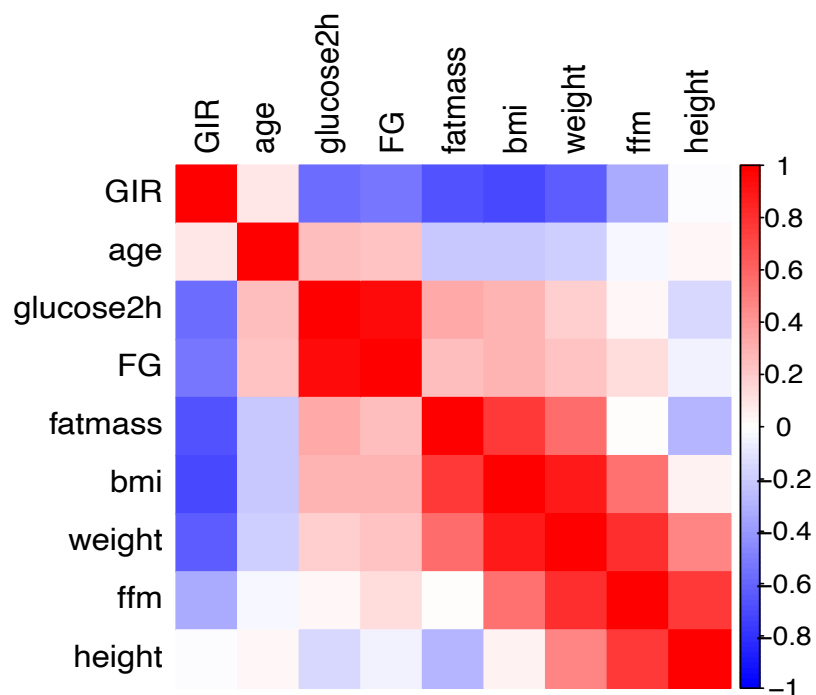
Figure 11.Pairwise correlation heatmap to depict the relationships between clinical variables. The intensity of color represents the strength of Pearson correlation coefficient and the value range between -1 and 1. Red indicates positive correlations and blue shows negative correlations.

5.2. Muscle and IMAT have distinct gene expression pattern.

A comprehensive transcriptome analysis across all study groups yielded a dataset consisting of 21,185 transcriptomes. Through a rigorous preprocessing step, 11,828 genes were identified for downstream analyses. Hierarchical clustering and Principal Component Analysis (PCA), powerful techniques for visualizing and understanding complex gene expression data, revealed different gene expression patterns between IMAT and muscle, suggesting that both tissues are regulated differently (Figure 12A and B). Additionally, we observed four distinct clusters within the IMAT expression patterns, indicating IMAT may not be a homogenous tissue but could encompass four different molecular subtypes, each characterized by unique gene expression profiles (Supplemental Figure 1).
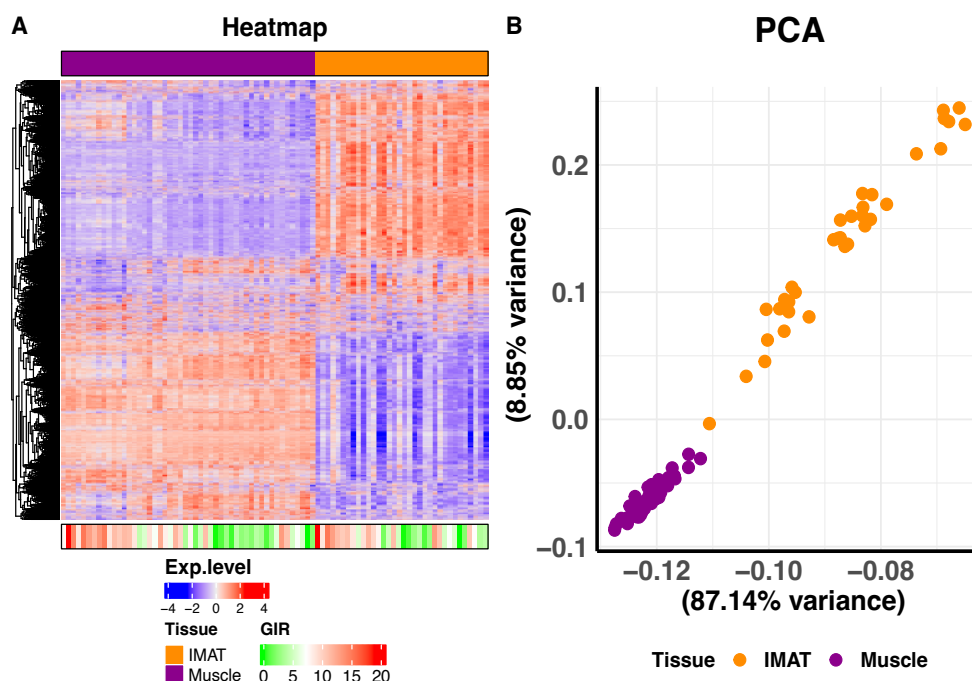
Figure 12.Heatmap and PCA plots. mRNA expression level of IMAT and skeletal muscle samples and how this expression level relates with GIR (A). Additionally, the PCA plot(B) demonstrated that muscle gene expression is different from the IMAT expression.

5.3. IMAT reveals higher DE genes in T2D people compared to the LC group.

IMAT gene expression shows relatively higher DE genes in the context of T2D compared to LC. The total number of DE genes in T2D was 47 out of 11828 preprocessed genes (Figure 13A). This finding suggests that T2D significantly impacts the gene expression of IMAT and may eventually affect the skeletal muscle tissue through crosstalk communication. Interestingly, we did not find DE genes when comparing OB versus LC, ATH versus LC, or T2D versus OB. Further analysis of the DE genes in the context of T2D revealed their functional relevance to critical metabolic pathways. These pathways included carbohydrate, fatty-acid, and amino-acid metabolic pathways. Notably, the genes within these metabolic pathways were predominantly dysregulated and may lead to abnormalities in metabolism (Figure 13B and C). Additionally, the enrichment analysis revealed that insulin, adipocytokine, and PPAR signaling pathways were among the most relevant pathways enriched in the GSEA. Importantly, in these pathways, we observed a consistent pattern of downregulation of genes (Figure 13C). This downregulation may indicate potential disruptions in key metabolic processes associated with T2D, warranting further investigation. In contrast, when examining the skeletal muscle tissue of ATH individuals, we observed a more variable gene expression profile compared to the other groups under consideration. In the ATH group, 121 genes displayed differential expression among the total 11,828 genes examined. This variability suggests that gene regulation within the muscle tissue of ATH individuals is significant and may be influenced by factors related to their athletic training and performance. Conversely, in the OB and T2D groups, when individually compared to the LC group, we identified 48 and 31 DE genes, respectively. These findings suggest that the degree of gene regulation within the muscle tissue of OB and T2D individuals is relatively decreased when compared to lean controls (Supplemental Figure 2).
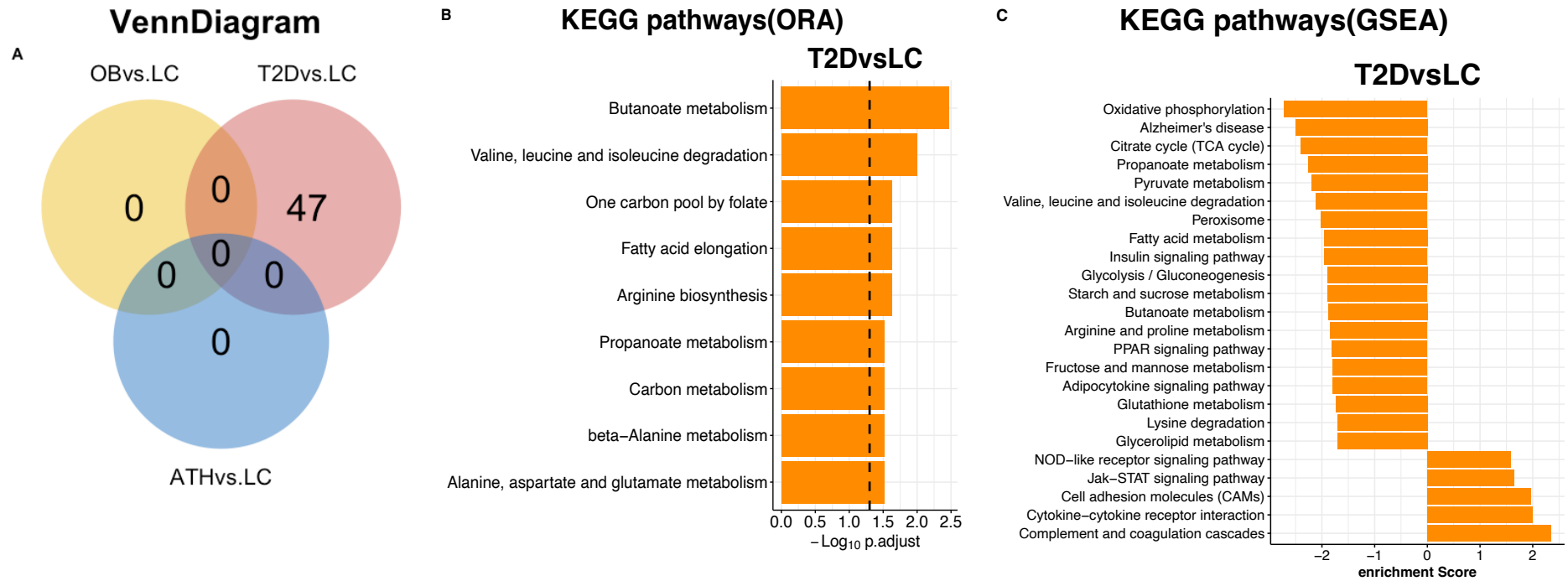
Figure 13.Number of DE genes and pathway enrichment analysis (FDR <0.05). Venn-diagram to indicate the number of DE genes in each group compared to the LC group (A). Bar plot to indicate KEGG pathways enriched for DE genes in T2D based on over representation analysis(ORA)(B). KEGG pathways based gene set enrichment analysis(GSEA) where all the genes in T2D are ranked by log fold change(log2FC) compared to LC expression and checked whether KEGG pathway genes overrepresented in the top or bottom of the ranked list (C).

5.4. Linking IMAT and muscle genes to insulin sensitivity.

The volcano and the histogram plot depict the relationship between gene expression in the muscle or IMAT and insulin sensitivity when BMI is adjusted as a covariate. In this analysis most muscle genes correlate to insulin sensitivity (Figure 14). These genes are involved in several crucial metabolic pathways, such as glycolysis, pyruvate metabolism, the citrate cycle, and oxidative phosphorylation, suggesting a strong link between energy metabolism and insulin sensitivity in muscle tissue. Furthermore, signaling pathways related to cytokine-cytokine receptor interaction and extracellular matrix (ECM)-receptor interaction were positively enriched in the muscle tissue. This implies that immune response and cell-matrix interactions may regulate insulin sensitivity in the muscle (Figure 15). In the IMAT, our analysis revealed a set of top-ranked genes demonstrated positive enrichment in specific KEGG pathways, such as Phenylalanine metabolism and Butanoate metabolism. Additionally, branched-chain amino acid (BCAA) degradation pathways were observed, indicating a connection between BCAA metabolism and insulin sensitivity in IMAT. However, when BMI is no longer adjusted for insulin sensitivity, our analysis in IMAT revealed a broader range of metabolic and signaling pathways positively associated with insulin sensitivity. For instance, insulin signaling pathways, PPAR signaling pathways, mTOR signaling pathways, peroxisome metabolism, fatty acid metabolism, propanoate metabolism, pyruvate metabolism, oxidative phosphorylation, and the Citrate cycle were among the top metabolic pathway hits in IMAT. Additionally, it was important that inflammatory pathways, including NOD-like receptor signaling, complement and coagulation cascades, B and T cell receptor signaling, and Chemokine signaling pathways, were found to be negatively correlated with insulin sensitivity in IMAT (Supplemental Figure 3).

Volcano and histogram plots
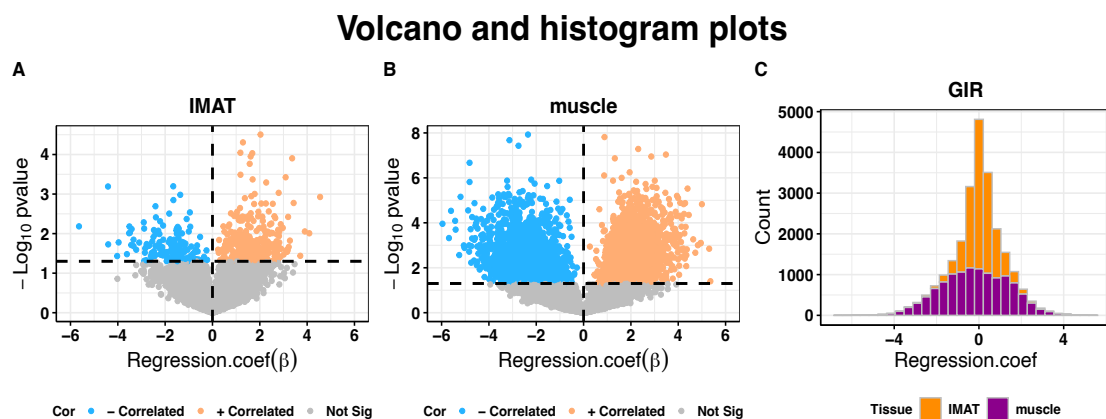
Figure 14. Volcano plot showing the regression coefficient of gene expression and insulin sensitivity in the IMAT(A) and muscle(B). Positively correlated genes are indicated in orange, while the light blue are the negatively correlated ones. Histogram plot showing the distribution of regression coefficient in IMAT and muscle.

KEGG pathways(GSEA)
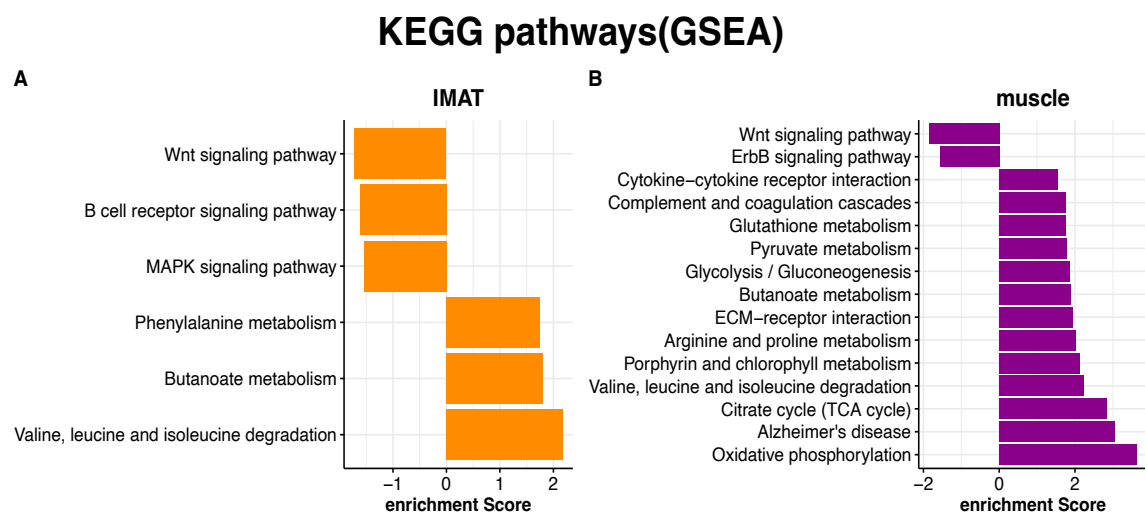
Figure 15. KEGG gene set enrichment analysis. Genes were ranked based on the regression coefficient they have with GIR. These pathways were significantly (FDR <0.05) enriched for the ranked genes in the IMAT(A) and muscle(B).

5.5. Cross-tissue gene correlation analysis demonstrate an increased molecular crosstalk communication from IMAT to muscle (IMCN) during insulin resistance.

We combined group specific expression data with the sender-receiver reference database to analyze the change in molecular crosstalk communication between IMAT and muscle in progressive insulin resistance. Using cross-tissue gene correlation analysis, the total number of significantly correlated pairs implying IMAT to muscle connections supported by our reference database in ATH, LC, OB, and T2D, were 65, 76, 82, and 94, respectively. In

53

addition, the number of genes in each network was 106,112,130,131, respectively. The size of OB or T2D network was higher compared to the ATH or LC indicating IMAT to muscle connectivity increased as insulin resistance advances. In addition, a minimal network size difference was observed between LC and ATH as well as between OB and T2D, while the identity of the network was different (Figure 16A and C and D). Overall, there was a substantial variation in connectivity and gene identity between and across groups. Furthermore, for group-specific genes in the network, we looked at the KEGG pathways to get a deeper understanding of the functions of those genes. Therefore, T2D-specific genes were enriched in more specific KEGG pathways associated with tissue damage and injury, such as complement and coagulation, leukocyte trans-endothelial migration, TGF-beta signaling, and cytoskeleton regulation pathways. Moreover, ECM-receptor interactions and focal adhesion pathways were over-presented in OB and T2D groups, suggesting matrix degradation, cell migration and loss of structural connectivity between cells as insulin resistance advance. Interestingly we did not see any KEGG pathway enrichments for ATH specific genes in the network.
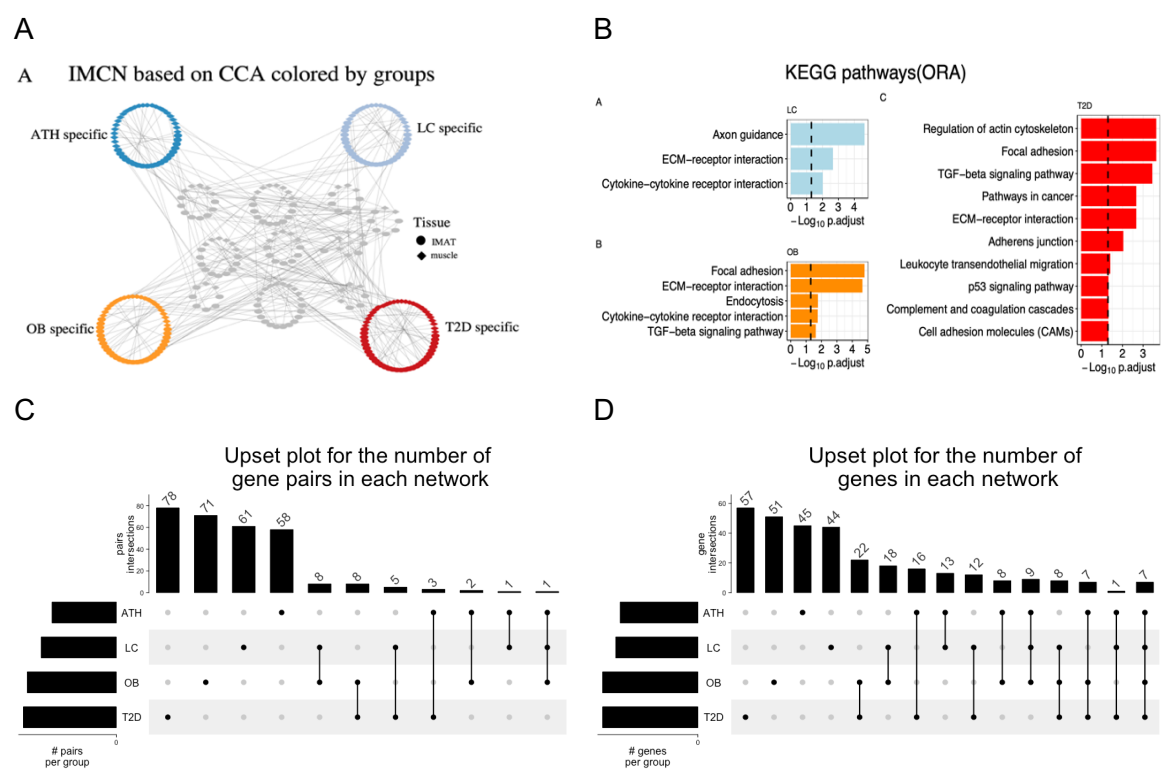
Figure 16.IMAT-muscle cross-correlations indicate increased molecular interactions as insulin resistance advances IMCN. In A, different colors indicate group-specific and shared interaction networks where each node in the network is representing a gene and the connection between nodes could be edge; in B, different colors indicate KEGG pathways significantly enriched (FDR < 0.05) for genes specific to each group. Upset plots to show the number of shared and unique interaction pairs(C) and genes(D) in the communication networks.

Moreover, we combined all the networks using the Dynet application in the cystoscope to determine the degree and rewiring rate of genes. The combined network of all conditions colored by the rewiring scores is illustrated in Figure 17A, where we did see a linear relationship between the degree and rewiring score of the genes (Figure 18A). This indicates hub genes in the network were changing due to condition changes. The subnetwork in figure 17B displays the top rewired genes (ITGB3, EGFR, ITGA10, CALM3, ITGAV, WNT5A, and ITGB1) in all IMAT to muscle communication networks under investigation. In the LC network, ITGB3 was found to interact with three IMAT genes: TGFB3, CX3CL1, and ADAM15. However, during the OB condition, ITGB3 exhibited changes in its interactions. Notably, it lost connections with TGFB3 and ADAM15 but formed new interactions with IGF2, COL1A2, NID1, FBN1, and TNXB. Furthermore, in the context of T2D, ITGB3 displayed an increased number of new connections with IMAT genes, including ITGB3BP, MFG38, and FGF1. Simultaneously, it lost connections with COL1A2, NID1, FBN1, and TNXB. Interestingly, in the ATH group, ITGB3 lost its interactions observed in the OB and T2D conditions but retained connections with IGF2 and TGFB3. Additionally, it established a new relationship with IL32. This demonstrates ITGB3 (the top rewired gene here) showing connectivity differences in different networks and may transduce different molecular signals to the target tissue to influence downstream activities in response to condition changes.
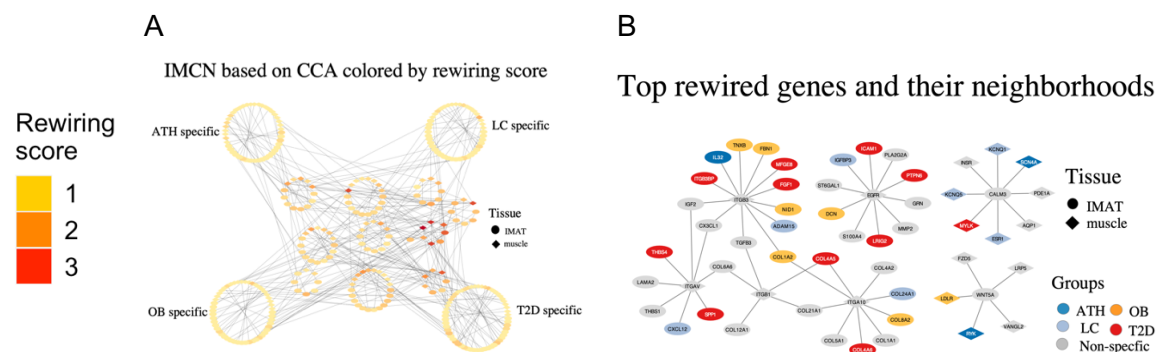
Figure 17.IMAT to muscle full communication network based on cross-tissue gene correlation analysis. Network colored by the rewiring score(A), where the reddest indicates a strong rewiring rate. The second network(B) is between the top-selected rewired genes in all groups and their interacting partners(neighborhoods). The neighborhoods of the rewired genes in the subnetwork are colored differently to designate group or condition-specific genes from shared ones. Thus, the neighborhood in grey denotes genes shared by two or more groups.

ITGB3, EGFR, ITGA10, ITGAV and ITGB1 are muscle-specific, and their expression level, as indicated in the heatmap, was low in all muscle samples compared to IMAT. CALM3 and WNT5A are IMAT specific, and their expression level across all IMAT samples was low compared to muscle (Figure 18 D).

Figure 18.Describing the rewiring rate of genes in the cross-tissue gene correlation network. The scatter plot(A) indicates the relationships between degree and rewiring scores in the cross-tissue gene correlation analysis. Boxplot(B) of gene rewiring scores in different networks, categorized by tissue. These genes in the networks were group specific or shared in two or more groups. The bar plot(C) displays the top rewired genes, and the heatmap (D) illustrates expression levels of rewired genes in IMAT and muscle across all groups.

5.6. The rewiring rate of genes in progressive insulin resistance remains unchanged based on DE analysis.

Using the reference database, upregulated IMAT sender genes were combined with their cognate upregulated muscle receiver genes to establish sender-receiver interaction from IMAT to muscle (Figure 19A). Among the four groups, the OB group demonstrated more inter-tissue connectivity and more genes involved in the interaction. Therefore, in OB, T2D, LC and ATH, the network size was 151, 128, 124 and 84, respectively, and the number of genes involved in the network was 154, 137, 126 and 95, respectively. Overall, 63 pairs involving 79 genes were common to all groups. In addition, 41 pairs from 34 genes overlapped between T2D, OB and LC and seven pairs involving three genes were shared among OB, LC and T2D (Figure 19C and D).
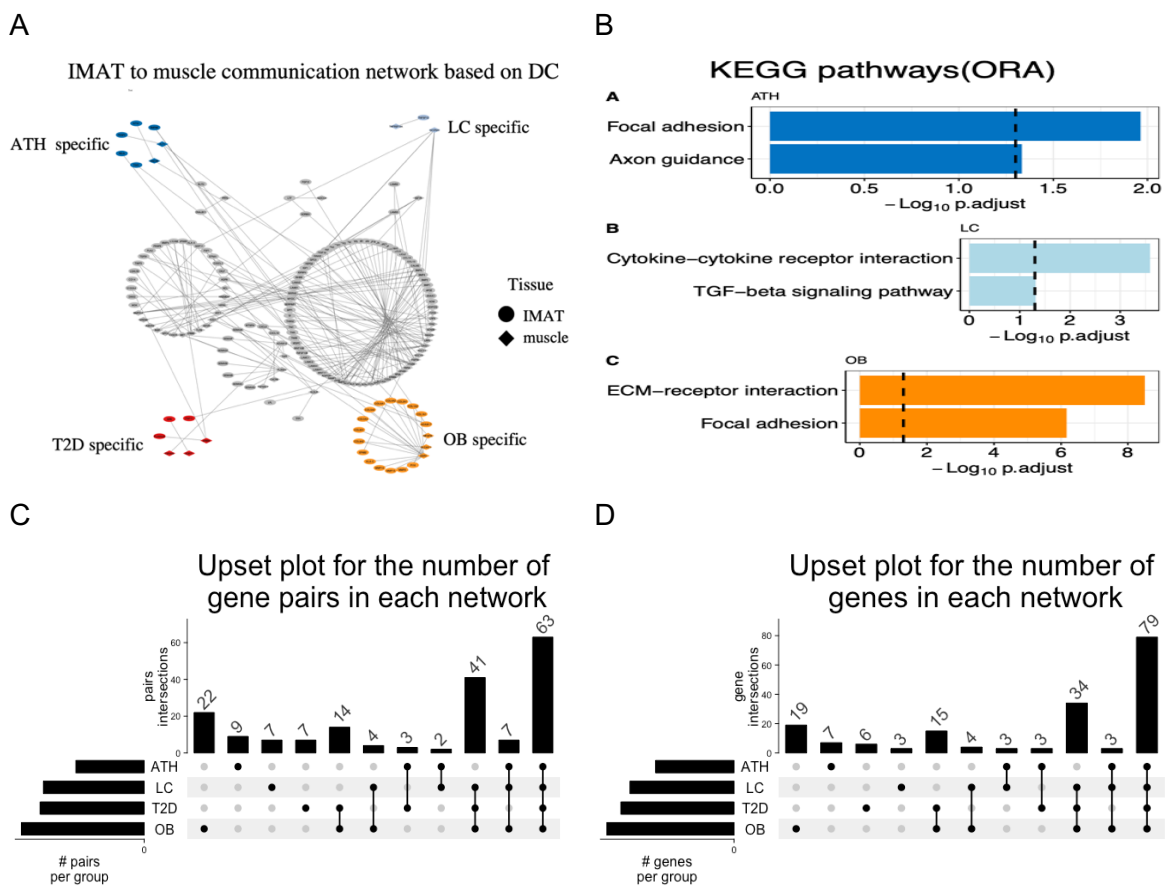
Figure 19.IMAT to muscle full communication network based on differential combinations. IMAT to muscle full communication network colored by the group(A). The enrichment bar plot to indicate significantly enriched KEGG pathways (FDR <0.05) for each group specific genes(B). The upset plot shows the distribution of connections and overall genes in each group (C and D).

ATH specific genes were found to be enriched in focal adhesion and axon guidance KEGG pathways, indicating that physical activity may activate the focal adhesion kinase (FAK) that decodes mechanical signals in the cytoskeletal system to transmitted across the cytoplasmic membrane by integrins to activate multiple anti-apoptotic and cell growth pathways, including the growth and development of nerve cell (Figure 19B, A). Also, impaired focal adhesion process was enriched along with ECM-receptor interaction pathways in the OB group, where the activities of FAK could be less active and induce apoptotic, cell death, and inflammation processes in response to lack of physical activities (Figure 19B, B). In terms of rewiring (gene connectivity difference across groups), significant changes in the molecular crosstalk between IMAT and muscle across groups were not uncovered (Figure 20 B and Figure 21B). However, there was a group-specific rewiring in the OB network, where the Discoidin Domain Receptor 1 (DDR1) gene ranked highest in the rewiring score and degree of centrality (Figure 5.20 A and B, Figure 21 B). DDR1 had 15 neighborhood IMAT genes; 13 were OB-specific, and LC, OB, and T2D shared the rest. In addition, the Plexin-A1 (PLXNA1) receiver gene was the second most rewired gene in the combined network, although PLXNA1 itself and all its connection partners were shared in OB and T2D networks only (Figure 20B and 21B).
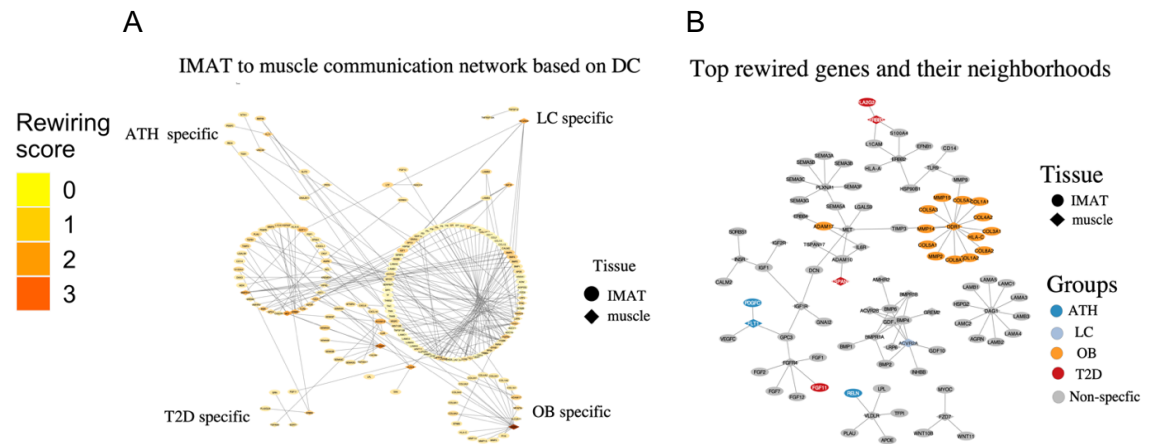
Figure 20.MAT to muscle full communication network based on differential combination did not show rewiring changes between networks. Network colored by rewiring score (A). A subnetwork (B) based on the top rewired genes in the combined network.
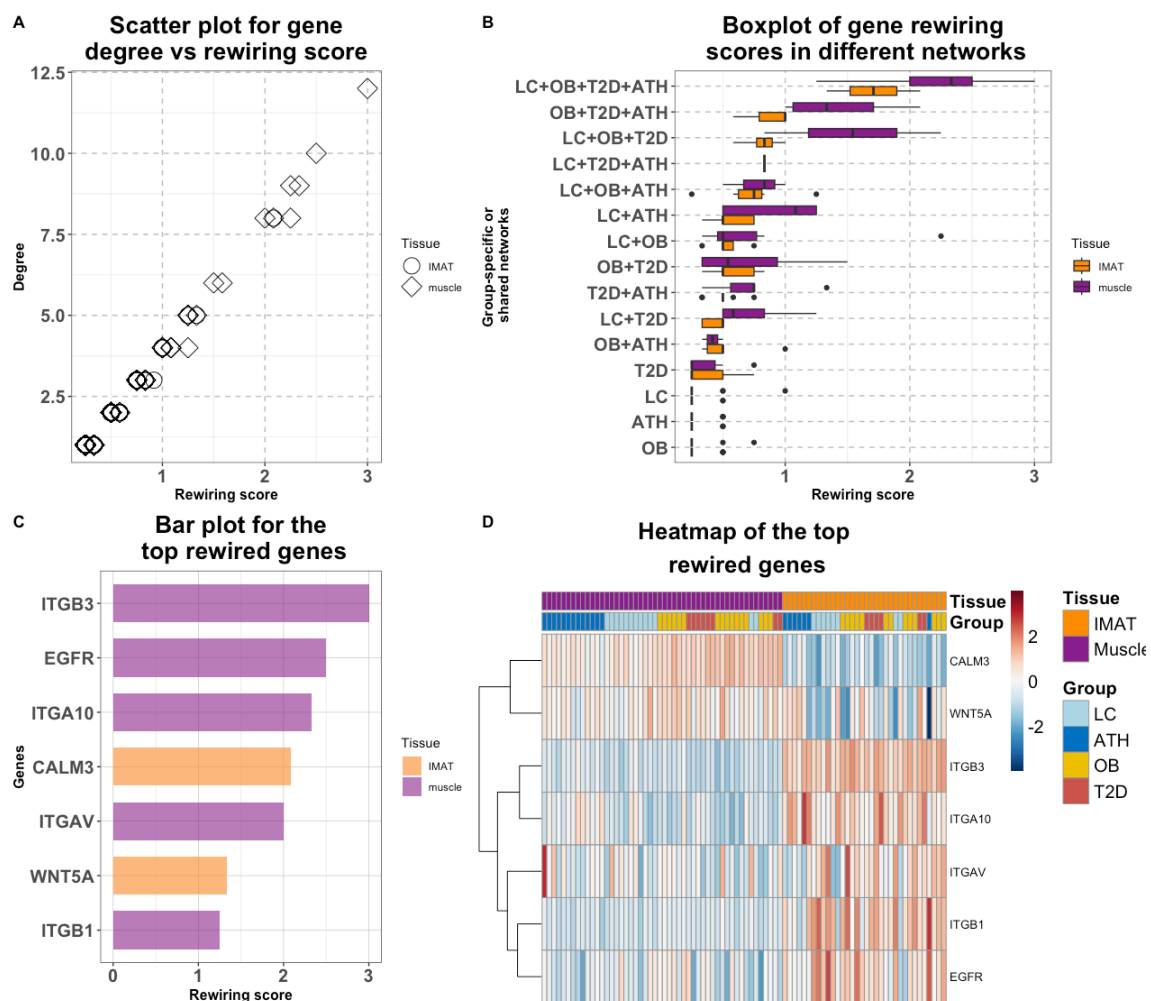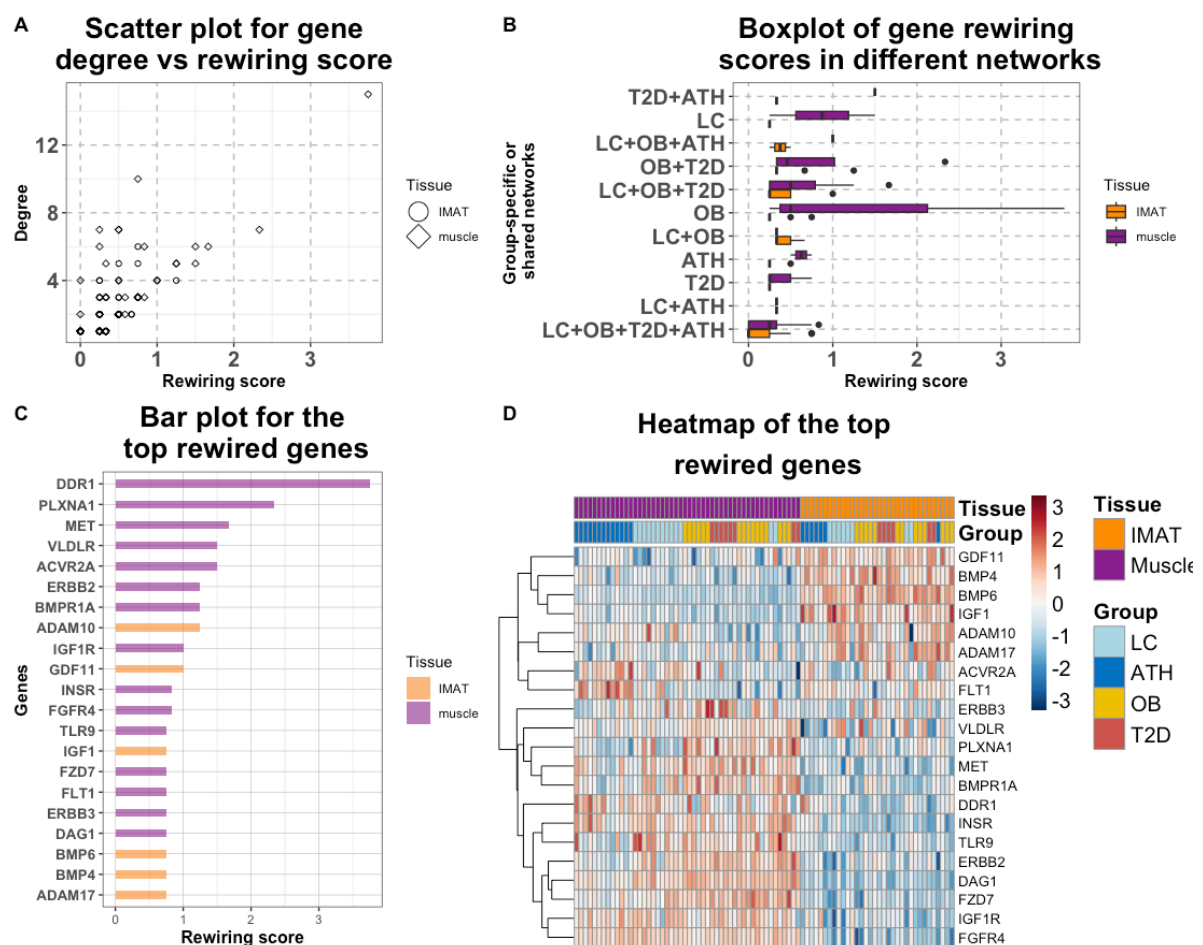
Figure 21.Describing the rewiring rate of genes in the differential combined networks. The scatter plot(A) indicates the relationships between degree and rewiring scores in the differential combination network. Boxplot(B) of gene rewiring scores in different networks, categorized by tissue. These genes in the networks were group specific or shared in two or more groups. The bar plot(C) displays the top rewired genes, and the heatmap(D) illustrates expression levels of rewired genes in IMAT and muscle across all groups

5.7. Communication between IMAT and muscle weighted by insulin sensitivity.

In this novel method, each gene from both IMAT and muscle samples with GIR and integrated them into a sender-receiver database to establish communication networks: IMAT to muscle (IMCN) and muscle to IMAT (MICN), as shown in Figure 22B and C. Every gene within these networks was endowed with insulin sensitivity attributes, signifying the correlation between gene expression in each tissue and GIR. The heatmap in Figure 22A illustrates the expression levels of all sender and receiver genes in both muscle and IMAT samples. In the IMCN network, we identified 488 nodes and 921 edges. Specifically, there were 250 nodes representing signaling genes from IMAT and 238 nodes representing receiver genes from muscle, as detailed in Figure 23A, A. On the contrary, MICN featured 510 nodes and 1084 edges, comprising 285 signaling genes from muscle and 225 receiver genes from IMAT, as depicted in Figure 23A, B. More signaling genes from muscle in MICN

suggest that muscle tissue may play a more significant role in transmitting signals to IMAT in the context of insulin sensitivity. Both networks shared 421 nodes and 796 edges, as shown in Figure 23A, C and D. Genes exclusively present in either IMCN or MICN demonstrated enrichment in the KEGG pathway of cytokine-cytokine receptor interaction, and the Disease Ontology (DO) pathway related to metabolic syndrome phenotypes (Figure 23 B, A:D). In both networks, secreted proteins and GPCRs covered the most significant part of the communication network.
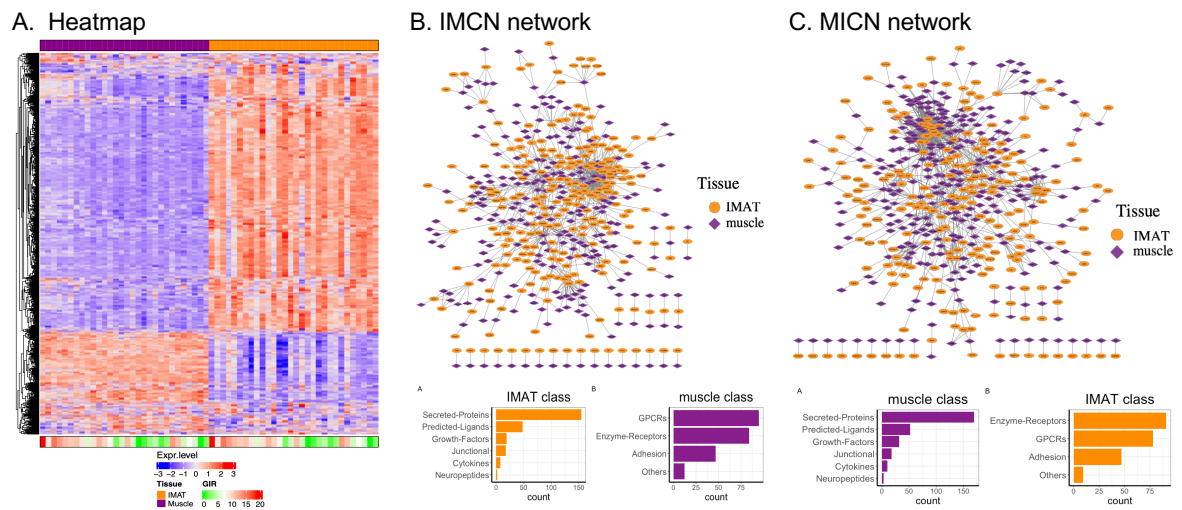
Figure 22.Crosstalk communication between IMAT and muscle weighted by insulin sensitivity. A, Heatmap for sender and receiver genes. B and C, represent the IMCN and MICN, where the class of the genes is indicated in the bar graph.

A. Number of node and edges
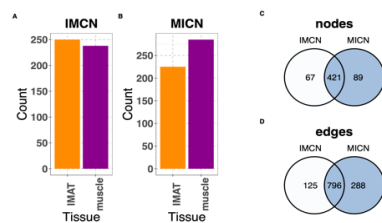
B. Pathway enrichments for genes present only in IMCN or MICN
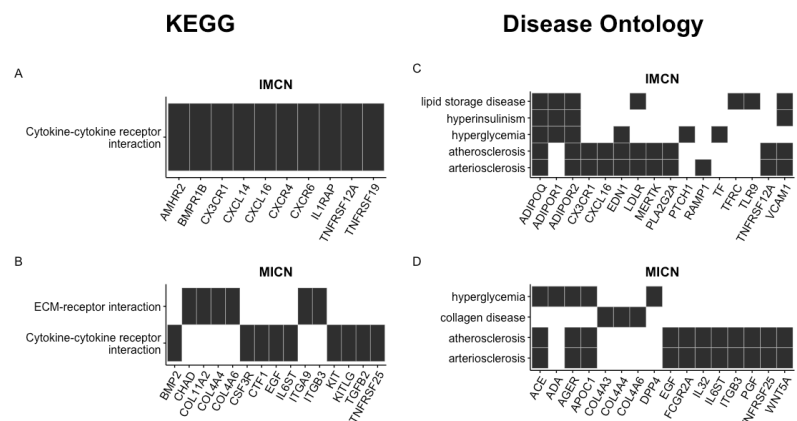
Figure 23.Network statistics. Bar plot and vendiagram for the number of nodes and edges of IMCN and MICN(A). Enrichment heat plot for the significantly (FDR < 0.05) enriched KEGG and disease ontology pathways(B).

5.8. Genes in the different network clusters revealed different KEGG pathways.

Both communication networks, IMCN and MICN, exhibited different communities based on the GLay community structure analysis method(226). Overall, 45 and 40 communities were detected for IMCN and MICN respectively (Figure 24 A and D). The number of genes for the largest ten modules were summarized as bar plots (Figure 24 B and E). Additionally, enrichment analysis found distinct pathways for dissimilar modules, indicating that different network clusters may present different function. Clusters 3, 4, 8, and 9 in IMCN showed the enrichment of complement and coagulation, TGF-beta signalling, Wnt signalling, and cell adhesion process, respectively. Cluster 7 also demonstrated functional pathways such as calcium and insulin signalling, and a metabolic disorder called Alzheimer's disease. Moreover, interlinked pathways such as Noch, ErbB, and calcium signalling involved in the activation, proliferation, and differentiation of cells are enriched in cluster 2 (Figure 24 C and F). In MICN, the same thing was observed because both networks had a huge gene overlap (Figure 24).
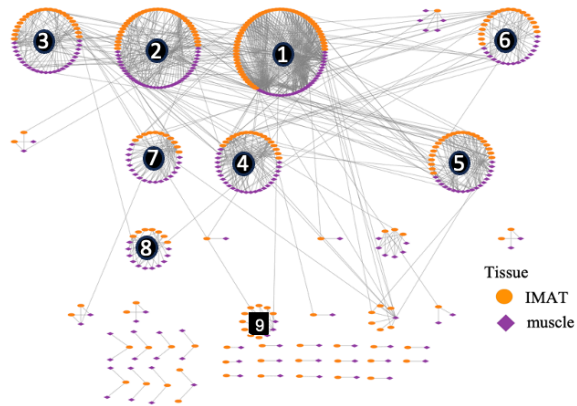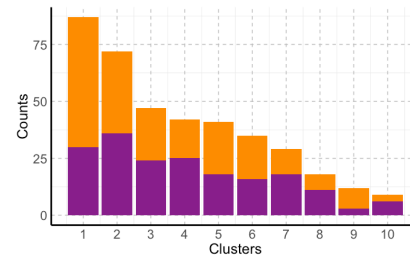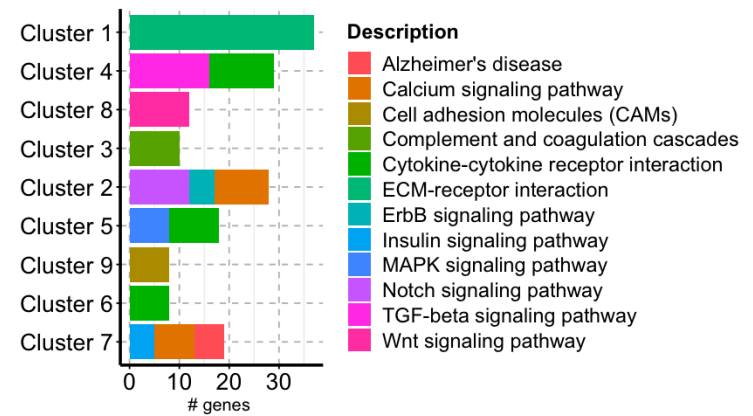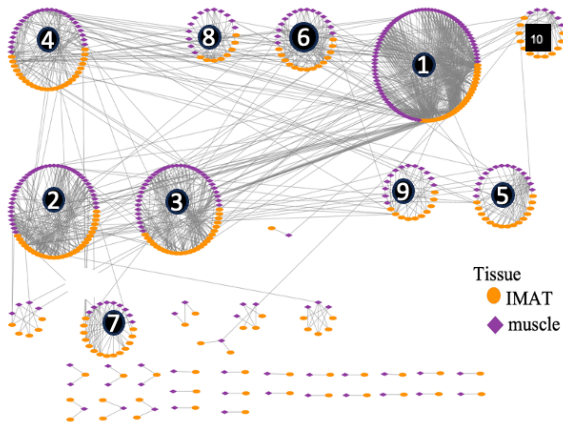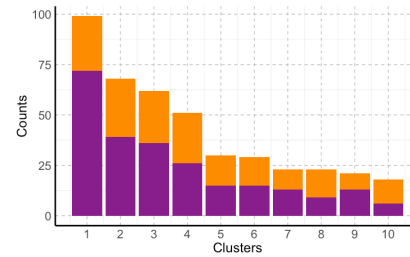
Figure 24.Clusters of gene networks in IMCN and MICN. 45 and 40 communities were detected for IMCN and MICN respectively (A, D), Bar plot to count the number of genes for the 10 largest modules (B, E). Enrichment bar plot to indicate significantly enriched (FDR < 0.05) KEGG pathways enriched for the genes in each module (C, F).

5.9. Insulin resistance increased ECM-receptor and Cytokine-Cytokine interaction.

In our pursuit to elucidate the roles of genes within the IMAT-muscle communication networks, we employed a logical classification approach, which separates the networks into insulin-sensitive and insulin-resistant states by adding the attributes of the interacting nodes in the network. In the insulin-sensitive (positive) network of IMCN, we identified 236 gene pairs involving 184 genes, signifying active communication between the tissues during periods of insulin sensitivity. Notably, most of these genes (97) originated from muscle tissue, which is considered the signal-receiving tissue. This observation suggests that, during insulin sensitivity, muscle actively participates in the signal transduction process, receiving a substantial influx of signals from IMAT (Figure 25A: C). Conversely, in the insulin-resistant(negative) network of IMCN, we recognized 185 gene pairs involving 159 genes, indicative of a decrease in signal transduction during insulin resistance. Interestingly, a shift in tissue involvement was observed, with most genes (87) originating from IMAT, the signaling tissue. This change suggests that, during insulin resistance, IMAT intensifies its signaling activity while muscle's role in signal transduction diminishes (Figure 25C). The KEGG pathway analysis (Figure 25D) highlights these findings. In the insulin-resistant state, IMCN exhibits an induction of pathways related to ECM-receptor interaction, Cytokine-Cytokine receptor interaction, and TGF-beta signaling. These pathways are commonly associated with inflammatory responses and tissue remodeling, aligning with the amplified signaling activity observed during insulin resistance. Moreover, in the MICN, we observed a similar interplay between tissues during insulin sensitivity. The insulin-sensitive network of MICN comprised 263 edges and 197 nodes, with a significant majority (126 genes) originating from the signaling tissue, muscle (Figure 25E: G). This finding implies that muscle actively participates in signaling activities. Those signaling proteins were associated with ECM-receptor interactions and inflammatory cytokines. Such signaling from skeletal muscle during insulin sensitivity may not be expected but could occur due to mechanical and physical activity stress, although validation may be required (Figure 25E: H).
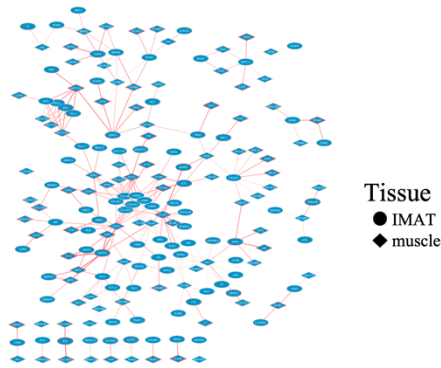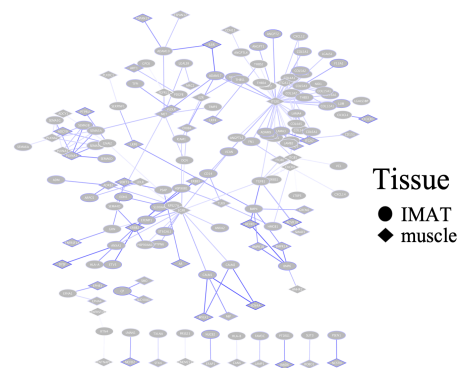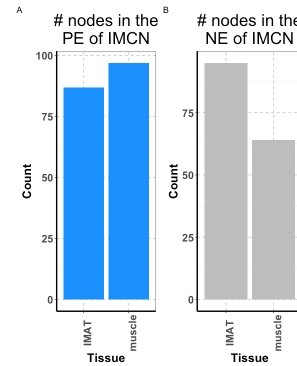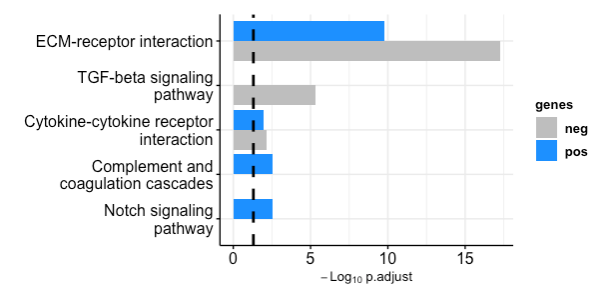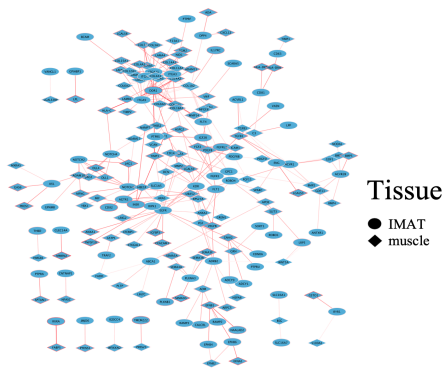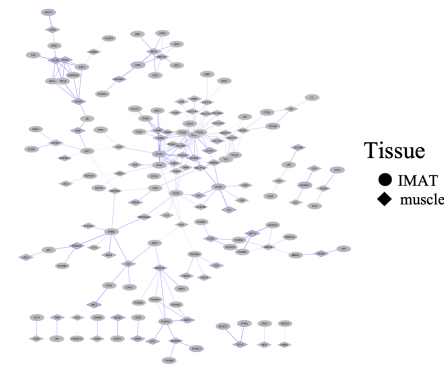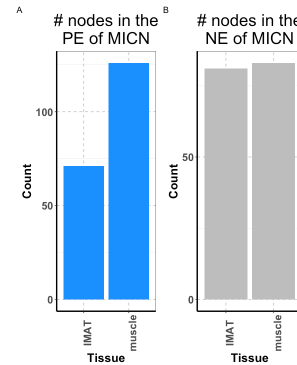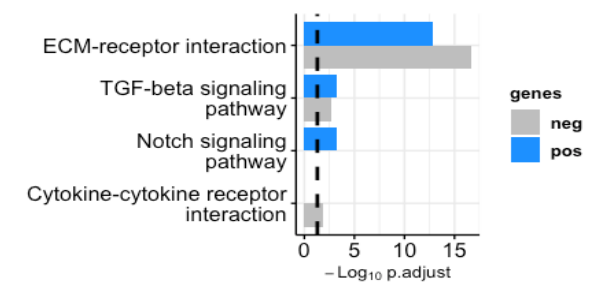
Figure 25.I Insulin-sensitive (Positive Edge(PE)) and insulin-resistance(Negative Edge(NE)) networks of IMCN and MICN (A, B, E, F). Insulin-sensitive networks were created when interacting nodes(genes) are positive in their insulin sensitivity attributes and insulin resistance network, when both nodes are negative. Bar plots to count the number of genes in the networks (C and G). Enrichment bar plots to show KEGG pathways enriched for network specific genes (D, H).

5.10. Rewiring analysis found most rewired genes in the IMAT during insulin sensitivity and resistance conditions.

Using variance analysis based on the insulin sensitivity attributes of the genes in the networks, 50 most rewired genes in the IMCN and 51 genes in the MICN were identified. From the top selected rewired genes in IMCN or MICN, 98% of the genes were from IMAT, indicating IMAT is a dynamic tissue during insulin sensitivity and resistance conditions (Figure 26E). That is in the cross talk between IMAT and muscle, the expression level of the top rewired IMAT genes was less affected during insulin sensitivity and resistance while their interacting partners from the skeletal muscles are changing (Supplemental Figure 4). The relationship between degree and rewiring was not linear, although the analysis considered highly connected genes to have a high rewiring rate in the network (Figure 26D). This indicates that few highly connected genes (CALM1, ADAM17, GDF9, APOE, BMP6 in the IMCN and CD44, ITGAV, CD44, and INSR in MICN) had interacting partners identical to each other in term of insulin sensitivity or were highly expressed in one condition (Supplemental Figure 4). However, few genes again followed a positive trend in rewiring and degree, especially in the MICN such as ITGB1 and EGFR (Figure 26D).

A. Full IMCN colored by rewiring score.

C. Rewiring score distrbution for the genes in IMCN and MICN.

E. List of the top reiwired genes.

B. Full MICN colored by rewiring score.
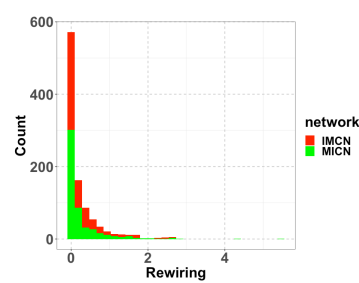
D. Rewiring score and degree centrality.
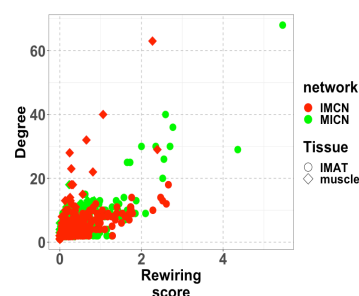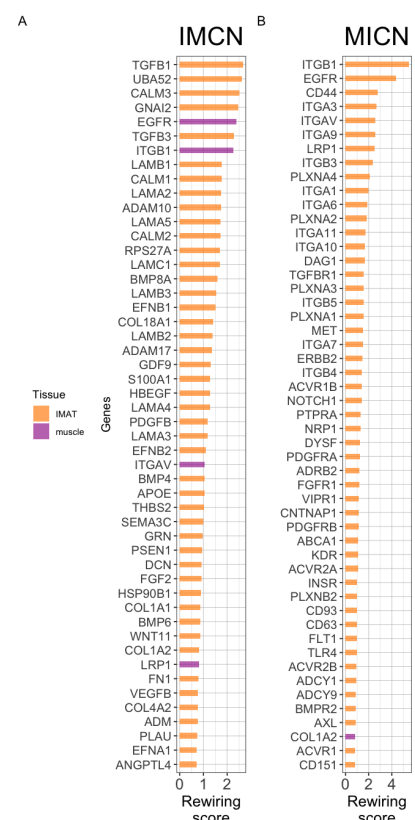
Figure 26.Rewiring analysis found higher variabilities in the IMAT. Networks (A and B) to indicate the full IMCN and MICN colored rewiring score. Bar plot to demonstrate the distribution of a rewiring score in the full networks(C) and top rewired genes(D) in both networks, the scatter plot(E) to display the correlation between rewiring and degree centrality.

Then, subnetworks based on the top rewired genes were created for IMCN and MICN, respectively (Figure 27A and E). Thus, 250 nodes (125 IMAT and 150 muscle) and 497 edges were identified in IMCN (Figure 27B). Those genes were enriched in TGF-beta signaling and ECM-receptor interaction KEGG pathways. Additionally, in collagen disease, atherosclerosis, and arteriosclerosis disease ontology terms (Figure 27C). Moreover, in MICN, 673 edges and 265 nodes (53 IMAT and 212 muscle) were identified (Figure 27F), and the genes were enriched in the TGF-beta, and calcium signaling, ECM-receptor and Cytokine-Cytokine interaction KEGG pathways. Similarly, myopathy, muscular dystrophy, lipid storage, hyperglycemia, atherosclerosis, and arteriosclerosis disease ontology terms were linked with the identified genes (Figure 27G). Furthermore, a pairwise similarities score was computed between the top rewired genes in both subnetworks using the Jaccard index to identify genes targeting similar target genes (Figure 27D and H).

A . Networks of the top rewired gene in IMCN
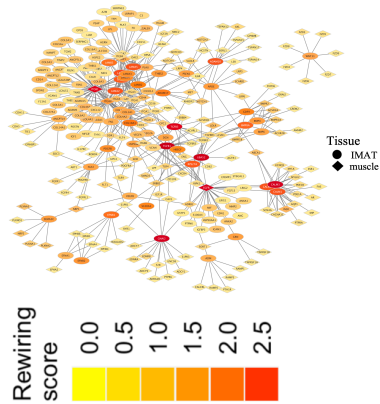
B. Number of nodes
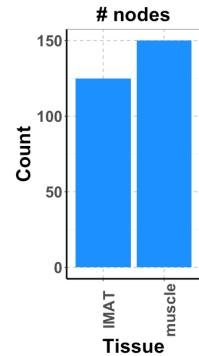
C. Pathway enrichment for top rewired genes network of IMCN
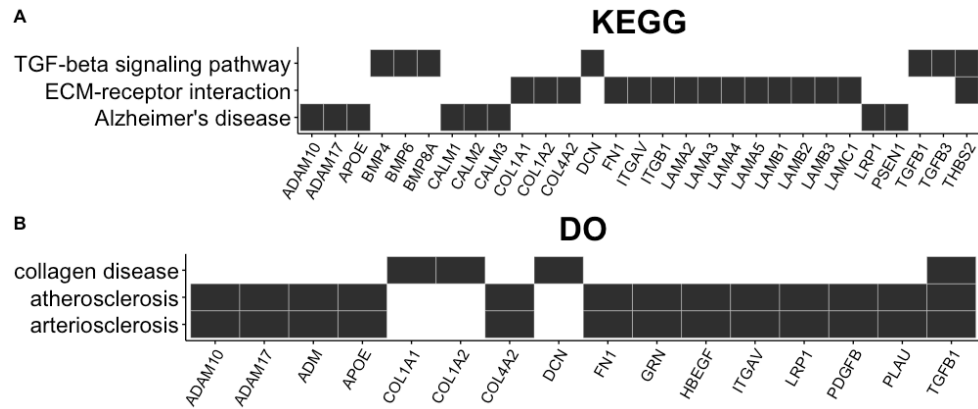
D. Jaccard similariy
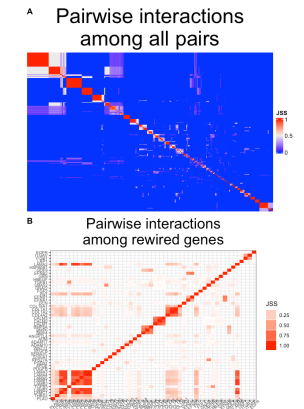
E. Networks of the top rewired gene in IMCN
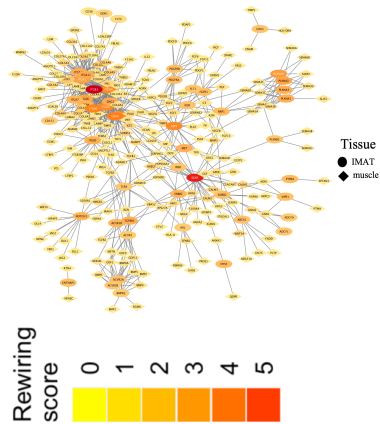
F. Number of nodes
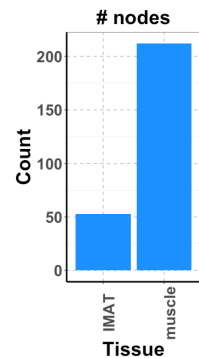
G. Pathway enrichment for top rewired genes network of MICN
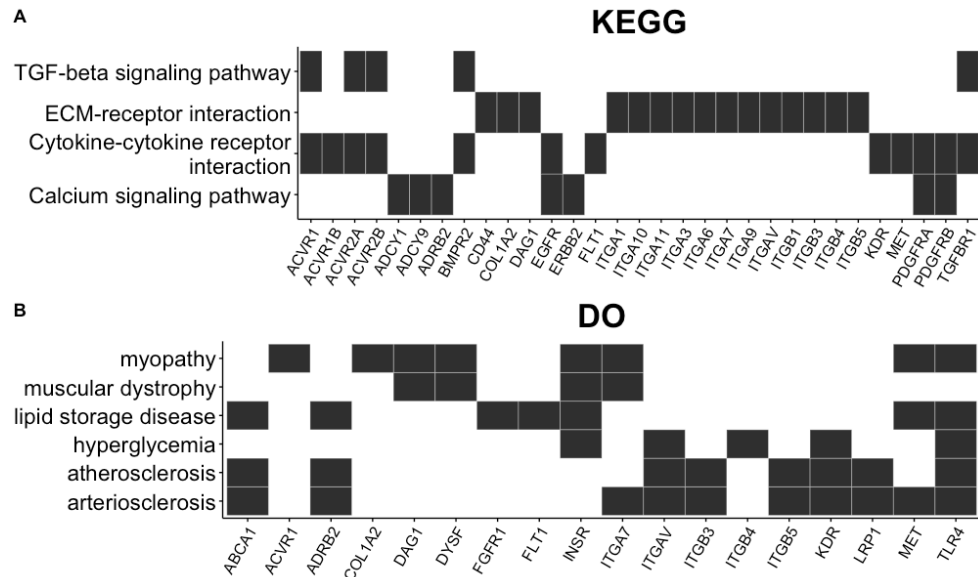
H. Jaccard similariy
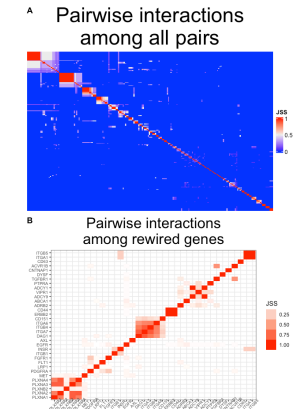
Figure 27.Subnetwork based on top rewired genes identified a more refined network cluster. A and E are networks of the top rewired genes with their interacting partners. The bar plot for the number of nodes for each network (B and F), heat plots for significantly enriched pathways (FDR < 0.05) terms (C and G). Heatmaps (D and H) for Jaccard index to find similarities between pairs of genes.

As a result, a strong similarity index emerged within the laminin, collagen, calmodulin, and bone morphogenetic gene clusters of the IMCN (Figure 27, panels D and H). This suggests that these groups of genes collectively influence target genes in the target tissues similarly. For instance, laminin genes (LAMC1, LAMB3, LAMB2, LAMA5, LAMA2, LAMA3, and LAMA4) from IMAT exhibit a comparable influence on muscle genes such as BCAM, CD151, CD44, DAG1, ITGA1, ITGA3, ITGA6, ITGA5, ITGA7, ITGAV, ITGB1, ITGB4, and RPSA (Figure 28, A and B). However, these genes' insulin sensitivity and rewiring score attributes are different (Figure 28, A and B). Additionally, the network of these genes was associated with KEGG terms such as ECM-receptor interaction and cell adhesion, as well as the disease ontology term muscular dystrophy (Figure 28 C). Likewise, IMAT collagen genes (COL1A1, COL1A2, COL4A2, and COL18A1) were observed to target cluster differentiation (CDs) and integrin genes in the muscle (Figure 28 D, and E). This specific network demonstrated strong associations with ECM-receptor interaction KEGG pathway, as well as with disease ontology terms such as myopathy, collagen diseases, hyperglycemia, atherosclerosis, and arteriosclerosis. Furthermore, CALM1, CALM2, and CALM3 expressions in the IMAT were negatively correlated to insulin sensitivity, and all of them target muscle genes such as AQP1, MYLK, PTPRA, ABCA1, PDE1A, PDE1B, INSR, CACNA1C, KCNQ5, FAS, ESR1, EGFR, MIP, AR, MYLK2 and SCN4A. Moreover, the network showed functions related to insulin, calcium, phosphatidylinositol signaling, and disease development, such as myopathy and atherosclerosis (Figure 28, G: I). Additionally, IMAT proteins BMP4, BMP6, and BMP8A have similar relationships to muscle insulin sensitive genes such as THFBR2, ACVR2A, BMPR2, TGFBR1, and ACVR2B, and insulin resistance genes such as GREM2, LRP6, BMPR1A, BMPR1B, and ACVR1. The network displayed functional enrichment-related inflammatory signaling pathways (Figure 28, J: L).

A. Laminin network in the IMCN

B. Heat and bar plots for laminin network in the IMCN

C. Enrichment pathways for laminin gene network in the IMCN

D. Collagen gene network in the IMCN

E. Heat and bar plots for collagen network in the IMCN

F. Enrichment pathways for collagen gene network in the IMCN

G. Bone morphogenetic network in the IMCN
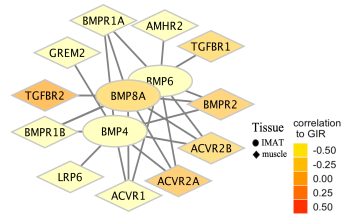
H. Heat and bar plots for Bone morphogenetic network in the MCN
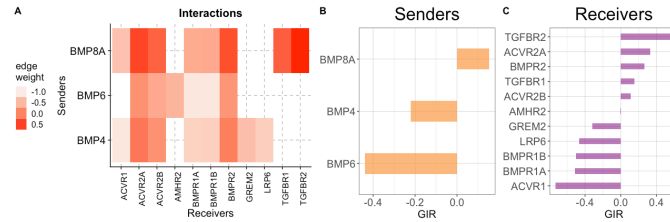
I. Enrichment pathways for bone morphogenetic gene network in the IMCN
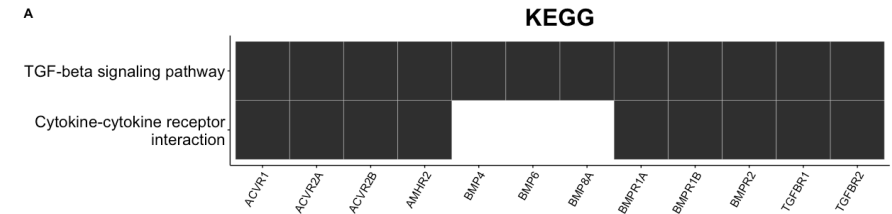
J. Calmodulin network, IMCN
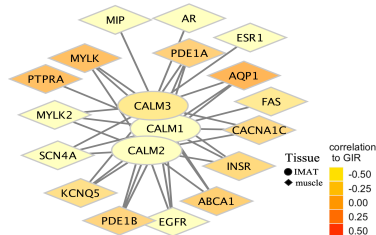
K. Heat and bar plots for calmodulin network, IMCN
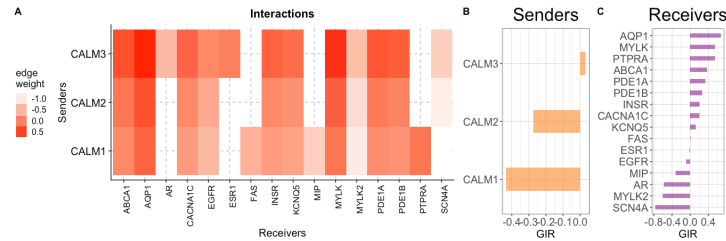
L. Enrichment pathways for calmodulin gene network, IMCN
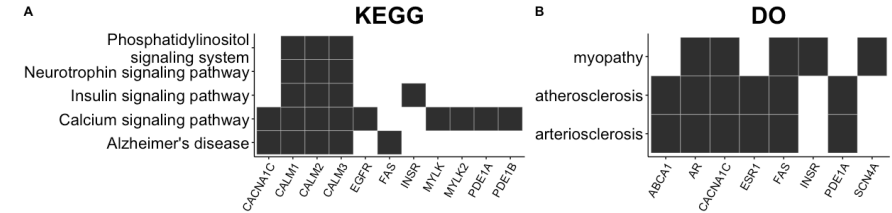
Figure 28. Laminin, Collagen, Calmodulin and Bone morphogenetic genes subnetwork in IMCN (A, D, G, and J). Colors in the network indicate the correlation between the gene and insulin sensitivity. Heat plot and the bar plot (B, E, H, K) to indicate interaction weights between sender and receiver as well as how much each gene was correlated to GIR. Significantly enriched KEGG pathways (FDR <0.05) are presented as heat plots (C, F, I, and L)

In the MICN, where muscle acts as a signaling tissue and IMAT as a signal-receiving tissue, the Jaccard index identified a group of Plexin genes in IMAT that showed substantial similarity among self-indicating they shared common interacting genes from muscle. Those genes were Semaphorins. In this case, the Plexins rewire similarly (with a slight difference) to respond to the incoming signals from muscle semaphorins (Figure 29 A:C). The same is true for Integrin genes of IMAT where they rewire in the similar rate to respond for the laminin signals from muscle

A.Semaphorins-Plexins network in the MICN
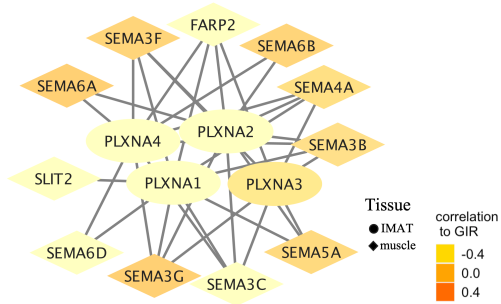
B. Heat and bar plots for Semaphorins-Plexins network
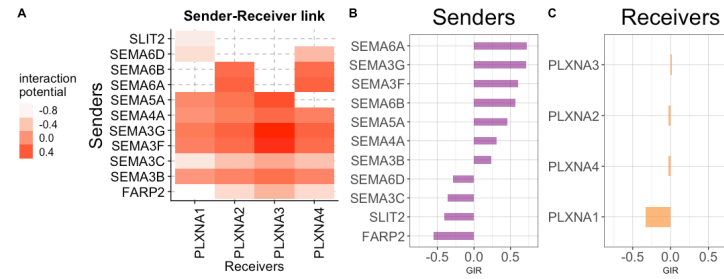
C

No significant enrichment pathways in the KEGG or DO

D.Laminin-Integrins network in the MICN
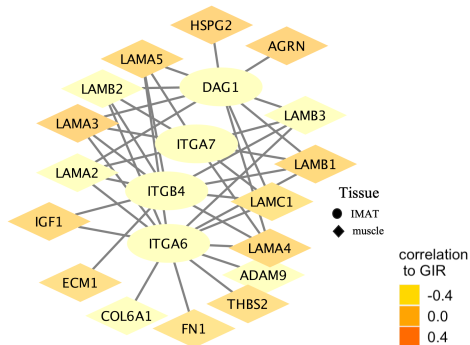
E. Heat and bar plots for Laminin-Integrins network
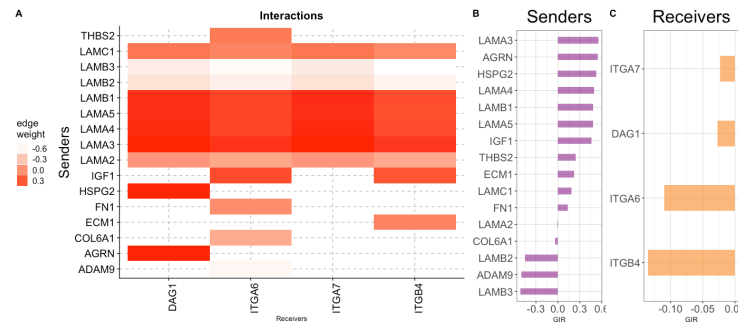
F. Enrichment pathways for Laminin-Integrins network, IMCN
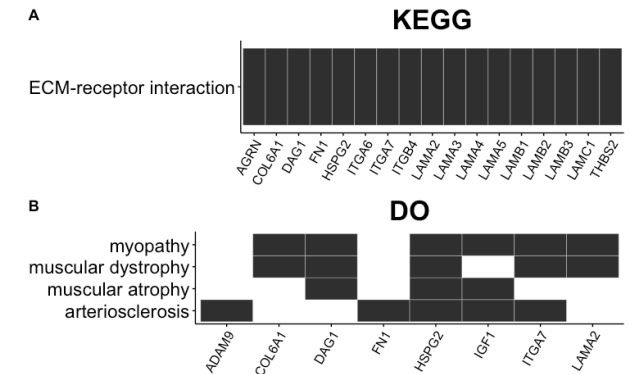
Figure 29. Semaphorins-plexins, and laminin-integrins gene subnetwork in MICN (A, D). Colors in the network indicate the correlation between the gene and insulin sensitivity. Heat plot and the bar plot (B, E) to indicate interaction weights and how much each gene was correlated to GIR. Significantly enriched KEGG pathways (FDR < 0.05) for the genes in the network is presented as heat plots (F).

6. Discussion

In recent years, a growing body of research has highlighted the significant impact of Intramuscular Adipose Tissue (IMAT) on metabolic and mobility dysfunctions in humans(97, 103, 105, 106, 110). Specifically, IMAT is closely linked to skeletal muscle insulin sensitivity, particularly in obese individuals(90). However, the intricate molecular mechanisms underlying the regulation of skeletal muscle insulin sensitivity by IMAT have remained elusive. Furthermore, little is known about how this regulation varies across different insulin sensitivity groups. To address these critical gaps in knowledge, we employed a computational approach, leveraging RNAseq data and clinical information from diverse insulin sensitivity groups. Our study discloses IMAT as a dynamic tissue actively engaged in communication with skeletal muscle during both insulin sensitivity and resistance states. These communication pathways predominantly involve interactions within the extracellular matrix (ECM) and between cytokines and cytokine receptors. Our findings demonstrated the potential consequences of these interactions, implicating them in various conditions, from inflammations and myopathies to muscular atrophy, dystrophy, collagen diseases, and hyperglycemia. This investigation not only deepens our understanding of the role of IMAT in metabolic regulation but also offers valuable insights into the complex molecular network that governs skeletal muscle insulin sensitivity, paving the way for targeted interventions and therapeutic strategies in the future.

6.1. GIR gold standard to measure insulin sensitivity of peripheral tissues.

GIR is the gold standard to measure insulin sensitivity of organs epically metabolic active organs such as muscle, adipose tissue, and liver(177). In our study, the GIR test was a crucial mechanism to assess the insulin sensitivity of different study groups and to correlate gene expression in muscle or IMAT with insulin sensitivity to identify genes that predict IMAT or muscle insulin sensitivity and to explore change in the communication network between IMAT and muscle in progressive insulin resistance. Similarly, in various research setups, GIR techniques have provided new insights into human obesity and type 2 diabetes and contributed significantly to understanding the role of liver and hepatic insulin resistance in these diseases(229, 230). Among the study groups in our data, T2D individuals had lower GIR and higher FPG levels, indicating this group of people was insulin resistant. Insulin resistance is a manifestation where metabolically active organs, such as skeletal muscle, liver, and adipose tissue, resist insulin action(177). As a result, the liver reduces glucose uptake rate while producing glucose and increasing the plasma glucose level(54, 56, 231). Additionally, in adipose tissue, the rate of lipolysis (the breakdown of triglycerides into fatty acids and glycerol) increased, leading to the release of more fat into the bloodstream

through free fatty acids, which other tissues, such as skeletal muscle and liver, can take up(64). While muscle can use these fatty acids for energy, fatty acid oxidation in liver is to supply energy for other organs functions(64, 71). Moreover liver may convert glycerol from triglycerides into new glucose through gluconeogenesis, eventually leading to elevated blood glucose levels contributing to hyperglycemia(64). Increased free fatty acids can promote fat accumulation in non-adipose tissues (liver, muscle, pancreas and many others)(48). They could be the primary source of inflammation within tissue and may affect insulin signaling. Insulin resistance in the skeletal muscle decreases glucose uptake and metabolism and increases glucose storage and the conversion of glycogen to lipid in the long run. This situation (insulin resistance) could eventually modify and reprogram the genetic makeup of the tissues, and intervention strategies through lifestyle modification may not work; instead, dependency on pharmacological or medical interventions(48, 232).

6.2. Muscle and IMAT gene expression profile and their predictive functions

Gene expression patterns in muscle and IMAT were compared to assess the possibility of contamination in the IMAT samples during isolation. We examined a dataset encompassing 11828 processed genes across all samples. Our results clearly demonstrated distinctive gene expression profiles between IMAT and muscle, providing strong evidence against contamination between these two tissue types (Figure 12A and B). This implies that IMAT constitutes a distinct tissue depot within the skeletal muscle, characterized by a unique gene expression signature. Although no analogous human data were available for direct comparison, previous investigations in livestock species have reported dissimilar genetic patterns between muscle and IMATA(233). Interestingly, their fundings also indicated that pathways that regulate cell adhesion, structure, and integrity were upregulated in IMATA and downregulated in muscle tissue. This is in harmony with our findings, where IMAT tissue showed a lot of enrichment in adhesion, ECM-receptor interaction, axon guidance, and actin cytoskeleton regulation (Figure 13C). Moreover, our data further support the notion that IMAT is not a homogeneous tissue but consists of distinct molecular subtypes. The existence of these subtypes within IMAT highlights the complexity and heterogeneity of this tissue, emphasizing the need for further investigation to delineate the functional implications of these subtypes (Supplemental Figure 1). Furthermore, our study provides important insights into distinct gene expression patterns within the skeletal muscle tissue and IMAT across various groups. Notably, we observed a significant number of DE genes in the IMAT among individuals with T2D. These genes showed functional enrichment in dysregulation metabolic pathways, as illustrated in Figures 13B and C, emphasizes the potential role of IMAT in the pathophysiology of T2D. One of the key findings is the downregulation of genes associated with oxidative phosphorylation, which is a fundamental process in cellular

energy production(234). This downregulation suggests a reduction in the capacity of IMAT to generate ATP through oxidative phosphorylation efficiently(235). This phenomenon aligns with the well-established concept of mitochondrial dysfunction in T2D, as impaired oxidative phosphorylation can contribute to an imbalance in cellular energy homeostasis(236, 237, 238, 239, 240). Furthermore, downregulated genes associated with the glycolysis, citrate cycle, and pyruvate metabolism advances metabolic dysregulations in IMAT. These pathways are intricately linked to energy metabolism and the production of metabolic intermediates that may disrupt various cellular processes and metabolic flux within IMAT, potentially contributing to insulin resistance and metabolic dysfunction. Additionally, the downregulation of genes related to fatty acid metabolism, Peroxisomes, and PPAR (Peroxisome Proliferator-Activated Receptor) signaling within IMAT is particularly significant because these pathways target lipids for energy production and storage, and the observed alterations in these pathways may disrupt lipid metabolism in the IMAT, potentially leading to lipid intermediates accumulation and insulin resistance. Besides their role in lipid metabolism, peroxisomes are involved in Reactive Oxygen Species(ROS) scavenging(241), and their downregulation may further exacerbate lipid-related disturbances within IMAT. PPARs are called lipid and insulin sensors(242) and have a DNA binding domain where they directly alter gene expression of target tissue(243); thus, they are master regulators of adipogenesis and lipid biosynthesis. When PPARs are downregulated as indicated in figure 13 C, insulin sensitization and fatty acid oxidation in IMAT are reduced. As a result, the lipolysis rate increases, and triglyceride levels might increase in the circulation and eventually lead to the accumulation of lipids in the local tissue(244, 245). This could worsen the situation by inducing inflammation and lead to peripheral tissue insulin resistance (primary to skeletal muscle and liver) and complications related to diabetes such as cardiovascular disorders, chronic kidney diseases, nerve damage, problems in vision and infection in the feet(48, 64). Also, very interestingly, in both ORA and GSEA (Figure 13 B and C), we marked the downregulation of genes with BCAA degradation pathway, Butanoate and Propanoate metabolism pathways suggest alterations in amino acid metabolism within IMAT. These pathways are interconnected with glucose and lipid metabolism and can impact cellular energy balance and insulin sensitivity. BCAAs are essential amino acids that must be obtained from food and have been shown to provide many physiological and metabolic benefits, such as stimulation of pancreatic insulin secretion, adipogenesis, and enhanced immune function(246), mainly mediated by the mammalian target of the rapamycin (mTOR) (246), known in its role in nutrition sensing, initiation of protein synthesis, cell growth, and proliferation(86, 87, 247). However, build-up of BCAAs in the circulation has been associated with metabolic syndrome in humans or animals(248, 249). Although no definite data that show the causal relationships between

BCAAs level and metabolic syndrome, studies have shown that 80% restriction of BCAAs for four weeks significantly improves glucose intolerance and insulin resistance in High Fat Diet(HFD) mice(250). Similarly, providing a diet low in isoleucine or valine, but not leucine, to diet-induced obese mice improved metabolic phenotypes (249). Consistent with these findings, BCAA supplementation with a HFD or defective BCAA oxidation through deleting methylmalonyl-CoA mutase in mice induces insulin resistance and impaired glucose tolerance(251, 252, 253), indicating that efficient BCAA breakdown is critical for decreasing plasma BCAAs and improving insulin sensitivity. Furthermore, in a human study, many enzymes responsible for breaking down BCAAs in visceral white adipose tissue were found to be significantly low in their expression among individuals with both obesity and metabolic syndrome compared to obese individuals without metabolic syndrome who had a similar weight(254). Combining these previous findings with our data, impaired BCAA degradation pathways in primary metabolic tissues, including IMAT, could raise plasma levels of BCAAs, activate mTOR signaling for more amino acid synthesis and impairs insulin mediated glucose transport and glycogen synthesis(234), increase oxidative stress that could lead to mitochondrial dysfunction, and eventually aggravate insulin resistance and T2D(255, 256). Propionate and Butyrate are metabolites formed by gut microbiota from complex dietary carbohydrates, and they were reported to protect against diet-induced obesity(257, 258). The dysregulated genes grouped in the propionate and butyrate metabolic pathways may explain altered gut microbiota that could induce the development of T2D and insulin resistance phenotype in the IMAT. Additionally, the propionate metabolic pathway has many overlaps with the distal part of BCAA degradation pathway (195), indicating both may have functional similarities in the IMAT during insulin resistance or T2D. In this analysis, dysregulated metabolic pathways in the IMAT may increase circulating amino acids (AA), free fatty acids (FFA), and glucose and directly affect skeletal muscle activity in T2D patients. Additionally, the enrichment of upregulated IMAT genes in the ECM-receptor interaction, cytokine-cytokine interaction, complement and coagulation cascades, and NOD-like receptor signaling pathways indicated inflammation and structural changes within IMAT due to diabetes. Briefly, in the skeletal muscle, higher number of DE genes (121 genes) observed in ATH individuals compared to other groups suggests the influence of athletic training on gene regulation in skeletal muscle (Supplemental Figure 2 A). These genes are enriched in a regulated metabolic pathway such as oxidative phosphorylation and PPAR signaling, indicating lipid metabolism has been maintained in the ATH muscle. However, cell structure modification markers such as ECM and adhesion protein, complement, and coagulation cascades were upregulated, which could explain the presence of cellular damages due to mechanical stress (Supplemental Figure 2 C). Further analysis was conducted to enhance our understanding of the role of IMAT in progressive

insulin resistance. Correlation analysis was performed between GIR, and all IMAT samples combined. In this analysis, BMI was considered a potential covariate for total adiposity to isolate the effect of IMAT on insulin sensitivity. As indicated by the distribution plot in figure 14C, IMAT appears to influence whole-body insulin sensitivity within a relatively narrow range through a smaller, more dynamic set of genes compared to skeletal muscle. In contrast, most muscle genes correlated with insulin sensitivity, indicating a broader regulation range. While further investigations are required, considering factors such as size, evolutionary advancement on glucose uptake, degradation, and storage, and with other physiological perspectives (having more insulin receptors, mitochondrial activity, and adaptability and more), it is plausible that muscle gene expression plays a role in regulating whole-body insulin sensitivity across a broader spectrum. Moreover, to give more biological inference on this finding, in the KEGG pathways (Figure 15 A), IMAT genes showed positive enrichment with the genes sets of Phenylalanine, Butanoate and BCAA degradation metabolic pathways during insulin sensitivity suggests that IMAT during insulin sensitivity facilitates a regulated metabolic function toward phenylalanine, butanoate and BCAAs. Dysregulated Butanoate and BCAAs could increase circulating amino acid levels and have been associated with the development of insulin resistance and T2D or could serve as indirect markers of developed metabolic syndromes, as discussed above. Phenylalanine is one of the aromatic amino acids repeatedly found in an abnormally higher amount in the blood sample of T2D patients(259). A recent discovery in mice has shown that a phenylalanine-rich chow diet or overexpression human phenylalanyl-tRNA synthetase(hFARS) stimulates the development of insulin resistance and T2D symptoms(260), suggesting abnormally regulated phenylalanine metabolic pathways in the IMAT could contribute for insulin resistance and T2D in humans too. Similarly, more regulated KEGG metabolic pathways related to glucose, amino acids, and fatty acids are observed during insulin sensitivity in the skeletal muscle (Figure 15 B). At the same time, cell injury and damage markers genes are indicated in the complement and coagulation cascade pathway. Additional investigation may be required to verify whether cellular damage to the muscle was primarily from physiological or pathological stress.

6.4. Crosstalk communication between IMAT and Muscle

Organ crosstalk communication is a phenomenon that refers to the dynamic exchange of signals among different organs and tissues, allowing them to coordinate their activities and respond to the ever-changing demands of the organism(64). It relies on a complex network of molecular messengers, responders, signaling pathways, and transcriptional factors that involve endocrine, paracrine, autocrine, juxtacrine, and neuronal signaling mechanisms (156, 157). Organ crosstalk communication is fundamental to the proper functioning of the body and ensures a stable internal condition(homeostasis). To illustrate, when the body

faces stress, organs like the hypothalamus, pituitary gland, and adrenal glands collaborate to provide a coordinated response. Organs like the liver, adipose tissue, and muscles cooperate to regulate metabolism and energy balance in the body to avoid metabolic disturbances(234).

The crosstalk between adipose tissue and skeletal muscle has gained notable interest since this process, specifically in obesity(261), substantially causes the development of muscle insulin resistance. During exercise, it reverses muscle insulin resistance and promotes insulin sensitivity(262). More specifically, IMAT directly impacts muscle insulin sensitivity due to its close physical proximity to muscles and ability to trigger local inflammation(90). The most compelling mechanism for IMAT and muscle crosstalk is paracrine signaling, where a signaling tissue releases the signaling molecules into the nearby extracellular fluid to affect neighboring tissues. Although numerous data support the endocrine signaling of muscle(myokines) to alter WAT phenotype including WAT "beiging", no data is found to verify the systemic effect of IMAT, even if IMAT has a similar molecular profile to visceral WAT(263).

The discussion below focuses on the paracrine signaling between IMAT and muscle in progressive insulin resistance. As described in the method and result section, three different computational approaches followed to dissect the crosstalk communication between IMAT and muscle. In the first two analysis, for each group, cross tissue gene correlation analysis and differential combination analysis based of DE between IMAT and muscle was performed. Both analyses found an increased molecular interaction in the direction of IMAT to muscle among OB and T2D groups and a decreased communication network in LC and ATH group. Overall, in the cross-tissue gene correlation, a significant number of interacting gene pairs (correlated pairs) or the identity of genes in the networks were different. T2D and OB networks, however, did not differ in size. The increase molecular cross during OB and T2D could be explained by the secretion of pro-inflammatory cytokines and chemokines from IMAT due metabolic disturbances and inflammation(234, 261). Additionally, on the muscle side, several molecules could be activated to correct the metabolic and inflammatory challenges. Our enrichment analysis has proven this, where group-specific genes in the OB and T2D have shown greater Cytokine-Cytokine receptor interactions, TGF-beta signaling, ECM-receptor interactions, and focal adhesion. Even in T2D-specific networks, genes were explicitly linked to pathways related to cancer, leukocyte migration, complement, and coagulation networks, and the activation of cell adhesion molecules indicates inflammatory cytokines mainly mediated the crosstalk between the tissues. The main question is how this could affect skeletal muscle insulin sensitivity. The molecular mechanism could be many. However, the expansion of adipocytes in the IMAT increases the release of FFA, tumor necrosis factors (TNF-alpha, beta), cytokine and

chemokines (like Interleukin-6(IL-6)) and monocyte chemoattractant molecules (MCP-1) and others(234, 261, 264, 265). This process increases the recrement of macrophages and other immune cells within the IMAT and increases inflammation within the IMAT, allowing the IMAT to release more FFA into surrounding muscle tissue. This could be beneficial in one way to the muscle because it can make more ATP from FFA when there is an energy crisis; at the same time, it could induce inflammation and block insulin signaling, eventually causing insulin resistance in the muscle.
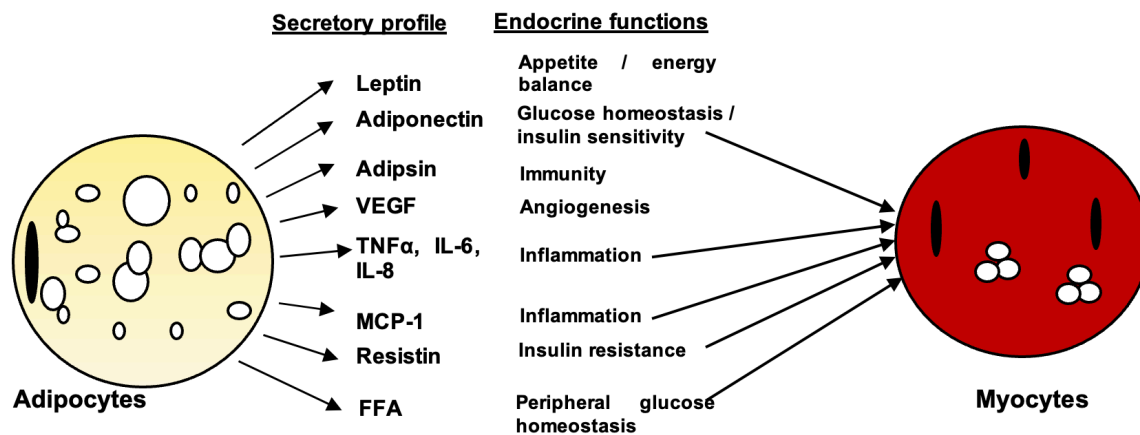
Figure 30.Secretory profile of adipocytes and potential functions in the skeletal muscle. The black filled oval shape is the nucleus, open circles represent lipid droplets in the adipocytes and muscle. Figure was adapted from(59, 231, 261, 262, 264, 265, 266, 267).

Rewiring analysis was employed to understand the changes in the molecular interaction networks between IMAT and muscle associated with the different phenotypes. The investigation found that ITGB3, EGFR, ITGA10, CALM3, ITGAV, WNT5A, and ITGB1 showed connectivity differences across all networks, indicating these genes and their interacting partners emerged as key influencers responsible for driving variations in the molecular communication from IMAT to muscle.

Integrin beta 3(ITGB3) is a cell surface receptor involved in cell adhesion and signaling. It plays an essential role in platelet aggregation, clot formation, and wound healing, indicating its involvement in tissue injury, damage, and inflammatory processes(194). In this context, ITGB3 was expressed in the muscle in all study groups and active enough to respond differently to IMAT signaling, depending on the condition. For example, it interacted with TGFB3, CX3CL1, and ADAM15 under LC network, whereas during obesity, it lost its connection with TGFB3 and ADAM15 but got new interactions with IGF2, COL1A2, NID1, FBN1, and TNXB. Interestingly, under diabetes conditions, it formed a new connection with ITGB3BP, MFG38, and FGF1 and simultaneously lost its associations with COL1A2, NID1, FBN1, and TNXB observed in obesity. Intriguingly, ITGB3 lost all the interactions observed in the OB and T2D conditions in the ATH group and maintained the connections with TGFB3 observed in LC, with IGF2 seen in OB; additionally, it established a new relationship with

IL32. Although no similar data was found to compare the findings, ITGB3 has been enormously investigated in cancer metastasis(268), tumor metabolism, epithelial to mesenchymal transition, and endothelial to mesenchymal transition(268, 269, 270). Moreover, ITGB3 found to be one of the gene identified as atherosclerosis inducing factor in the Azorean population study(271) indicating a potent pro-inflammatory mediator to induce metabolic syndrome(272). Considering its pro-inflammatory roles described in the previous studies and the interaction difference observed in the various insulin sensitivity groups in the current study, ITGB3 may have a role to play in muscle metabolism, exercise adaptions, vascularization, and regeneration and, when dysregulated, may cause muscular disorder, including insulin resistance.

Epidermal Growth Factor Receptor (EGFR) is a cell surface protein that binds to epidermal growth factor to induce receptor dimerization and tyrosine autophosphorylation, leading to cell proliferation. Mutations in this gene have been associated with cancer and inflammatory disorders(194). The metabolic role of EGFR, specifically in the skeletal muscle and adipose tissue, is lacking. One study has shown that HFD increases the expression of EGFR and its ligands in the adipose tissue macrophages (ATM). This could indicate that obesity-induced macrophage recruitment may activate the expression of EGFR and its ligands, a source of proinflammatory cytokines that increase crosstalk between macrophages adipocyte, and selective deletion of EGFR in ATM reduced HFD-induced obesity, adipose tissue derangements, resident ATM proliferation, and monocyte recruitment and insulin resistance (273). Additionally, a cross-sectional study involving humans found that EGFR gene expression was associated with adipogenesis in the SAT and VAT regardless of obesity status(274). Also, EGFR inhibitors showed promising results in lowering obesity in leptin receptor-deficient type II diabetes mice(275) and improved glucose control among lung cancer patients with diabetes(276). In our data, EGFR, like ITGB3, is expressed in the skeletal muscle of all study groups and showed higher and variable connectivity with IMAT genes. EGFR interacted with GRN, IGFBP3, S100A4, MMP2, and ST6GAL1 in the LC network and lost its connection with IGFBP3, S100A4, and MMP2 while gaining a unique relationship with DCN in the OB network. Furthermore, during the T2D state, EGFR formed new connections with LRIG2, ICAM1, ST6GAL1, and PTPN6 and regained the lost connection during OB with MMP2, while missing IGFBP3, S100A4, and DCN. Surprisingly in the ATH network, EGFR lost all the connection observed in LC, OB and T2D and maintained its connection only with PLA2G2A and ST6GAL1. Although these data need validation, the higher connectivity of EGFR observed in T2D could indicate the increased release of inflammatory cytokines from the IMAT side and their relations with the muscle. This interaction is diminished when the inflammatory reactions are decreased during ATH.

Wnt family member 5A (WNT5A) was one of the genes identified as a most rewired gene in our analysis. WNT5A is a secreted glycoprotein, it binds to G-protein coupled receptors from the Frizzled (FZD) family, low-density lipoprotein receptor-related proteins, and many tyrosine kinase-like related receptor proteins(277). It regulates cellular functions, such as proliferation, differentiation, migration, adhesion, and polarity. Interestingly, dysregulation of WNT5A signaling, usually due to WNT5A overexpression, has been implicated in developing various pathological conditions in humans, such as fibrosis, cancer, inflammatory diseases, and metabolic disorders(278). In our finding, WNT5A expression in the IMAT was correlated considerably with different signal receiver genes in the muscle under different conditions. For example, in the LC network with FZD5 and LRP5, additional interactions with VANGL2 and LDLR exist in the OB network. However, in the T2D network, its interaction was limited to VANGL2, and in the ATH network, it was only with FZD5 and RYK. The interaction of WNT5A with LDLR and LRP5 observed in OB network may suggest metabolic involvement of WNT5A particularly in lipid transport, storage, and clearance and in the inflammatory process associated with lipid metabolism. Although there is no direct relation with our data, in vitro studies in human carotid atherosclerotic tissue indicated that WNT5A significantly increased the expression of lipid uptake receptors CD36 and enhanced lipid accumulation and its inhibition with BOX5 reversed the effect suggesting there is a strong link between WNT5A expression and lipid metabolism(279). Similar studies on the atherosclerotic (vascular smooth muscle) clinical samples and in vivo experiment targeting on apolipoprotein E knockout demonstrated higher expression of WNT5A that conforms its role in cholesterol accumulation and inflammatory process(280). Additionally, in subjects with diabetes, WNT5A levels were elevated and significantly associated with fasting plasma glucose concentrations(281). Therefore, WNT5a expression in IMAT and its interaction with the skeletal muscle genes may indicate its potential role in lipid accumulation and inflammation to induce insulin resistance in the skeletal muscle.

In the differential combination network, the second approach we applied to explore the IMCN, DE analysis between IMAT and muscle was performed to identify DE senders in the IMAT and receiver genes in the muscle. In this investigation, although there were variations in network sizes across different groups, we observed a considerable overlap in the connections (edges) and genes (nodes) between these networks. However, it's important to note that we did not identify any genes expressed in all groups(networks) and exhibited differential connectivity across all networks in our rewiring analysis. In other words, this approach did not provide the insights we were seeking. Therefore, a detailed discussion of this negative result would not improve the overall clarity of this thesis. Instead, we decided for a third approach that aligns more with our research objectives and significantly enhances

our understanding of how IMAT and muscle communicate in the context of progressive insulin resistance.

6.5. GIR weighted communication network between IMAT and Muscle

In the third method, we employed a novel approach correlating gene expression data from IMAT and muscle samples with GIR to generate a bidirectional network, IMCN and MICN. This study emphasizes how the insulin sensitivity attributes linked to each gene within the communication networks give valuable insights into elucidating the rewiring mechanism of each gene under insulin-sensitive and insulin-resistant conditions.

6.5.1. Overview on the networks

In both networks (IMCN or MICN), majority of the interaction was mediated by secreted proteins and GPCRs indicating the communication mechanism was primally paracrine. Although, in the network property analysis, we observed notable differences between IMCN and MICN in the edges and nodes, both shared 421 nodes and 796 edges. This commonality indicates a substantial overlap in the molecular components of the two networks, highlighting the existence of core signaling pathways and genes essential for communication between IMAT and muscle tissues in the context of insulin sensitivity regulation. Genes exclusive to each of the communication networks exhibited significant enrichment in pathways related to Cytokine-Cytokine receptor and ECM-receptor interactions, along with associations with disease ontology terms, including hyperglycemia, hyperinsulinemia, atherosclerosis, lipid storage, and collagen diseases (Figure 23 B). The enrichment of specific genes from the communication networks in these pathways and disease terms implies that these genes have a significant role in mediating intercellular communication between IMAT and muscle, and they could be implicated in various physiological and pathological processes related to insulin sensitivity and metabolic health. For example, among pathway enriched genes in the IMCN, we found some chemokines (CXCL14 and CXCL16 are crucial for immune cell recruitment in the IMAT), tumor necrosis factors receptors (TNFRSF12A and TNFRSF19), chemokine and interleukin receptors (CXCR4, CXCR6, CX3CR1, and IL1RAP), AMHR2, and BMPR1B are well-documented in immune cell activation and migration and can modulate inflammatory responses. Additionally, ADIPOQ, CXCL16, EDN1, TF, PLA2G2A, VCAM1, ADIPOR1, ADIPOR2, CX3CR1, LDLR, MERTK, PTCH1, TFRC, TLR9, and TNFRSF12A have been identified as genes involved in various aspects of metabolic syndrome, highlighting the potential involvement of inter-tissue communication in the development or progression of metabolic disorders. Further investigation of these genes could provide cherished insights into the

molecular mechanisms underlying these conditions and potentially lead to the development of targeted therapies or interventions.

6.5.1. Clustering analysis

Clustering analysis and community detection within biological networks serve as pivotal tools in comprehending intricate biological systems(226). These techniques enable the identification of tightly interacting groups of genes, proteins, or molecules, referred to as "clusters" or "communities," which often represent functional modules with specific roles in biological processes or pathways(282). The ability to pinpoint clusters is particularly relevant in disease research, as it can unveil potential biomarkers, aiding in early diagnosis and therapeutic strategies(283, 284, 285, 286). Our study employed these methods to analyze the IMCN and MICN, uncovering 45 communities within the IMCN and 40 within the MICN, as visually presented in Figure 24A and D, respectively. This community detection revealed a diverse landscape within the network, suggesting that different modules may serve distinct biological functions. Furthermore, the enrichment analysis of these communities yielded intriguing insights into the underlying biology. Specifically, the largest modules in both networks prominently featured the Cytokine-Cytokine receptor interaction pathway. This observation underlines the significance of inflammatory processes in the context of progressive insulin resistance, as summarized in Figure 24C and F. Additionally, this inflammatory event was mediated by various pathways, including complement and coagulation cascades, Wnt signaling, and TGF signaling, as evidenced by their enrichment within clusters 3, 8, and 4 in MICN and clusters 4, 8, and 2 in IMCN. Furthermore, modules that did not exhibit tissue-specificity in both networks revealed the enrichment of insulin signaling, suggesting that the communication between IMAT and muscle tissues involves metabolic pathways. However, it is important to mark that the enrichment patterns in both IMCN and MICN were highly comparable, reflecting the substantial gene overlap between the two networks, which amounted to 73% shared genes.

6.5.2. Insulin sensitive and resistance networks of IMCN

Muscle tissue actively engages in signal transduction processes in the IMCN network, particularly in the insulin sensitivity network. This active involvement of muscle in signal processing is coupled with a significant input of inflammatory signals originating from IMAT. The activation of genes such as tumor necrosis factor receptors (TNFRs), platelet-derived growth factor receptors (PDGFRs), integrins, CD44, and CD36 in skeletal muscle signifies an influx of inflammatory signaling molecules from IMAT. TNFRs (TNFRSF10D, TNFRSF21, TNFRSF14, and TNFRSF12A, TNFRSF12) are known mediators of inflammation(59, 102, 131, 149), PDGFR (PDGFRA, and PDGFRB) signaling may reflect efforts to repair or adapt to inflammatory challenges in muscle(287, 288), integrins suggest cell adhesion and signaling interactions(120, 289), and CD44 and CD36 play roles in cell

adhesion, migration, and fatty acid uptake, respectively(147, 270, 279). Most importantly, the expression of CD36 in muscle indicates continuous stimulation by signaling molecules, including fatty acids, collagen proteins (COL1A1, COL6A3, COL4A2), ECM proteins (LAMAs and LAMBs), and Notch proteins (DDL1, DDL4, JAG1, and JAG2) from IMAT (Supplemental Table 1). The uninterrupted entry of signaling molecules from IMAT into muscle over time contributes to skeletal muscle insulin resistance characterized by a diminished response of muscle tissue to insulin, leading to impaired glucose uptake and utilization(90, 95). This can eventually result in elevated blood glucose levels and metabolic disorders like type 2 diabetes. Conversely, in the insulin resistance network of IMCN, there is a tangible shift in the skeletal muscle signal processing activity where IMAT assumes a more prominent role by intensifying it signaling output, while muscle involvement in signal processing reduces (Supplemental Table 2). This event further complicates overall metabolic health and could induces such as diabetic neuropathy, nephropathy, retinopathy, and many others(16, 25, 26, 28, 290, 291).

6.5.3. Rewired genes in the IMAT muscle communication networks.

All biological systems are inherently dynamic and entail dynamic features, such as rewiring in response to different internal and external stimuli, such as adaptation needs due to changes in nutrient availability, exercise, or cellular processes, such as cell division(292, 293, 294, 295). As described earlier, this feature in network biology is essential for studying changes in the molecular interaction network of organisms during healthy and disease states or at different time points in treatment or disease progression to facilitate innovative drug discovery endeavors. A prime example of the significance of network rewiring is evident in type T2D. In T2D, organ crosstalk triggers a complex cascade, leading to numerous genes and proteins being rewired across multiple tissues(222). This rewiring ultimately culminates in the development of insulin resistance in the target tissues. The definition of rewiring analysis should be context-specific. In this study, our rewiring analysis focused on identifying hub and rewired genes that showed variable connectivity in the crosstalk communication network between IMAT and muscle, where every gene in the network was weighted by insulin sensitivity. Our analysis identified top 50 most wired genes within the IMCN and 51 genes within the MICN. These findings are particularly intriguing because 98% of the top-selected rewired genes from IMCN or MICN were derived from IMAT. This observation indicates that IMAT exhibits dynamic behavior under conditions of insulin sensitivity and resistance. In other words, IMAT genes actively interact with muscle genes during periods of insulin sensitivity and resistance, although they have a narrow range of insulin regulation (Supplemental Figure 5). Furthermore, this phenomenon underscores the variability of muscle genes in terms of insulin sensitivity, as exemplified in Figure 26 E.

Moreover, the Jaccard index highlights striking similarities among the top rewired genes within the IMCN, particularly within the laminin IMAT genes (LAMC1, LAMB3, LAMB2, LAMA5, LAMA2, LAMA3, and LAMA4), which target muscle genes, such as BCAM, CD151, CD44, DAG1, ITGA1, ITGA3, ITGA6, ITGA5, ITGA7, ITGAV, ITGB1, ITGB4, and RPSA(Figure 28A:C). The similarity found by the Jaccard index does not indicate expression similarities among the genes. Instead, it signifies similarity in their interaction partners (they share common interaction partners). Pathway analysis of the laminin network suggested an association with extracellular matrix (ECM) proteins, cell adhesion molecules (CAMs), and muscular dystrophy. The ECM, which comprises various proteins and proteoglycans, plays a vital role in regulating processes such as differentiation, migration, repair, survival, and development. Although ECM remodeling is essential for the healthy expansion of adipose tissue, in the cases of obesity, excessive lipid accumulation in adipocytes triggers immune cell infiltration, fibrosis (excessive deposition of ECM components such as collagens, elastin, and fibronectin), and inflammation, which is often a consequence of local hypoxia and ultimately leads to insulin resistance(116, 289, 296, 297). Laminins are a group of ECM proteins found within the basement membrane, which provide structural support and facilitate cellular adhesion and migration. By interacting with cell surface receptors, laminins initiate intracellular signaling pathways that guide distinct survival and differentiation processes(298). While no directly comparable data are available, most existing evidence points to the involvement of laminins in cancer and cancer-related phenotypes; interestingly, in the context of obesity, both mRNA and protein expression levels of LAMA4 are elevated in the Subcutaneous Adipose Tissue (SAT) and Visceral Adipose Tissue (VAT) of obese individuals. This observation strongly suggests its role in adipogenesis and in the development of insulin resistance(299). Furthermore, studies in male mice revealed that the absence of LAMA4 resulted in enhanced energy expenditure and promotion of a beige phenotype in the SAT(300). Additionally, it leads to decreased adipose tissue expansion and reduced weight gain(301). Similarly, in our datasets, LAMA4 expression in IMAT negatively correlated with insulin sensitivity. This suggests a potential role for LAMA4 in adipocyte expansion, and its interaction with DAG1 and ITGA7 in the muscle could indicate the development of skeletal muscle insulin resistance. Because DAG1 and ITGA7 had a strong negative correlation with insulin sensitivity in the muscle, they were further indicated in muscular dystrophy in the enrichment analysis. Therefore, LAMA4, DAG1, and ITGA7 could be ideal candidates to understand how LAMA4 via DAG1 and ITGA7 induces skeletal muscle insulin resistance.

The collagen genes in IMAT (COL1A1, COL1A2, COL4A2, and COL18A1) had common target genes in the muscle (CD36, CD93, and CD44) and integrins (ITGAs and ITGBs) (Figure 28 D:F). This network is enriched with many disease ontology terms, such as

myopathy, collagen diseases, hyperglycemia, atherosclerosis, and arteriosclerosis. The metabolic role of collagen proteins is not well documented, particularly in the context of adipocyte and muscle insulin resistance. Few human studies have demonstrated that COL1A1 is positively associated with increased muscle stiffening(302) and the pathogenesis of T2D and CVD (303, 304). In contrast, IMAT COL1A1 expression is positively correlated with insulin sensitivity in our study. Additionally, a study in the jejunum of diabetic rats confirmed that COL1A1 has hypoglycemic activity(305), indicating that this gene may play a role in insulin sensitivity and resistance in selective tissues. One study showed that COL4A2 is highly expressed in the SAT of obese individuals with and without T2D compared to normal individuals(306). IMAT COL4A2 positively and weakly correlated with insulin sensitivity in the current dataset. CD36 is one of the target genes in the muscle for COL4A2. CD36 expression in the muscle is also weakly and positively correlated with insulin sensitivity, indicating that its expression decreases as insulin resistance advances. Subsequently, muscle FFA uptake rate decreases, and increased lipid accumulation in the myocyte blocks insulin signaling. Our data indicate that CD36 is associated with the development of metabolic syndrome and muscular dysfunction, making it a promising candidate for future validation with the aim of understanding how disturbed collagen proteins(COL4A2) in the IMAT accelerate skeletal muscle adiposity and insulin resistance. Furthermore, the Jaccard index identified strong similarities among bone morphogenetic genes such as BMP4, BMP6, and BMP8A in IMAT (Figure 28 G: I). These genes have a common target in the muscle (TGFBR2, ACVR2A, BMPR2, TGFBR1, ACVR2B, AMHR2, GREM2, LRP6, BMPR1B, BMPR1A, and ACVR1) and show variable positive and negative correlations with insulin sensitivity. This module is functionally associated with TGF-β signaling and cytokine-cytokine receptor interactions, suggesting its role in inflammatory responses. Research on the role of bone morphogenetic genes or proteins associated with metabolic syndrome is notably lacking despite the reasonably documented functions of these genes in cancer and bone formation. Limited in vivo and in vitro studies on adipocytes have revealed potential connections between specific bone morphogenetic genes, specifically BMP4, BMP6, BMP7, and BMP9, and the regulation of adipogenesis(307). Our analysis uncovered a significant negative correlation between insulin sensitivity and BMP4 and BMP6 expression in the IMAT. These findings align with similar reports in humans, where elevated serum BMP4 levels were observed in individuals with obesity and metabolic syndrome (307, 308, 309, 310, 311, 312). Furthermore, animal models have provided additional insights into BMP4 expression. Hyperglycemia and high levels of free fatty acids have been shown to stimulate BMP4 expression (311), while inhibition of glucose-stimulated insulin secretion in diabetic rodents results in upregulation of BMP4 expression in pancreatic islets(312). Collectively, these findings collectively suggest the crucial role of

BMP4 in body metabolism. However, literature evidence on BMP6 shows that obese and T2D mice treated with BMP6 exhibit lower circulating lipid and glucose levels, in contrast to our findings. Therefore, based on the data, BMP4 expression in IMAT and its interaction with various muscle genes during insulin sensitivity and resistance could be potential research targets to understand muscle insulin resistance in response to IMAT signaling.

Calmodulin proteins in IMAT would be an exciting area to explore how they affect skeletal muscle metabolism, as they are involved in insulin, calcium, phosphatidylinositol signaling, and disease development, such as myopathy and atherosclerosis, particularly CALM1, CALM2, and CAML3, which showed a positive correlation with insulin resistance in the IMAT (Figure 28 J: L). Their interaction with MIP, MYLK2, and SCN4A genes, which are correlated with insulin resistance in the muscle, could potentially facilitate the discovery of therapeutics to treat myopathy and other muscular disorders.

In the context of MICN, a unique pattern emerges in the Plexin IMAT genes, which exhibit a significantly higher Jaccard similarity amongst themselves. This finding strongly suggests that these Plexin IMAT genes interact with muscle semaphorins and other genes within the network. Furthermore, IMAT integrin genes (specifically, ITGA7, ITGB4, ITGA6, and DAG1) serve as targets for a diverse array of laminin genes, including IGF1, ECM1, COL6A1, FN1, THBS2, and ADAM9. Importantly, all these genes are integral components of the ECM. As previously discussed, the enrichment of ECM genes signifies ECM remodeling and adipocyte expansion within the tissue, a characteristic feature associated with insulin resistance. In light of these findings, it is increasingly apparent that the signaling pathways involving semaphorins or laminins from muscle to IMAT through Plexin or integrin channels hold immense potential for uncovering novel therapeutic avenues for addressing insulin resistance and muscular disorders, as illustrated in Figure 29A: F.

7. Perspective

Our study has disclosed the dynamic nature of IMAT during interactions with skeletal muscle under changing insulin sensitivity and resistance conditions. This discovery holds significant promise, as it opens new avenues for research and potential therapeutic targets for addressing conditions such as diabetes, insulin resistance, and muscular disorders.

In the future, further investigations aided by single-cell RNA sequencing will be essential to look deeper into the cellular heterogeneity within IMAT. This approach will enable us to pinpoint specific cell populations within IMAT that directly impact skeletal muscle insulin sensitivity. Understanding this cellular heterogeneity could lead to more precise and effective interventions.

Additionally, incorporating metabolomics profiling of both IMAT and muscle will provide valuable insights into the interactions of metabolites between these tissues. This approach can identify candidate metabolites crucial in regulating muscle insulin sensitivity. Such findings could lay out the way for targeted interventions at the metabolic level to enhance insulin sensitivity and overall metabolic health.

8. Summary reports for the side projects

8.1. Skeletal muscle and IMAT gene expression profiling identifies new biomarkers with prognostic significance for insulin resistance progression and intervention response.

In this project, we applied a predictive module to identify genes in IMAT or muscle that hold prognostic significance in the development and treatment of insulin resistance. This study utilized samples from individuals with OB and T2D in both IMAT and muscle tissues. We employed multivariate regression analysis to simultaneously predict FPG and GIR based on gene expression in skeletal muscle and IMAT. Subsequently, we identified the top 59 genes in both tissues that significantly correlated with insulin resistance, as measured by FPG and GIR, for further analysis.

Upon performing clustering analysis on these genes, we observed three distinct clusters in the muscle sample, displaying clear expression patterns during insulin sensitivity and resistance conditions. However, the IMAT sample did not exhibit a similar expression pattern. Furthermore, we utilized this molecular information from skeletal muscle and IMAT in clinically classified OB and T2D individuals for genetic classification. Our analysis aimed to test the hypothesis that genetic classification is more robust than conventional clinical markers for disease diagnosis and treatment. To achieve this, we employed a k-Nearest Neighbors (kNN) algorithm(313) to classify tissue samples based on their expression profiles. The kNN method is non-parametric and relies on measuring the distance between data points to classify new data points. Consequently, we generated three nearest neighbor networks (NNNs) per tissue, indicating the similarity of samples within the three expression clusters. We calculated a predictive classification score for each sample using these networks and direct network neighbors. In the case of muscle tissue, the sample classification was identical across all three NNNs, except for two OB samples (Pb029 and Pb043) and three T2D samples (Pb034, PB053, and Pb032) that clustered differently. However, when averaging the predictive classification scores across the three clusters, one participant with OB (Pb043) was classified as T2D, and two participants with T2D (Pb034 and Pb053) were classified as OB.

In the IMAT analysis, averaging across the three clusters led to different genetic classifications for patients Pb043 and Pb033, who were clinically diagnosed as OB and T2D, respectively. These results suggest that traditional blood-based patient classification may not accurately represent the actual genetic makeup of individual disease states. An incorrect diagnosis could result in unintended treatment that negatively impacts a patient's quality of life.

To further investigate whether gene expression profiles within muscle and IMAT could predict disease progression, we analyzed clinical and mRNA data from individuals with obesity undergoing a combined weight loss and exercise training intervention in a separate cohort. From the initial cohort, we selected fifteen candidate genes from the top 59 genes based on their predictive power for insulin sensitivity (SIN3A, UBTD1, ST3GAL2, and NAPB)(263), linkage to diabetes-associated SNPs (AASS, DBNDD1, PDK4, PIGA, POLR3GL, SNAP23, SPCS2, SSU72, and UBTD1), and their involvement in skeletal muscle lipid and glucose metabolism (ARF1, BCAT2, and LDHD)(263). We then measured the expression of these 15 genes in the muscle among individuals with obesity in the second cohort, both before and after exercise intervention. Among these genes, LDHD, ARF1, NAPB, POLR3GL, and SNAP23 showed significant changes in expression between the pre- and post-intervention phases. However, only ARF1 expression significantly correlated with the change in FPG, while none of the differentially expressed genes could significantly predict other clinical variables measured. Furthermore, the change in GIR did not significantly correlate with any of the 15 genes, while changes in FPG, BW, FFM, and BMI could be significantly predicted by ST3GAL2 expression. Additionally, FG, FFM, and BMI changes were associated with SIN3A expression, and FFM was associated with AASS expression.

These findings led us to the conclusion that individual susceptibility to an exercise intervention aimed at improving glucose homeostasis is independent of individual clinical factors but correlates with individual gene expression profiles before the intervention. Moreover, low AASS, ARF1, and SIN3A expression on exercise intervention was associated with a favorable health prognosis, while an increase in ST3GAL2 expression increased the likelihood of an effective intervention. In summary, gene expression profiles in muscle tissues hold predictive potential for individual insulin resistance states.

Note: The project is published and can be found in the following link.
https://pubmed.ncbi.nlm.nih.gov/36790478/

8.2. Circadiomics analysis to understand the role of Class 3 phosphatidylinositol-3 kinase (PI3K) signaling.

In this collaborative project with Dr. Ganna Panasyuk (PI) and others, we have shown class 3 PI3K coactivates the circadian clock to promote rhythmic de novo purine synthesis.

Briefly, class 3 phosphatidylinositol-3-kinase (PI3K) has a canonical pro-catabolic function and is known best for its essential role as a lipid kinase in endocytosis and lysosomal degradation by autophagy(314). Furthermore, PI3K has a nuclear function in gene transcription as a coactivator of the heterodimer of two transcription factors, Bmal1 and Clock to act as a master regulator of the mammalian circadian clock gene network(315). However, class 3 PI3K activity relies on the lipid kinase Vps34 and regulatory subunit Vps15. Although both subunits of class 3 PI3K interact with RNA polymerase II and co-localize with active transcription sites, exclusive loss of Vps15 in cells blunts the transcriptional activity of Bmal1–Clock(314). Thus, we could show the ability of Vps15 to coactivate Bmal1–Clock independently in liver cells. Vps15 is required for liver metabolic rhythmicity, and our study has shown that Vps15 promotes pro-anabolic de novo purine nucleotide synthesis. Furthermore, our study has displayed that Vps15 activates the transcription of Ppat, a key enzyme for the production of inosine monophosphate, a central metabolic intermediate for purine synthesis. Finally, we demonstrate that Vps15 levels are decreased on the promoters of Bmal1 targets, Nr1d1, and Ppat in fasting, which represses clock transcriptional activity. In conclusion, this study has established the role of class 3 PI3K signaling in the temporal regulation of energy homeostasis.

Note: In this project I did the bioinformatics works particular analyzing and identifying the circadian genes, proteins, and metabolites in the liver wide type(WT) cells, Vps15 positive and negative cells, Vps34 positive and negative cells. The work is published in nature cell biology and can be accessed freely using the link.

https://www.nature.com/articles/s41556-023-01171-3

8.3. Unveiling early development and complications of T2D through cell-free DNA biomarkers.

Liquid biopsy offers a valuable opportunity to detect, analyze, and monitor disease progression through molecular profiling(316). It encompasses various biological components, such as circulating tumor DNA (ctDNA), mitochondrial DNA (mtDNA), and cell-free DNA (cfDNA)(317). Although the cfDNA test is less invasive and enhances clinical decision-making, it has the drawback of yielding relatively small amounts of cfDNA using current isolation techniques(318). cfDNA is released into the bloodstream from cells undergoing apoptosis or necrosis, and its levels are correlated with inflammation and tissue injury in various diseases(319). Unfortunately, cfDNA lacks specificity for tissue or cell types(320), making extensive genomic profiling necessary to identify cfDNA from specific sources(321, 322). In this study, we aimed to identify specific biomarkers relevant to the early diagnosis, progression, and complications of type 2 diabetes (T2D) using cfDNA.

Our study collected cfDNA samples from healthy individuals, individuals with T2D, and individuals with T2D and complications (25 samples in each group) at Heidelberg University Hospital in Germany. These samples were sent to GenxPro (Frankfurt, Germany) for whole-exome and methylation sequencing.

In exome sequencing, our primary goal was to identify differential gene reads that were mapped to the exome region of the genome among the groups. We checked the quality of the sequencing data in FASTQ format using the FASTQC tool(323). All sequencing reads met the quality requirements, although we observed a high level of PCR amplification, which was likely due to the low abundance of cfDNA in the samples. Sequencing reads were mapped to the human reference genome (hg38) using Bowtie2(324), a fast and memory-efficient tool for aligning short reads to a long reference sequence (hg38). Subsequently, we generated Binary Alignment Map (BAM) files indicating the positions of the reads on the chromosomes and their mapping qualities. We performed read summarization using the featureCounts function in the subread tool (325) by counting mapped reads in the BAM files for genes in the exon region of the genome. This process is based on a General Feature Format (GFF) file that describes gene annotations. As a result, we identified the read counts for 44,714 genes in each library. After creating the count matrix, we preprocessed the data for differential expression (DE) and functional enrichment analysis. Preliminary results showed no DE genes between conditions, and clear clusters between groups were not observed (Supplemental Figure 6).

In DNA methylation sequencing, our primary objective was to determine the specific cell or tissue type responsible for releasing cfDNA by analyzing different methylation patterns in each group. Methylation is an epigenetic mechanism that regulates gene expression and contributes to cellular development(326). We used Bismark for DNA methylation data

analysis, a popular bioinformatics tool for bisulfite sequencing data analysis, commonly used for studying DNA methylation patterns at single-base resolution(327). Bisulfite treatment converts unmethylated cytosine residues to uracil while leaving methylated cytosines unchanged. First, we removed all sequences containing adapters from the raw data using Trim Galore(328). We then aligned the raw methylation sequencing data to a bisulfite-converted reference genome and methylation information from the aligned BAM files was extracted. This reports the methylation status at each cytosine position in the reference genome. Methylation alignment and pattern extraction are computationally intensive processes requiring expertise. Our initial analysis using the R package EdgeR (329)and methylkit(330) revealed no differences in methylation patterns among the study subjects(Supplemental Figure 6).

This project is currently ongoing, and we will continue to communicate new data as they become available.

9. Reference

1.   Petersmann A, Müller-Wieland D, Müller UA, Landgraf R, Nauck M, Freckmann G, et al. Definition, Classification and Diagnosis of Diabetes Mellitus. Exp Clin Endocrinol Diabetes. 2019;127(S 01):S1-s7.

2.   Wilcox G. Insulin and insulin resistance. Clin Biochem Rev. 2005;26(2):19-39.

3.   Association AD. 2. Classification and Diagnosis of Diabetes. Diabetes Care. 2014;38(Supplement_1):S8-S16.

4.   Magliano DJ, Boyko EJ. IDF Diabetes Atlas. 10th ed. Brussels2021.

5.   Ogurtsova K, Guariguata L, Barengo NC, Ruiz PL, Sacre JW, Karuranga S, et al. IDF diabetes Atlas: Global estimates of undiagnosed diabetes in adults for 2021. Diabetes Res Clin Pract. 2022;183:109118.

6.   Tonnies T, Rathmann W, Hoyer A, Brinks R, Kuss O. Quantifying the underestimation of projected global diabetes prevalence by the International Diabetes Federation (IDF) Diabetes Atlas. BMJ Open Diabetes Res Care. 2021;9(1).

7.   Marks BE, Wolfsdorf JI. Monitoring of Pediatric Type 1 Diabetes. Front Endocrinol (Lausanne). 2020;11:128.

8.   Primavera M, Giannini C, Chiarelli F. Prediction and Prevention of Type 1 Diabetes. Front Endocrinol (Lausanne). 2020;11:248.

9.   Haak T, Gölz S, Fritsche A, Füchtenbusch M, Siegmund T, Schnellbächer E, et al. Therapy of Type 1 Diabetes. Exp Clin Endocrinol Diabetes. 2019;127(S 01):S27-s38.

10.   Landgraf R, Aberle J, Birkenfeld AL, Gallwitz B, Kellerer M, Klein H, et al. Therapy of Type 2 Diabetes. Exp Clin Endocrinol Diabetes. 2019;127(S 01):S73-s92.

11.   Laakso M. Biomarkers for type 2 diabetes. Mol Metab. 2019;27s(Suppl):S139-s46.

12.   Tanase DM, Gosav EM, Costea CF, Ciocoiu M, Lacatusu CM, Maranduca MA, et al. The Intricate Relationship between Type 2 Diabetes Mellitus (T2DM), Insulin Resistance (IR), and Nonalcoholic Fatty Liver Disease (NAFLD). J Diabetes Res. 2020;2020:3920196.

13.   Szmuilowicz ED, Josefson JL, Metzger BE. Gestational Diabetes Mellitus. Endocrinol Metab Clin North Am. 2019;48(3):479-93.

14.   Sweeting A, Wong J, Murphy HR, Ross GP. A Clinical Update on Gestational Diabetes Mellitus. Endocr Rev. 2022;43(5):763-93.

15.   Damanik J, Yunir E. Type 2 Diabetes Mellitus and Cognitive Impairment. Acta Med Indones. 2021;53(2):213-20.

16.   Demir S, Nawroth PP, Herzig S, Ekim Üstünel B. Emerging Targets in Type 2 Diabetes and Diabetic Complications. Adv Sci (Weinh). 2021;8(18):e2100275.

17.   Cole JB, Florez JC. Genetics of diabetes mellitus and diabetes complications. Nat Rev Nephrol. 2020;16(7):377-90.

18.	Biondi B, Kahaly GJ, Robertson RP. Thyroid Dysfunction and Diabetes Mellitus: Two Closely Associated Disorders. Endocr Rev. 2019;40(3):789-824.

19.	Agashe S, Petak S. Cardiac Autonomic Neuropathy in Diabetes Mellitus. Methodist Debakey Cardiovasc J. 2018;14(4):251-6.

20.	Winters B. Promoting wound healing in the diabetic patient. AORN J. 1982;35(6):1083-7.

21.	Burgess JL, Wyant WA, Abdo Abujamra B, Kirsner RS, Jozic I. Diabetic Wound-Healing Science. Medicina (Kaunas). 2021;57(10).

22.	Tchero H, Kangambega P, Fluieraru S, Bekara F, Teot L. Management of infected diabetic wound: a scoping review of guidelines. F1000Res. 2019;8:737.

23.	Association AD. Diagnosis and Classification of Diabetes Mellitus. Diabetes Care. 2004;27(suppl_1):s5-s10.

24.	Powers AC. Diabetes mellitus: Diagnosis, Classification, and Pathophysiology. Harrison's principles of internal medicine. 19 ed: McGraw Hill; 2015. p. 2399-407.

25.	Prevention CfDCa. Diabetes Symptoms 2023 [Available from: https://www.cdc.gov/diabetes/basics/symptoms.html.

26.	Prevention CfDCa. Prevent Diabetes Complications 2023 [Available from: https://www.cdc.gov/diabetes/managing/problems.html#:~:text=Common%20diabetes%20 health%20complications%20include,how%20to%20improve%20overall%20health.&text= How%20to%20be%20heart%2Dhealthy%20if%20you%20have%20diabetes.

27.	Powers AC. Diabetes mellitus: management and Therapies. Harrison's principles of internal medicine: McGraw Hill; 2015. p. 2405-14.

28.	Endalifer ML, Diress G. Epidemiology, Predisposing Factors, Biomarkers, and Prevention Mechanism of Obesity: A Systematic Review. J Obes. 2020;2020:6134362.

29.	Kwansa AL, Akparibo R, Cecil JE, Infield Solar G, Caton SJ. Risk Factors for Overweight and Obesity within the Home Environment of Preschool Children in Sub-Saharan Africa: A Systematic Review. Nutrients. 2022;14(9).

30.	Lin X, Li H. Obesity: Epidemiology, Pathophysiology, and Therapeutics. Front Endocrinol (Lausanne). 2021;12:706978.

31.	Marcelin G, Silveira ALM, Martins LB, Ferreira AV, Clément K. Deciphering the cellular interplays underlying obesity-induced adipose tissue fibrosis. J Clin Invest. 2019;129(10):4032-40.

32.	WHO. Obesity 2023 [Available from: https://www.who.int/health-topics/obesity/#tab=tab_1.

33.	Caballero B. Humans against Obesity: Who Will Win? Adv Nutr. 2019;10(suppl_1):S4-s9.

34.	Qatanani M, Lazar MA. Mechanisms of obesity-associated insulin resistance: many choices on the menu. Genes Dev. 2007;21(12):1443-55.

35.   Safaei M, Sundararajan EA, Driss M, Boulila W, Shapi'i A. A systematic literature review on obesity: Understanding the causes & consequences of obesity and reviewing various machine learning approaches used to predict obesity. Comput Biol Med. 2021;136:104754.

36.   Pi-Sunyer FX. Obesity: criteria and classification. Proc Nutr Soc. 2000;59(4):505-9.

37.   Michel S, Linder N, Eggebrecht T, Schaudinn A, Blüher M, Dietrich A, et al. Abdominal subcutaneous fat quantification in obese patients from limited field-of-view MRI data. Scientific Reports. 2020;10(1):19039.

38.   Fang H, Berg E, Cheng X, Shen W. How to best assess abdominal obesity. Curr Opin Clin Nutr Metab Care. 2018;21(5):360-5.

39.   Sizoo D, de Heide LJM, Emous M, van Zutphen T, Navis G, van Beek AP. Measuring Muscle Mass and Strength in Obesity: a Review of Various Methods. Obesity Surgery. 2021;31(1):384-93.

40.   Björntorp P. The regulation of adipose tissue distribution in humans. Int J Obes Relat Metab Disord. 1996;20(4):291-302.

41.   Chait A, den Hartigh LJ. Adipose Tissue Distribution, Inflammation and Its Metabolic Consequences, Including Diabetes and Cardiovascular Disease. Front Cardiovasc Med. 2020;7:22.

42.   Gil A, Olza J, Gil-Campos M, Gomez-Llorente C, Aguilera CM. Is adipose tissue metabolically different at different sites? Int J Pediatr Obes. 2011;6 Suppl 1:13-20.

43.   Kwok KHM, Lam KSL, Xu A. Heterogeneity of white adipose tissue: molecular basis and clinical implications. Experimental & Molecular Medicine. 2016;48(3):e215-e.

44.   Hansen E, Hajri T, Abumrad NN. Is all fat the same? The role of fat in the pathogenesis of the metabolic syndrome and type 2 diabetes mellitus. Surgery. 2006;139(6):711-6.

45.   Jensen MD. Role of body fat distribution and the metabolic complications of obesity. J Clin Endocrinol Metab. 2008;93(11 Suppl 1):S57-63.

46.   Ibrahim MM. Subcutaneous and visceral adipose tissue: structural and functional differences. Obes Rev. 2010;11(1):11-8.

47.   Jensen MD. Is visceral fat involved in the pathogenesis of the metabolic syndrome? Human model. Obesity (Silver Spring). 2006;14 Suppl 1:20s-4s.

48.   Dennis L. Kasper ASF, Stephen L. Hauser, Dan L. Longo, J. Larry Jameson, Joseph Loscalzo. Harrison's Principles of Internal Medicine: McGraw Hill; 2015.

49.   Sethi JK. Obesity: Adipogenesis and Insulin Resistance. IDrugs. 2000;3(8):884-6.

50.   Mayoral LP, Andrade GM, Mayoral EP, Huerta TH, Canseco SP, Rodal Canales FJ, et al. Obesity subtypes, related biomarkers & heterogeneity. Indian J Med Res. 2020;151(1):11-21.

51.   Ahmed B, Sultana R, Greene MW. Adipose tissue and insulin resistance in obese. Biomed Pharmacother. 2021;137:111315.

52.   DeFronzo RA. Insulin resistance, lipotoxicity, type 2 diabetes and atherosclerosis: the missing links. The Claude Bernard Lecture 2009. Diabetologia. 2010;53(7):1270-87.

53.   Engin ABEA. Obesity and Lipotoxicity. AtillaEngin ABE, editor: Springer; 2017. 618 p.

54.   Jeong EM, Chung J, Liu H, Go Y, Gladstein S, Farzaneh-Far A, et al. Role of Mitochondrial Oxidative Stress in Glucose Tolerance, Insulin Resistance, and Cardiac Diastolic Dysfunction. J Am Heart Assoc. 2016;5(5).

55.   Wang CH, Wei YH. Role of mitochondrial dysfunction and dysregulation of Ca(2+) homeostasis in the pathophysiology of insulin resistance and type 2 diabetes. J Biomed Sci. 2017;24(1):70.

56.   Tangvarasittichai S. Oxidative stress, insulin resistance, dyslipidemia and type 2 diabetes mellitus. World J Diabetes. 2015;6(3):456-80.

57.   Sergi D, Naumovski N, Heilbronn LK, Abeywardena M, O'Callaghan N, Lionetti L, et al. Mitochondrial (Dys)function and Insulin Resistance: From Pathophysiological Molecular Mechanisms to the Impact of Diet. Front Physiol. 2019;10:532.

58.   Garcia-Rio F, Alvarez-Puebla MJ, Esteban-Gorgojo I, Barranco P, Olaguibel JM. Obesity and Asthma: Key Clinical Questions. J Investig Allergol Clin Immunol. 2019;29(4):262-71.

59.   Kawai T, Autieri MV, Scalia R. Adipose tissue inflammation and metabolic dysfunction in obesity. Am J Physiol Cell Physiol. 2021;320(3):C375-C91.

60.   Muller TD, Bluher M, Tschop MH, DiMarchi RD. Anti-obesity drug discovery: advances and challenges. Nat Rev Drug Discov. 2022;21(3):201-23.

61.   Nogueiras R, Nauck MA, Tschop MH. Gut hormone co-agonists for the treatment of obesity: from bench to bedside. Nat Metab. 2023;5(6):933-44.

62.   Yoo ES, Yu J, Sohn JW. Neuroendocrine control of appetite and metabolism. Exp Mol Med. 2021;53(4):505-16.

63.   Joly-Amado A, Cansell C, Denis RG, Delbes AS, Castel J, Martinez S, et al. The hypothalamic arcuate nucleus and the control of peripheral substrates. Best Pract Res Clin Endocrinol Metab. 2014;28(5):725-37.

64.   Hall JE. Guyton and hall textbook of medical physiology. 13 ed: Saunders; 2015.

65.   Tran LT, Park S, Kim SK, Lee JS, Kim KW, Kwon O. Hypothalamic control of energy expenditure and thermogenesis. Exp Mol Med. 2022;54(4):358-69.

66.   Friedman JM. Leptin and the regulation of body weigh. Keio J Med. 2011;60(1):1-9.

67.   Friedman JM. Leptin and the endocrine control of energy balance. Nat Metab. 2019;1(8):754-64.

68.   Yu CD, Xu QJ, Chang RB. Vagal sensory neurons and gut-brain signaling. Curr Opin Neurobiol. 2020;62:133-40.

69. Browning KN, Verheijden S, Boeckxstaens GE. The Vagus Nerve in Appetite Regulation, Mood, and Intestinal Inflammation. Gastroenterology. 2017;152(4):730-44.

70. Chadt A, Al-Hasani H. Glucose transporters in adipose tissue, liver, and skeletal muscle in metabolic health and disease. Pflugers Arch. 2020;472(9):1273-98.

71. Sharabi K, Tavares CD, Rines AK, Puigserver P. Molecular pathophysiology of hepatic glucose production. Mol Aspects Med. 2015;46:21-33.

72. Rorsman P, Ashcroft FM. Pancreatic beta-Cell Electrical Activity and Insulin Secretion: Of Mice and Men. Physiol Rev. 2018;98(1):117-214.

73. Weiss M, Steiner DF, Philipson LH. Insulin Biosynthesis, Secretion, Structure, and Structure-Activity Relationships. In: Feingold KR, Anawalt B, Blackman MR, Boyce A, Chrousos G, Corpas E, et al., editors. Endotext. South Dartmouth (MA)2000.

74. Hulse RE, Ralat LA, Wei-Jen T. Structure, function, and regulation of insulin-degrading enzyme. Vitam Horm. 2009;80:635-48.

75. Campbell JE, Newgard CB. Mechanisms controlling pancreatic islet cell function in insulin secretion. Nat Rev Mol Cell Biol. 2021;22(2):142-58.

76. De Meyts P. The Insulin Receptor and Its Signal Transduction Network. In: Feingold KR, Anawalt B, Blackman MR, Boyce A, Chrousos G, Corpas E, et al., editors. Endotext. South Dartmouth (MA)2000.

77. Leto D, Saltiel AR. Regulation of glucose transport by insulin: traffic control of GLUT4. Nat Rev Mol Cell Biol. 2012;13(6):383-96.

78. Saltiel AR, Kahn CR. Insulin signalling and the regulation of glucose and lipid metabolism. Nature. 2001;414(6865):799-806.

79. Norton L, Shannon C, Gastaldelli A, DeFronzo RA. Insulin: The master regulator of glucose metabolism. Metabolism. 2022;129:155142.

80. Ruderman NB, Carling D, Prentki M, Cacicedo JM. AMPK, insulin resistance, and the metabolic syndrome. J Clin Invest. 2013;123(7):2764-72.

81. Santoro A, McGraw TE, Kahn BB. Insulin action in adipocytes, adipose remodeling, and systemic effects. Cell Metab. 2021;33(4):748-57.

82. Perry RJ, Samuel VT, Petersen KF, Shulman GI. The role of hepatic lipids in hepatic insulin resistance and type 2 diabetes. Nature. 2014;510(7503):84-91.

83. Richter EA, Hargreaves M. Exercise, GLUT4, and skeletal muscle glucose uptake. Physiol Rev. 2013;93(3):993-1017.

84. Hammond ML, Bowman LH. Insulin stimulates the translation of ribosomal proteins and the transcription of rDNA in mouse myoblasts. J Biol Chem. 1988;263(33):17785-91.

85. Kelmer Sacramento E, Kirkpatrick JM, Mazzetto M, Baumgart M, Bartolome A, Di Sanzo S, et al. Reduced proteasome activity in the aging brain results in ribosome stoichiometry loss and aggregation. Mol Syst Biol. 2020;16(6):e9596.

86. Yoon MS. The Role of Mammalian Target of Rapamycin (mTOR) in Insulin Signaling. Nutrients. 2017;9(11).

87.   Wang X, Proud CG. The mTOR pathway in the control of protein synthesis. Physiology (Bethesda). 2006;21:362-9.

88.   Goodpaster BH, Bergman BC, Brennan AM, Sparks LM. Intermuscular adipose tissue in metabolic disease. Nat Rev Endocrinol. 2023;19(5):285-98.

89.   Rossi AP, Gottin L, Donadello K, Schweiger V, Brandimarte P, Zamboni GA, et al. Intermuscular Adipose Tissue as a Risk Factor for Mortality and Muscle Injury in Critically Ill Patients Affected by COVID-19. Front Physiol. 2021;12:651167.

90.   Sachs S, Zarini S, Kahn DE, Harrison KA, Perreault L, Phang T, et al. Intermuscular adipose tissue directly modulates skeletal muscle insulin sensitivity in humans. Am J Physiol Endocrinol Metab. 2019;316(5):E866-e79.

91.   Sparks LM, Goodpaster BH, Bergman BC. The Metabolic Significance of Intermuscular Adipose Tissue: Is IMAT a Friend or a Foe to Metabolic Health? Diabetes. 2021;70(11):2457-67.

92.   Addison O, Marcus RL, Lastayo PC, Ryan AS. Intermuscular fat: a review of the consequences and causes. Int J Endocrinol. 2014;2014:309570.

93.   Ogawa M, Lester R, Akima H, Gorgey AS. Quantification of intermuscular and intramuscular adipose tissue using magnetic resonance imaging after neurodegenerative disorders. Neural Regen Res. 2017;12(12):2100-5.

94.   Waters DL. Intermuscular Adipose Tissue: A Brief Review of Etiology, Association With Physical Function and Weight Loss in Older Adults. Ann Geriatr Med Res. 2019;23(1):3-8.

95.   Kim JE, Dunville K, Li J, Cheng JX, Conley TB, Couture CS, et al. Intermuscular Adipose Tissue Content and Intramyocellular Lipid Fatty Acid Saturation Are Associated with Glucose Homeostasis in Middle-Aged and Older Adults. Endocrinol Metab (Seoul). 2017;32(2):257-64.

96.   Borghi S, Bonato M, La Torre A, Banfi G, Vitale JA. Interrelationship among thigh intermuscular adipose tissue, cross-sectional area, muscle strength, and functional mobility in older subjects. Medicine (Baltimore). 2022;101(26):e29744.

97.   Carbone S. Intramuscular and Intermuscular Adipose Tissue in Older Adults: Noncardiac Body Composition Depots and HF Risk. JACC Heart Fail. 2022;10(7):494-7.

98.   Ruan XY, Gallagher D, Harris T, Albu J, Heymsfield S, Kuznia P, et al. Estimating whole body intermuscular adipose tissue from single cross-sectional magnetic resonance images. J Appl Physiol (1985). 2007;102(2):748-54.

99.   Gamboa JL, Carranza-Leon D, Crescenzi R, Pridmore M, Peng D, Marton A, et al. Intermuscular adipose tissue in patients with systemic lupus erythematosus. Lupus Sci Med. 2022;9(1).

100.   Vella CA, Allison MA. Associations of abdominal intermuscular adipose tissue and inflammation: The Multi-Ethnic Study of Atherosclerosis. Obes Res Clin Pract. 2018;12(6):534-40.

101.   Wang Y, Wang Y, Li G, Zhang H, Yu H, Xiang J, et al. Associations of intermuscular adipose tissue and total muscle wasting score in PG-SGA with low muscle radiodensity and

mass in nonmetastatic colorectal cancer: A two-center cohort study. Front Nutr. 2022;9:967902.

102.	Yu F, Fan Y, Sun H, Li T, Dong Y, Pan S. Intermuscular adipose tissue in Type 2 diabetes mellitus: Non-invasive quantitative imaging and clinical implications. Diabetes Res Clin Pract. 2022;187:109881.

103.	Suka Aryana IGP, Paulus IB, Kalra S, Daniella D, Kuswardhani RAT, Suastika K, et al. The Important Role of Intermuscular Adipose Tissue on Metabolic Changes Interconnecting Obesity, Ageing and Exercise: A Systematic Review. touchREV Endocrinol. 2023;19(1):54-9.

104.	Frank AP, de Souza Santos R, Palmer BF, Clegg DJ. Determinants of body fat distribution in humans may provide insight about obesity-related health risks. J Lipid Res. 2019;60(10):1710-9.

105.	Boettcher M, Machann J, Stefan N, Thamer C, Haring HU, Claussen CD, et al. Intermuscular adipose tissue (IMAT): association with other adipose tissue compartments and insulin sensitivity. J Magn Reson Imaging. 2009;29(6):1340-5.

106.	Lim JP, Chong MS, Tay L, Yang YX, Leung BP, Yeo A, et al. Inter-muscular adipose tissue is associated with adipose tissue inflammation and poorer functional performance in central adiposity. Arch Gerontol Geriatr. 2019;81:1-7.

107.	Konopka AR, Wolff CA, Suer MK, Harber MP. Relationship between intermuscular adipose tissue infiltration and myostatin before and after aerobic exercise training. Am J Physiol Regul Integr Comp Physiol. 2018;315(3):R461-R8.

108.	Haam JH, Kim YS, Koo HS, Haam J, Seo NK, Kim HY, et al. Intermuscular adipose tissue is associated with monocyte chemoattractant protein-1, independent of visceral adipose tissue. Clin Biochem. 2016;49(6):439-43.

109.	Scherzer R, Shen W, Heymsfield SB, Lewis CE, Kotler DP, Punyanitya M, et al. Intermuscular adipose tissue and metabolic associations in HIV infection. Obesity (Silver Spring). 2011;19(2):283-91.

110.	Marcus RL, Addison O, Dibble LE, Foreman KB, Morrell G, Lastayo P. Intramuscular adipose tissue, sarcopenia, and mobility function in older individuals. J Aging Res. 2012;2012:629637.

111.	Delmonico MJ, Harris TB, Visser M, Park SW, Conroy MB, Velasquez-Mieyer P, et al. Longitudinal study of muscle strength, quality, and adipose tissue infiltration. Am J Clin Nutr. 2009;90(6):1579-85.

112.	Song MY, Ruts E, Kim J, Janumala I, Heymsfield S, Gallagher D. Sarcopenia and increased adipose tissue infiltration of muscle in elderly African American women. Am J Clin Nutr. 2004;79(5):874-80.

113.	Marcus RL, Addison O, Kidde JP, Dibble LE, Lastayo PC. Skeletal muscle fat infiltration: impact of age, inactivity, and exercise. J Nutr Health Aging. 2010;14(5):362-6.

114.	Asakura A, Komaki M, Rudnicki M. Muscle satellite cells are multipotential stem cells that exhibit myogenic, osteogenic, and adipogenic differentiation. Differentiation. 2001;68(4-5):245-53.

115.   Yu D, Cai Z, Li D, Zhang Y, He M, Yang Y, et al. Myogenic Differentiation of Stem Cells for Skeletal Muscle Regeneration. Stem Cells Int. 2021;2021:8884283.

116.   Alexakis C, Partridge T, Bou-Gharios G. Implication of the satellite cell in dystrophic muscle fibrosis: a self-perpetuating mechanism of collagen overproduction. Am J Physiol Cell Physiol. 2007;293(2):C661-9.

117.   Pallafacchina G, Francois S, Regnault B, Czarny B, Dive V, Cumano A, et al. An adult tissue-specific stem cell in its niche: a gene profiling analysis of in vivo quiescent and activated muscle satellite cells. Stem Cell Res. 2010;4(2):77-91.

118.   Yin H, Price F, Rudnicki MA. Satellite cells and the muscle stem cell niche. Physiol Rev. 2013;93(1):23-67.

119.   Collins CA, Olsen I, Zammit PS, Heslop L, Petrie A, Partridge TA, et al. Stem cell function, self-renewal, and behavioral heterogeneity of cells from the adult muscle satellite cell niche. Cell. 2005;122(2):289-301.

120.   Boonen KJ, Post MJ. The muscle stem cell niche: regulation of satellite cells during regeneration. Tissue Eng Part B Rev. 2008;14(4):419-31.

121.   Molina T, Fabre P, Dumont NA. Fibro-adipogenic progenitors in skeletal muscle homeostasis, regeneration and diseases. Open Biol. 2021;11(12):210110.

122.   Arrighi N, Moratal C, Clement N, Giorgetti-Peraldi S, Peraldi P, Loubat A, et al. Characterization of adipocytes derived from fibro/adipogenic progenitors resident in human skeletal muscle. Cell Death Dis. 2015;6(4):e1733.

123.   Contreras O, Rossi FMV, Theret M. Origins, potency, and heterogeneity of skeletal muscle fibro-adipogenic progenitors-time for new definitions. Skelet Muscle. 2021;11(1):16.

124.   Gil-Ortega M, Garidou L, Barreau C, Maumus M, Breasson L, Tavernier G, et al. Native adipose stromal cells egress from adipose tissue in vivo: evidence during lymph node activation. Stem Cells. 2013;31(7):1309-20.

125.   Girousse A, Gil-Ortega M, Bourlier V, Bergeaud C, Sastourne-Arrey Q, Moro C, et al. The Release of Adipose Stromal Cells from Subcutaneous Adipose Tissue Regulates Ectopic Intramuscular Adipocyte Deposition. Cell Rep. 2019;27(2):323-33 e5.

126.   Kim NK, Lim JH, Song MJ, Kim OH, Park BY, Kim MJ, et al. Comparative studies of skeletal muscle proteome and transcriptome profilings between pig breeds. Mol Cell Proteomics. 2006;5(10):S93-S.

127.   Kim NK, Park HR, Lee HC, Yoon D, Son ES, Kim YS, et al. Comparative studies of skeletal muscle proteome and transcriptome profilings between pig breeds. Mamm Genome. 2010;21(5-6):307-19.

128.   Bong JJ, Cho KK, Baik M. Comparison of gene expression profiling between bovine subcutaneous and intramuscular adipose tissues by serial analysis of gene expression. Cell Biol Int. 2010;34(1):125-33.

129.   Lee HJ, Park HS, Kim W, Yoon D, Seo S. Comparison of Metabolic Network between Muscle and Intramuscular Adipose Tissues in Hanwoo Beef Cattle Using a Systems Biology Approach. Int J Genomics. 2014;2014.

130.   Mourot J, Kouba M. Development of intra- and intermuscular adipose tissue in growing Large White and Meishan pigs. Reprod Nutr Dev. 1999;39(1):125-32.

131.   Kahn D, Macias E, Zarini S, Garfield A, Zemski Berry K, Gerszten R, et al. Quantifying the inflammatory secretome of human intermuscular adipose tissue. Physiol Rep. 2022;10(16):e15424.

132.   Gallagher D, Kuznia P, Heshka S, Albu J, Heymsfield SB, Goodpaster B, et al. Adipose tissue in muscle: a novel depot similar in size to visceral adipose tissue. Am J Clin Nutr. 2005;81(4):903-10.

133.   Gallagher D, Kelley DE, Yim JE, Spence N, Albu J, Boxt L, et al. Adipose tissue distribution is different in type 2 diabetes. Am J Clin Nutr. 2009;89(3):807-14.

134.   Goodpaster BH, Krishnaswami S, Resnick H, Kelley DE, Haggerty C, Harris TB, et al. Association between regional adipose tissue distribution and both type 2 diabetes and impaired glucose tolerance in elderly men and women. Diabetes Care. 2003;26(2):372-9.

135.   Goodpaster BH, Thaete FL, Simoneau JA, Kelley DE. Subcutaneous abdominal fat and thigh muscle composition predict insulin sensitivity independently of visceral fat. Diabetes. 1997;46(10):1579-85.

136.   Albu JB, Kovera AJ, Allen L, Wainwright M, Berk E, Raja-Khan N, et al. Independent association of insulin resistance with larger amounts of intermuscular adipose tissue and a greater acute insulin response to glucose in African American than in white nondiabetic women. American Journal of Clinical Nutrition. 2005;82(6):1210-7.

137.   Durheim MT, Slentz CA, Bateman LA, Mabe SK, Kraus WE. Relationships between exercise-induced reductions in thigh intermuscular adipose tissue, changes in lipoprotein particle size, and visceral adiposity. Am J Physiol-Endoc M. 2008;295(2):E407-E12.

138.   Yim JE, Heshka S, Albu J, Heymsfield S, Kuznia P, Harris T, et al. Intermuscular adipose tissue rivals visceral adipose tissue in independent associations with cardiovascular risk. Int J Obes (Lond). 2007;31(9):1400-5.

139.   Kim SK, Park SW, Hwang IJ, Lee YK, Cho YW. High fat stores in ectopic compartments in men with newly diagnosed type 2 diabetes: an anthropometric determinant of carotid atherosclerosis and insulin resistance. Int J Obes (Lond). 2010;34(1):105-10.

140.   Goodpaster BH, Krishnaswami S, Harris TB, Katsiaras A, Kritchevsky SB, Simonsick EM, et al. Obesity, regional body fat distribution, and the metabolic syndrome in older men and women. Arch Intern Med. 2005;165(7):777-83.

141.   Kannan R, Palmquist DL, Baker N. Contribution of intermuscular fat to lipogenesis from dietary glucose carbon in mice. Biochim Biophys Acta. 1976;431(2):225-32.

142.   Mattacks CA, Sadler D, Pond CM. The effects of exercise and dietary restriction on the activities of hexokinase and phosphofructokinase in superficial, intra-abdominal and intermuscular adipose tissue of guinea-pigs. Comp Biochem Physiol B. 1987;87(3):533-42.

143.   Mattacks CA, Pond CM. Site-specific and sex differences in the rates of fatty acid/triacylglycerol substrate cycling in adipose, tissue and muscle of sedentary and exercised dwarf hamsters (Phodopus sungorus). Int J Obes. 1988;12(6):585-97.

144.   Goodpaster BH, Sparks LM. Metabolic Flexibility in Health and Disease. Cell Metab. 2017;25(5):1027-36.

145.   Lehr S, Hartwig S, Lamers D, Famulla S, Muller S, Hanisch FG, et al. Identification and validation of novel adipokines released from primary human adipocytes. Mol Cell Proteomics. 2012;11(1):M111 010504.

146.   Dietze D, Koenen M, Rohrig K, Horikoshi H, Hauner H, Eckel J. Impairment of insulin signaling in human skeletal muscle cells by co-culture with human adipocytes. Diabetes. 2002;51(8):2369-76.

147.   Taube A, Lambernd S, van Echten-Deckert G, Eckardt K, Eckel J. Adipokines promote lipotoxicity in human skeletal muscle cells. Arch Physiol Biochem. 2012;118(3):92-101.

148.   Lam YY, Janovska A, McAinch AJ, Belobrajdic DP, Hatzinikolas G, Game P, et al. The use of adipose tissue-conditioned media to demonstrate the differential effects of fat depots on insulin-stimulated glucose uptake in a skeletal muscle cell line. Obes Res Clin Pract. 2011;5(1):e1-e78.

149.   Pellegrinelli V, Rouault C, Rodriguez-Cuenca S, Albert V, Edom-Vovard F, Vidal-Puig A, et al. Human Adipocytes Induce Inflammation and Atrophy in Muscle Cells During Obesity. Diabetes. 2015;64(9):3121-34.

150.   Laurens C, Louche K, Sengenes C, Coue M, Langin D, Moro C, et al. Adipogenic progenitors from obese human skeletal muscle give rise to functional white adipocytes that contribute to insulin resistance. Int J Obes (Lond). 2016;40(3):497-506.

151.   Bonnans C, Chou J, Werb Z. Remodelling the extracellular matrix in development and disease. Nat Rev Mol Cell Bio. 2014;15(12):786-801.

152.   Zhou X, Franklin RA, Adler M, Jacox JB, Bailis W, Shyer JA, et al. Circuit Design Features of a Stable Two-Cell System. Cell. 2018;172(4):744-+.

153.   Physiology in perspective: cell-cell interactions: the physiological basis of communication. Physiology (Bethesda). 2014;29(4):220-1.

154.   Armingol E, Officer A, Harismendy O, Lewis NE. Deciphering cell-cell interactions and communication from gene expression. Nat Rev Genet. 2021;22(2):71-88.

155.   Browaeys R, Saelens W, Saeys Y. NicheNet: modeling intercellular communication by linking ligands to target genes. Nat Methods. 2020;17(2):159-62.

156.   Armingol E, Officer A, Harismendy O, Lewis NE. Deciphering cell-cell interactions and communication from gene expression. Nat Rev Genet. 2021;22(2):71-88.

157.   Cao YH, Ding J, Tang QH, Zhang J, Huang ZY, Tang XM, et al. Deciphering cell-cell interactions and communication in the tumor microenvironment and unraveling intratumoral genetic heterogeneity via single-cell genomic sequencing. Bioengineered. 2022;13(7-12):14974-86.

158.   Turei D, Valdeolivas A, Gul L, Palacio-Escat N, Klein M, Ivanova O, et al. Integrated intra- and intercellular signaling knowledge for multicellular omics analysis. Mol Syst Biol. 2021;17(3).

159.   Shao X, Liao J, Li CY, Lu XY, Cheng JY, Fan XH. CellTalkDB: a manually curated database of ligand-receptor interactions in humans and mice. Brief Bioinform. 2021;22(4).

160.   Jin SQ, Guerrero-Juarez CF, Zhang LH, Chang I, Ramos R, Kuan CH, et al. Inference and analysis of cell-cell communication using CellChat. Nat Commun. 2021;12(1).

161.   Efremova M, Vento-Tormo M, Teichmann SA, Vento-Tormo R. CellPhoneDB: inferring cell-cell communication from combined expression of multi-subunit ligand-receptor complexes. Nat Protoc. 2020;15(4):1484-506.

162.   Turei D, Valdeolivas A, Gul L, Palacio-Escat N, Klein M, Ivanova O, et al. Integrated intra- and intercellular signaling knowledge for multicellular omics analysis. Mol Syst Biol. 2021;17(3):e9923.

163.   Efremova M, Vento-Tormo M, Teichmann SA, Vento-Tormo R. CellPhoneDB: inferring cell-cell communication from combined expression of multi-subunit ligand-receptor complexes. Nat Protoc. 2020;15(4):1484-506.

164.   Shao X, Liao J, Li C, Lu X, Cheng J, Fan X. CellTalkDB: a manually curated database of ligand-receptor interactions in humans and mice. Brief Bioinform. 2021;22(4).

165.   Dimitrov D, Turei D, Garrido-Rodriguez M, Burmedi PL, Nagai JS, Boys C, et al. Comparison of methods and resources for cell-cell communication inference from single-cell RNA-Seq data. Nat Commun. 2022;13(1):3224.

166.   Yang Y, Li G, Zhong Y, Xu Q, Lin YT, Roman-Vicharra C, et al. scTenifoldXct: A semi-supervised method for predicting cell-cell interactions and mapping cellular communication graphs. Cell Syst. 2023;14(4):302-11 e4.

167.   Pavlicev M, Wagner GP, Chavan AR, Owens K, Maziarz J, Dunn-Fletcher C, et al. Single-cell transcriptomics of the human placenta: inferring the cell communication network of the maternal-fetal interface. Genome Res. 2017;27(3):349-61.

168.   Cabello-Aguilar S, Alame M, Kon-Sun-Tack F, Fau C, Lacroix M, Colinge J. SingleCellSignalR: inference of intercellular networks from single-cell transcriptomics. Nucleic Acids Res. 2020;48(10):e55.

169.   Kanehisa MaG, S. KEGG: Kyoto Encyclopedia of Genes and Genomes 2000 [Available from: https://www.genome.jp/kegg/.

170.   GO[Internet]. Gene Ontology 2000 [Available from: http://geneontology.org/.

171.   team[Internet] s. The string database 2008 [Available from: https://string-db.org/.

172.   Heise T, Zijlstra E, Nosek L, Heckermann S, Plum-Morschel L, Forst T. Euglycaemic glucose clamp: what it can and cannot do, and how to do it. Diabetes Obes Metab. 2016;18(10):962-72.

173.   Soop M, Nygren J, Brismar K, Thorell A, Ljungqvist O. The hyperinsulinaemic-euglycaemic glucose clamp: reproducibility and metabolic effects of prolonged insulin infusion in healthy subjects. Clin Sci (Lond). 2000;98(4):367-74.

174.   Simonson DC. Insulin Resistance and the Metabolic Syndrome in Chronic Renal Disease. In: Williams AKSaGH, editor. Textbook of Nephro-Endocrinology. 2 ed: Academic Press; 2018. p. 233-28.

175.   Schmitz O, Arnfred J, Nielsen OH, Beck-Nielsen H, Orskov H. Glucose uptake and pulsatile insulin infusion: euglycaemic clamp and [3-3H]glucose studies in healthy subjects. Acta Endocrinol (Copenh). 1986;113(4):559-63.

176.   Nieuwenhuizen AG, Schuiling GA, Bonen A, Paans AM, Vaalburg W, Koiter TR. Glucose consumption by various tissues in pregnant rats: effects of a 6-day euglycaemic hyperinsulinaemic clamp. Acta Physiol Scand. 1998;164(3):325-34.

177.   DeFronzo RA, Tobin JD, Andres R. Glucose clamp technique: a method for quantifying insulin secretion and resistance. Am J Physiol. 1979;237(3):E214-23.

178.   Finegood DT, Bergman RN, Vranic M. Estimation of endogenous glucose production during hyperinsulinemic-euglycemic glucose clamps. Comparison of unlabeled and labeled exogenous glucose infusates. Diabetes. 1987;36(8):914-24.

179.   Team RC. R: A language and environment for statistical computing. . R Foundation for Statistical Computing; 2023.

180.   Love MI, Huber W, Anders S. Moderated estimation of fold change and dispersion for RNA-seq data with DESeq2. Genome Biol. 2014;15(12):550.

181.   Anders S, Huber W. Differential expression analysis for sequence count data. Genome Biol. 2010;11(10):R106.

182.   [Available   from: https://hbctraining.github.io/DGE_workshop/lessons/02_DGE_count_normalization.html.

183.   Mark D. Robinson DJM, Gordon K. Smyth edgeR: a Bioconductor package for differential expression analysis of digital gene expression data. Bioinformatics. 2010;26(1):139-40.

184.   Robinson MD, Oshlack A. A scaling normalization method for differential expression analysis of RNA-seq data. Genome Biol. 2010;11(3):R25.

185.   Zhao S, Ye Z, Stanton R. Misuse of RPKM or TPM normalization when comparing across samples and sequencing protocols. Rna. 2020;26(8):903-9.

186.   Johnson KA, Krishnan A. Robust normalization and transformation techniques for constructing gene coexpression networks from RNA-seq data. Genome Biology. 2022;23(1):1.

187.   Cameron AC TP. Regression Analysis of Count Data: Cambridge University Press; 1988.

188.   Love MI, Anders S, Kim V, Huber W. RNA-Seq workflow: gene-level exploratory analysis and differential expression. F1000Res. 2015;4:1070.

189.   Boyle EI, Weng S, Gollub J, Jin H, Botstein D, Cherry JM, et al. GO::TermFinder—open source software for accessing Gene Ontology information and finding significantly enriched Gene Ontology terms associated with a list of genes. Bioinformatics. 2004;20(18):3710-5.

190.   Liberzon A. A description of the Molecular Signatures Database (MSigDB) Web site. Methods Mol Biol. 2014;1150:153-60.

191.   Subramanian A, Tamayo P, Mootha VK, Mukherjee S, Ebert BL, Gillette MA, et al. Gene set enrichment analysis: a knowledge-based approach for interpreting genome-wide expression profiles. Proc Natl Acad Sci U S A. 2005;102(43):15545-50.

192.   Hollander M, Wolfe DA, Chicken E. Nonparametric statistical methods: John Wiley & Sons; 2013.

193.   Wu T, Hu E, Xu S, Chen M, Guo P, Dai Z, et al. clusterProfiler 4.0: A universal enrichment tool for interpreting omics data. Innovation (Camb). 2021;2(3):100141.

194.   Sayers EW, Beck J, Bolton EE, Bourexis D, Brister JR, Canese K, et al. Database resources of the National Center for Biotechnology Information. Nucleic Acids Res. 2021;49(D1):D10-d7.

195.   Kanehisa M, Goto S. KEGG: kyoto encyclopedia of genes and genomes. Nucleic Acids Res. 2000;28(1):27-30.

196.   Conesa A, Götz S, García-Gómez JM, Terol J, Talón M, Robles M. Blast2GO: a universal tool for annotation, visualization and analysis in functional genomics research. Bioinformatics. 2005;21(18):3674-6.

197.   UniProt: a worldwide hub of protein knowledge. Nucleic Acids Res. 2019;47(D1):D506-d15.

198.   Alexander SP, Kelly E, Mathie A, Peters JA, Veale EL, Armstrong JF, et al. THE CONCISE GUIDE TO PHARMACOLOGY 2021/22: Introduction and Other Protein Targets. Br J Pharmacol. 2021;178 Suppl 1(Suppl 1):S1-s26.

199.   Cell-Cell Interaction Database [Internet]. 2013. Available from: https://zenodo.org/record/7589953.

200.   Jin S, Guerrero-Juarez CF, Zhang L, Chang I, Ramos R, Kuan CH, et al. Inference and analysis of cell-cell communication using CellChat. Nat Commun. 2021;12(1):1088.

201.   Yuanxin Wang RW, Shaojun Zhang, Shumei Song, Changying Jiang, Guangchun Han, Michael Wang, Jaffer Ajani, Andy Futreal, Linghua Wang. iTALK: an R Package to Characterize and Illustrate Intercellular Communication. bioRxiv 2019.

202.   Ceccarelli F, Turei D, Gabor A, Saez-Rodriguez J. Bringing data from curated pathway resources to Cytoscape with OmniPath. Bioinformatics. 2020;36(8):2632-3.

203.   Zaidel-Bar R, Itzkovitz S, Ma'ayan A, Iyengar R, Geiger B. Functional atlas of the integrin adhesome. Nature Cell Biology. 2007;9(8):858-67.

204.   Zhang Y, Liu T, Wang J, Zou B, Li L, Yao L, et al. Cellinker: a platform of ligand-receptor interactions for intercellular communication analysis. Bioinformatics. 2021.

205.   Noël F, Massenet-Regad L, Carmi-Levy I, Cappuccio A, Grandclaudon M, Trichot C, et al. Dissection of intercellular communication using the transcriptome-based framework ICELLNET. Nature Communications. 2021;12(1):1089.

206.   Dimitrov D, Türei D, Garrido-Rodriguez M, Burmedi PL, Nagai JS, Boys C, et al. Comparison of methods and resources for cell-cell communication inference from single-cell RNA-Seq data. Nature Communications. 2022;13(1):3224.

207.   Hou R, Denisenko E, Ong HT, Ramilowski JA, Forrest ARR. Predicting cell-to-cell communication networks using NATMI. Nat Commun. 2020;11(1):5011.

208.   Ramilowski JA, Goldberg T, Harshbarger J, Kloppmann E, Lizio M, Satagopam VP, et al. A draft network of ligand-receptor-mediated multicellular signalling in human. Nat Commun. 2015;6:7866.

209.   Hermjakob H, Montecchi-Palazzi L, Lewington C, Mudali S, Kerrien S, Orchard S, et al. IntAct: an open source molecular interaction database. Nucleic Acids Res. 2004;32(Database issue):D452-5.

210.   Oughtred R, Stark C, Breitkreutz BJ, Rust J, Boucher L, Chang C, et al. The BioGRID interaction database: 2019 update. Nucleic Acids Res. 2019;47(D1):D529-d41.

211.   Szklarczyk D, Gable AL, Nastou KC, Lyon D, Kirsch R, Pyysalo S, et al. The STRING database in 2021: customizable protein-protein networks, and functional characterization of user-uploaded gene/measurement sets. Nucleic Acids Res. 2021;49(D1):D605-d12.

212.   Kosti I, Jain N, Aran D, Butte AJ, Sirota M. Cross-tissue Analysis of Gene and Protein Expression in Normal and Cancer Tissues. Sci Rep. 2016;6:24799.

213.   Hu Y, Li M, Lu Q, Weng H, Wang J, Zekavat SM, et al. A statistical framework for cross-tissue transcriptome-wide association analysis. Nat Genet. 2019;51(3):568-76.

214.   Long Q, Argmann C, Houten SM, Huang T, Peng S, Zhao Y, et al. Inter-tissue coexpression network analysis reveals DPP4 as an important gene in heart to blood communication. Genome Medicine. 2016;8(1):15.

215.   Csárdi GN, Tamás; Müller, Kirill; Horvát, Szabolcs; Traag, Vincent; Zanini, Fabio; Noom, Daniel. igraph: Network Analysis and Visualization in R. 2023.

216.   Gustavsen JA, Pai S, Isserlin R, Demchak B, Pico AR. RCy3: Network biology using Cytoscape from within R. F1000Res. 2019;8:1774.

217.   Shannon P, Markiel A, Ozier O, Baliga NS, Wang JT, Ramage D, et al. Cytoscape: a software environment for integrated models of biomolecular interaction networks. Genome Res. 2003;13(11):2498-504.

218.   Suoqin Jin CFG-J, Lihua Zhang, Ivan Chang, Peggy Myung, Maksim V. Plikus, Qing Nie. **Inference and analysis of cell-cell communication using CellChat**. bioRxiv. 2020.

219.   Goenawan IH, Bryan K, Lynn DJ. DyNet: visualization and analysis of dynamic molecular interaction networks. Bioinformatics. 2016;32(17):2713-5.

220.   Hollander M, Do T, Will T, Helms V. Detecting Rewiring Events in Protein-Protein Interaction Networks Based on Transcriptomic Data. Front Bioinform. 2021;1:724297.

221.   Kim Y, Han S, Choi S, Hwang D. Inference of dynamic networks using time-course data. Brief Bioinform. 2014;15(2):212-28.

222.   Hu JX, Thomas CE, Brunak S. Network biology concepts in complex disease comorbidities. Nat Rev Genet. 2016;17(10):615-29.

223.   Barabasi AL, Gulbahce N, Loscalzo J. Network medicine: a network-based approach to human disease. Nat Rev Genet. 2011;12(1):56-68.

224.   Bowler EH, Wang Z, Ewing RM. How do oncoprotein mutations rewire protein-protein interaction networks? Expert Rev Proteomics. 2015;12(5):449-55.

225.   Greene CS, Krishnan A, Wong AK, Ricciotti E, Zelaya RA, Himmelstein DS, et al. Understanding multicellular function and disease with human tissue-specific networks. Nature Genetics. 2015;47(6):569-76.

226.   Su G, Kuchinsky A, Morris JH, States DJ, Meng F. GLay: community structure analysis of biological networks. Bioinformatics. 2010;26(24):3135-7.

227.   Newman ME, Girvan M. Finding and evaluating community structure in networks. Phys Rev E Stat Nonlin Soft Matter Phys. 2004;69(2 Pt 2):026113.

228.   Kim J, Kim I, Han SK, Bowie JU, Kim S. Network rewiring is an important mechanism of gene essentiality change. Scientific Reports. 2012;2(1):900.

229.   Chung ST, Chacko SK, Sunehag AL, Haymond MW. Measurements of Gluconeogenesis and Glycogenolysis: A Methodological Review. Diabetes. 2015;64(12):3996-4010.

230.   Rizza RA, Mandarino LJ, Gerich JE. Dose-response characteristics for effects of insulin on production and utilization of glucose in man. Am J Physiol. 1981;240(6):E630-9.

231.   Guerreiro VA, Carvalho D, Freitas P. Obesity, Adipose Tissue, and Inflammation Answered in Questions. J Obes. 2022;2022:2252516.

232.   Fink J, Seifert G, Blüher M, Fichtner-Feigl S, Marjanovic G. Obesity Surgery. Dtsch Arztebl Int. 2022;119(5):70-80.

233.   Lee H-J, Park H-S, Kim W, Yoon D, Seo S. Comparison of Metabolic Network between Muscle and Intramuscular Adipose Tissues in Hanwoo Beef Cattle Using a Systems Biology Approach. Int J Genomics. 2014;2014:679437.

234.   Gancheva S, Jelenik T, Alvarez-Hernandez E, Roden M. Interorgan Metabolic Crosstalk in Human Insulin Resistance. Physiol Rev. 2018;98(3):1371-415.

235.   Bellanti F, Lo Buglio A, Vendemiale G. Muscle Delivery of Mitochondria-Targeted Drugs for the Treatment of Sarcopenia: Rationale and Perspectives. Pharmaceutics. 2022;14(12).

236.   Patti ME, Corvera S. The role of mitochondria in the pathogenesis of type 2 diabetes. Endocr Rev. 2010;31(3):364-95.

237.   Pinti MV, Fink GK, Hathaway QA, Durr AJ, Kunovac A, Hollander JM. Mitochondrial dysfunction in type 2 diabetes mellitus: an organ-based analysis. Am J Physiol Endocrinol Metab. 2019;316(2):E268-e85.

238.   Bhatti JS, Kumar S, Vijayan M, Bhatti GK, Reddy PH. Therapeutic Strategies for Mitochondrial Dysfunction and Oxidative Stress in Age-Related Metabolic Disorders. Prog Mol Biol Transl Sci. 2017;146:13-46.

239.   Bhatti JS, Bhatti GK, Reddy PH. Mitochondrial dysfunction and oxidative stress in metabolic disorders - A step towards mitochondria based therapeutic strategies. Biochim Biophys Acta Mol Basis Dis. 2017;1863(5):1066-77.

240.   Stepien KM, Heaton R, Rankin S, Murphy A, Bentley J, Sexton D, et al. Evidence of Oxidative Stress and Secondary Mitochondrial Dysfunction in Metabolic and Non-Metabolic Disorders. J Clin Med. 2017;6(7).

241.   Bruce Alberts AJ, Julian Lewis, Martin Raff, Keith Roberts, and Peter Walte. Molecular Biology of the Cell. 4 ed. New York2002.

242.   Grygiel-Górniak B. Peroxisome proliferator-activated receptors and their ligands: nutritional and clinical implications--a review. Nutr J. 2014;13:17.

243.   Schoonjans K, Staels B, Auwerx J. Role of the peroxisome proliferator-activated receptor (PPAR) in mediating the effects of fibrates and fatty acids on gene expression. J Lipid Res. 1996;37(5):907-25.

244.   Tyagi S, Gupta P, Saini AS, Kaushal C, Sharma S. The peroxisome proliferator-activated receptor: A family of nuclear receptors role in various diseases. J Adv Pharm Technol Res. 2011;2(4):236-40.

245.   Yang XF, Shang DJ. The role of peroxisome proliferator-activated receptor gamma in lipid metabolism and inflammation in atherosclerosis. Cell Biol Int. 2023;47(9):1469-87.

246.   Siddik MAB, Shin AC. Recent Progress on Branched-Chain Amino Acids in Obesity, Diabetes, and Beyond. Endocrinol Metab (Seoul). 2019;34(3):234-46.

247.   Mao Z, Zhang W. Role of mTOR in Glucose and Lipid Metabolism. Int J Mol Sci. 2018;19(7).

248.   Tan HC, Hsu JW, Khoo CM, Tai ES, Yu S, Chacko S, et al. Alterations in branched-chain amino acid kinetics in nonobese but insulin-resistant Asian men. Am J Clin Nutr. 2018;108(6):1220-8.

249.   Yu D, Richardson NE, Green CL, Spicer AB, Murphy ME, Flores V, et al. The adverse metabolic effects of branched-chain amino acids are mediated by isoleucine and valine. Cell Metab. 2021;33(5):905-22 e6.

250.   Newgard CB. Interplay between lipids and branched-chain amino acids in development of insulin resistance. Cell Metab. 2012;15(5):606-14.

251.   Newgard CB, An J, Bain JR, Muehlbauer MJ, Stevens RD, Lien LF, et al. A branched-chain amino acid-related metabolic signature that differentiates obese and lean humans and contributes to insulin resistance. Cell Metab. 2009;9(4):311-26.

252.   Lerin C, Goldfine AB, Boes T, Liu M, Kasif S, Dreyfuss JM, et al. Defects in muscle branched-chain amino acid oxidation contribute to impaired lipid metabolism. Mol Metab. 2016;5(10):926-36.

253.   Zhang F, Zhao S, Yan W, Xia Y, Chen X, Wang W, et al. Branched Chain Amino Acids Cause Liver Injury in Obese/Diabetic Mice by Promoting Adipocyte Lipolysis and Inhibiting Hepatic Autophagy. EBioMedicine. 2016;13:157-67.

254.   Lackey DE, Lynch CJ, Olson KC, Mostaedi R, Ali M, Smith WH, et al. Regulation of adipose branched-chain amino acid catabolism enzyme expression and cross-adipose amino acid flux in human obesity. Am J Physiol Endocrinol Metab. 2013;304(11):E1175-87.

255.   Jang C, Oh SF, Wada S, Rowe GC, Liu L, Chan MC, et al. A branched-chain amino acid metabolite drives vascular fatty acid transport and causes insulin resistance. Nat Med. 2016;22(4):421-6.

256.   Zhao X, Han Q, Liu Y, Sun C, Gang X, Wang G. The Relationship between Branched-Chain Amino Acid Related Metabolomic Signature and Insulin Resistance: A Systematic Review. J Diabetes Res. 2016;2016:2794591.

257.   Lin HV, Frassetto A, Kowalik EJ, Jr., Nawrocki AR, Lu MM, Kosinski JR, et al. Butyrate and propionate protect against diet-induced obesity and regulate gut hormones via free fatty acid receptor 3-independent mechanisms. PLoS One. 2012;7(4):e35240.

258.   van Deuren T, Blaak EE, Canfora EE. Butyrate to combat obesity and obesity-associated metabolic disorders: Current status and future implications for therapeutic use. Obes Rev. 2022;23(10):e13498.

259.   Bloomgarden Z. Diabetes and branched-chain amino acids: What is the link? J Diabetes. 2018;10(5):350-2.

260.   Zhou Q, Sun WW, Chen JC, Zhang HL, Liu J, Lin Y, et al. Phenylalanine impairs insulin signaling and inhibits glucose uptake through modification of IRβ. Nat Commun. 2022;13(1):4291.

261.   Indrakusuma I, Sell H, Eckel J. Novel Mediators of Adipose Tissue and Muscle Crosstalk. Curr Obes Rep. 2015;4(4):411-7.

262.   Stanford KI, Goodyear LJ. Muscle-Adipose Tissue Cross Talk. Cold Spring Harb Perspect Med. 2018;8(8).

263.   Lutter D, Sachs S, Walter M, Kerege A, Perreault L, Kahn DE, et al. Skeletal muscle and intermuscular adipose tissue gene expression profiling identifies new biomarkers with prognostic significance for insulin resistance progression and intervention response. Diabetologia. 2023;66(5):873-83.

264.   Zamboni M, Mazzali G, Brunelli A, Saatchi T, Urbani S, Giani A, et al. The Role of Crosstalk between Adipose Cells and Myocytes in the Pathogenesis of Sarcopenic Obesity in the Elderly. Cells. 2022;11(21).

265.   Wilhelmsen A, Tsintzas K, Jones SW. Recent advances and future avenues in understanding the role of adipose tissue cross talk in mediating skeletal muscle mass and function with ageing. Geroscience. 2021;43(1):85-110.

266.   da Silva Rosa SC, Nayak N, Caymo AM, Gordon JW. Mechanisms of muscle insulin resistance and the cross-talk with liver and adipose tissue. Physiol Rep. 2020;8(19):e14607.

267.   Smith U, Kahn BB. Adipose tissue regulates insulin sensitivity: role of adipogenesis, de novo lipogenesis and novel lipids. J Intern Med. 2016;280(5):465-75.

268.   Fuentes P, Sese M, Guijarro PJ, Emperador M, Sanchez-Redondo S, Peinado H, et al. ITGB3-mediated uptake of small extracellular vesicles facilitates intercellular communication in breast cancer cells. Nat Commun. 2020;11(1):4261.

269.   Zhu C, Kong Z, Wang B, Cheng W, Wu A, Meng X. ITGB3/CD61: a hub modulator and target in the tumor microenvironment. Am J Transl Res. 2019;11(12):7195-208.

270.   Misra A, Feng Z, Chandran RR, Kabir I, Rotllan N, Aryal B, et al. Integrin beta3 regulates clonality and fate of smooth muscle-derived atherosclerotic plaque cells. Nat Commun. 2018;9(1):2073.

271.   Cymbron T, Raposo M, Kazachkova N, Bettencourt C, Silva F, Santos C, et al. Cross-sectional study of risk factors for atherosclerosis in the Azorean population. Ann Hum Biol. 2011;38(3):354-9.

272.   Zotova TY, Kubanova AP, Azova MM, Aissa AA, Gigani OO, Frolov VA. Analysis of Polymorphism of Angiotensin System Genes (ACE, AGTR1, and AGT) and Gene ITGB3 in Patients with Arterial Hypertension in Combination with Metabolic Syndrome. Bull Exp Biol Med. 2016;161(3):334-8.

273.   Cao S, Pan Y, Tang J, Terker AS, Arroyo Ornelas JP, Jin GN, et al. EGFR-mediated activation of adipose tissue macrophages promotes obesity and insulin resistance. Nat Commun. 2022;13(1):4684.

274.   Latorre J, Martinez C, Ortega F, Oliveras-Canellas N, Diaz-Saez F, Aragones J, et al. The relevance of EGFR, ErbB receptors and neuregulins in human adipocytes and adipose tissue in obesity. Biomed Pharmacother. 2022;156:113972.

275.   Li Z, Li Y, Overstreet JM, Chung S, Niu A, Fan X, et al. Inhibition of Epidermal Growth Factor Receptor Activation Is Associated With Improved Diabetic Nephropathy and Insulin Resistance in Type 2 Diabetes. Diabetes. 2018;67(9):1847-57.

276.   Costa DB, Huberman MS. Improvement of Type 2 Diabetes in a Lung Cancer Patient Treated With Erlotinib. Diabetes Care. 2006;29(7):1711-.

277.   Relling I, Akcay G, Fangmann D, Knappe C, Schulte DM, Hartmann K, et al. Role of wnt5a in Metabolic Inflammation in Humans. The Journal of Clinical Endocrinology & Metabolism. 2018;103(11):4253-64.

278.   Lopez-Bergami P, Barbero G. The emerging role of Wnt5a in the promotion of a pro-inflammatory and immunosuppressive tumor microenvironment. Cancer Metastasis Rev. 2020;39(3):933-52.

279.   Ackers I, Szymanski C, Duckett KJ, Consitt LA, Silver MJ, Malgor R. Blocking Wnt5a signaling decreases CD36 expression and foam cell formation in atherosclerosis. Cardiovasc Pathol. 2018;34:1-8.

280.   Zhang CJ, Zhu N, Liu Z, Shi Z, Long J, Zu XY, et al. Wnt5a/Ror2 pathway contributes to the regulation of cholesterol homeostasis and inflammatory response in atherosclerosis. Biochim Biophys Acta Mol Cell Biol Lipids. 2020;1865(2):158547.

281.   Kikuchi A, Yamamoto H, Sato A, Matsumoto S. Wnt5a: its signalling, functions and implication in diseases. Acta Physiol (Oxf). 2012;204(1):17-33.

282.   Langfelder P, Horvath S. WGCNA: an R package for weighted correlation network analysis. BMC Bioinformatics. 2008;9:559.

283.   Desquilles L, Musso O. Metabolic Networks: Weighted Gene Correlation Network Analysis. Methods Mol Biol. 2023;2675:317-25.

284. Li L, Kan K, Pallavi P, Keese M. Identification of the Key Genes and Potential Therapeutic Compounds for Abdominal Aortic Aneurysm Based on a Weighted Correlation Network Analysis. Biomedicines. 2022;10(5).

285. Song C, Qiao Z, Chen L, Ge J, Zhang R, Yuan S, et al. Identification of Key Genes as Early Warning Signals of Acute Myocardial Infarction Based on Weighted Gene Correlation Network Analysis and Dynamic Network Biomarker Algorithm. Front Immunol. 2022;13:879657.

286. Ghafouri-Fard S, Safarzadeh A, Taheri M, Jamali E. Identification of diagnostic biomarkers via weighted correlation network analysis in colorectal cancer using a system biology approach. Sci Rep. 2023;13(1):13637.

287. Purdy JC, Shatzel JJ. The hematologic consequences of obesity. Eur J Haematol. 2021;106(3):306-19.

288. Mallard J, Hucteau E, Bender L, Charlot A, Debrut L, Pflumio C, et al. Development of skeletal muscle atrophy and intermuscular adipose tissue in patients with early breast cancer treated with chemotherapy. Am J Physiol Cell Physiol. 2022;323(4):C1325-C32.

289. Aleksandrowicz R, Straczkowski M. Link between insulin resistance and skeletal muscle extracellular matrix remodeling. Endocr Connect. 2023.

290. Sun H, Saeedi P, Karuranga S, Pinkepank M, Ogurtsova K, Duncan BB, et al. IDF Diabetes Atlas: Global, regional and country-level diabetes prevalence estimates for 2021 and projections for 2045. Diabetes Res Clin Pract. 2022;183:109119.

291. Moselakgomo KV, Van Staden M. Diagnostic comparison of Centers for Disease Control and Prevention and International Obesity Task Force criteria for obesity classification in South African children. Afr J Prim Health Care Fam Med. 2017;9(1):e1-e7.

292. Diss G, Filteau M, Freschi L, Leducq JB, Rochette S, Torres-Quiroz F, et al. Integrative avenues for exploring the dynamics and evolution of protein interaction networks. Curr Opin Biotechnol. 2013;24(4):775-83.

293. Liu CH, Chen TC, Chen CH, Kao CY, Huang CY. Differential network biology reveals a positive correlation between a novel protein-protein interaction and cancer cells migration. Annu Int Conf IEEE Eng Med Biol Soc. 2013;2013:2700-3.

294. Ideker T, Krogan NJ. Differential network biology. Mol Syst Biol. 2012;8:565.

295. Califano A. Rewiring makes the difference. Mol Syst Biol. 2011;7:463.

296. Ruiz-Ojeda FJ, Mendez-Gutierrez A, Aguilera CM, Plaza-Diaz J. Extracellular Matrix Remodeling of Adipose Tissue in Obesity and Metabolic Diseases. Int J Mol Sci. 2019;20(19).

297. Guzman-Ruiz R, Tercero-Alcazar C, Rabanal-Ruiz Y, Diaz-Ruiz A, El Bekay R, Rangel-Zuniga OA, et al. Adipose tissue depot-specific intracellular and extracellular cues contributing to insulin resistance in obese individuals. FASEB J. 2020;34(6):7520-39.

298. Goddi A, Schroedl L, Brey EM, Cohen RN. Laminins in metabolic tissues. Metabolism. 2021;120:154775.

299.   Goddi A, Carmona A, Schroedl L, White JM, Piron MJ, De Leon A, et al. Laminin-α4 Is Upregulated in Both Human and Murine Models of Obesity. Front Endocrinol (Lausanne). 2021;12:698621.

300.   Vaicik MK, Blagajcevic A, Ye H, Morse MC, Yang F, Goddi A, et al. The Absence of Laminin α4 in Male Mice Results in Enhanced Energy Expenditure and Increased Beige Subcutaneous Adipose Tissue. Endocrinology. 2018;159(1):356-67.

301.   Vaicik MK, Thyboll Kortesmaa J, Movérare-Skrtic S, Kortesmaa J, Soininen R, Bergström G, et al. Laminin α4 deficient mice exhibit decreased capacity for adipose tissue expansion and weight gain. PLoS One. 2014;9(10):e109854.

302.   Moriggi M, Belloli S, Barbacini P, Murtaj V, Torretta E, Chaabane L, et al. Skeletal Muscle Proteomic Profile Revealed Gender-Related Metabolic Responses in a Diet-Induced Obesity Animal Model. Int J Mol Sci. 2021;22(9).

303.   Chan KH, Huang YT, Meng Q, Wu C, Reiner A, Sobel EM, et al. Shared molecular pathways and gene networks for cardiovascular disease and type 2 diabetes mellitus in women across diverse ethnicities. Circ Cardiovasc Genet. 2014;7(6):911-9.

304.   Liu J, Liu S, Yu Z, Qiu X, Jiang R, Li W. Uncovering the gene regulatory network of type 2 diabetes through multi-omic data integration. J Transl Med. 2022;20(1):604.

305.   Lin G, Wan X, Liu D, Wen Y, Yang C, Zhao C. COL1A1 as a potential new biomarker and therapeutic target for type 2 diabetes. Pharmacol Res. 2021;165:105436.

306.   Dong Z, Lei X, Kujawa SA, Bolu N, Zhao H, Wang C. Identification of core gene in obese type 2 diabetes patients using bioinformatics analysis. Adipocyte. 2021;10(1):310-21.

307.   Chen Y, Ma B, Wang X, Zha X, Sheng C, Yang P, et al. Potential Functions of the BMP Family in Bone, Obesity, and Glucose Metabolism. J Diabetes Res. 2021;2021:6707464.

308.   Macotela Y, Emanuelli B, Mori MA, Gesta S, Schulz TJ, Tseng YH, et al. Intrinsic differences in adipocyte precursor cells from different white fat depots. Diabetes. 2012;61(7):1691-9.

309.   Son JW, Kim MK, Park YM, Baek KH, Yoo SJ, Song KH, et al. Association of serum bone morphogenetic protein 4 levels with obesity and metabolic syndrome in non-diabetic individuals. Endocr J. 2011;58(1):39-46.

310.   Kim MK, Jang EH, Hong OK, Chun HJ, Yoo SJ, Baek KH, et al. Changes in serum levels of bone morphogenic protein 4 and inflammatory cytokines after bariatric surgery in severely obese korean patients with type 2 diabetes. Int J Endocrinol. 2013;2013:681205.

311.   Hong OK, Yoo SJ, Son JW, Kim MK, Baek KH, Song KH, et al. High glucose and palmitate increases bone morphogenic protein 4 expression in human endothelial cells. Korean J Physiol Pharmacol. 2016;20(2):169-75.

312.   Christensen GL, Jacobsen MLB, Wendt A, Mollet IG, Friberg J, Frederiksen KS, et al. Bone morphogenetic protein 4 inhibits insulin secretion from rodent beta cells through regulation of calbindin1 expression and reduced voltage-dependent calcium currents. Diabetologia. 2015;58(6):1282-90.
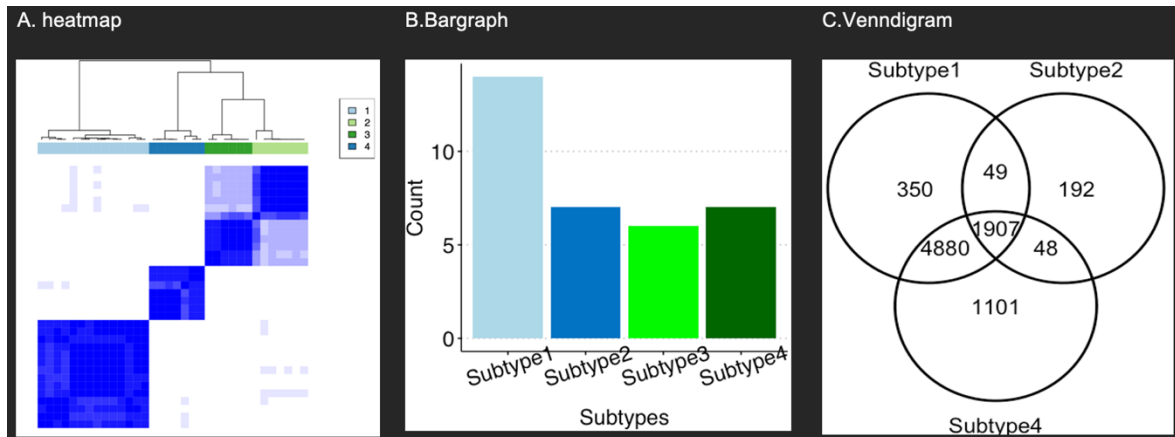
313.   Guo G, Wang H, Bell D, Bi Y, Greer K, editors. KNN Model-Based Approach in Classification2003; Berlin, Heidelberg: Springer Berlin Heidelberg.

314.   Alkhoury C, Henneman NF, Petrenko V, Shibayama Y, Segaloni A, Gadault A, et al. Class 3 PI3K coactivates the circadian clock to promote rhythmic de novo purine synthesis. Nat Cell Biol. 2023;25(7):975-88.

315.   Marri D, Filipovic D, Kana O, Tischkau S, Bhattacharya S. Prediction of mammalian tissue-specific CLOCK–BMAL1 binding to E-box DNA motifs. Scientific Reports. 2023;13(1):7742.

316.   Poulet G, Massias J, Taly V. Liquid Biopsy: General Concepts. Acta Cytol. 2019;63(6):449-55.

317.   Nikanjam M, Kato S, Kurzrock R. Liquid biopsy: current technology and clinical applications. Journal of Hematology & Oncology. 2022;15(1):131.

318.   Janku F, Huang HJ, Pereira DY, Kobayashi M, Chiu CH, Call SG, et al. A novel method for liquid-phase extraction of cell-free DNA for detection of circulating tumor DNA. Scientific Reports. 2021;11(1):19653.

319.   Drag MH, Kilpeläinen TO. Cell-free DNA and RNA-measurement and applications in clinical diagnostics with focus on metabolic disorders. Physiol Genomics. 2021;53(1):33-46.

320.   Ding SC, Lo YMD. Cell-Free DNA Fragmentomics in Liquid Biopsy. Diagnostics (Basel). 2022;12(4).

321.   Spector BL, Harrell L, Sante D, Wyckoff GJ, Willig L. The methylome and cell-free DNA: current applications in medicine and pediatric disease. Pediatric Research. 2023;94(1):89-95.

322.   Moss J, Magenheim J, Neiman D, Zemmour H, Loyfer N, Korach A, et al. Comprehensive human cell-type methylation atlas reveals origins of circulating cell-free DNA in health and disease. Nature Communications. 2018;9(1):5068.

323.   FastQC. 2015.

324.   Langmead B, Salzberg SL. Fast gapped-read alignment with Bowtie 2. Nature Methods. 2012;9(4):357-9.

325.   Liao Y, Smyth GK, Shi W. featureCounts: an efficient general purpose program for assigning sequence reads to genomic features. Bioinformatics. 2014;30(7):923-30.

326.   Plumbridge J. The role of dam methylation in controlling gene expression. Biochimie. 1987;69(5):439-43.

327.   Krueger F, Andrews SR. Bismark: a flexible aligner and methylation caller for Bisulfite-Seq applications. Bioinformatics. 2011;27(11):1571-2.

328.   Krueger   F.   Trim   Galore   [Available   from: https://github.com/FelixKrueger/TrimGalore.

329.   Robinson MD, McCarthy DJ, Smyth GK. edgeR: a Bioconductor package for differential expression analysis of digital gene expression data. Bioinformatics. 2010;26(1):139-40.

330. Akalin A, Kormaksson M, Li S, Garrett-Bakelman FE, Figueroa ME, Melnick A, et al. methylKit: a comprehensive R package for the analysis of genome-wide DNA methylation profiles. Genome Biol. 2012;13(10):R87.
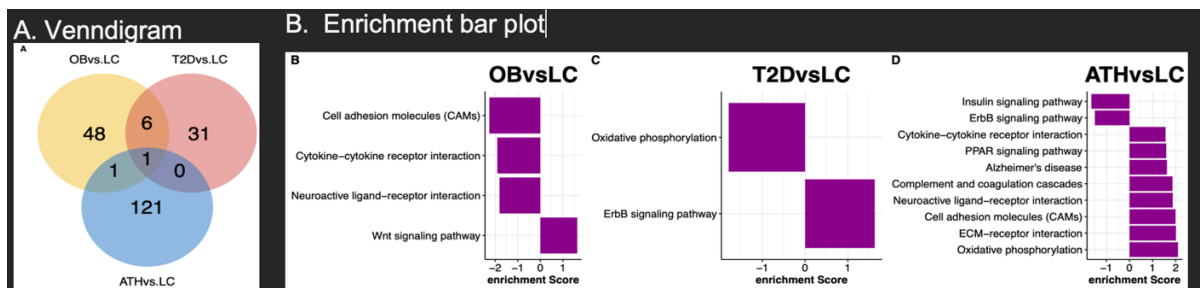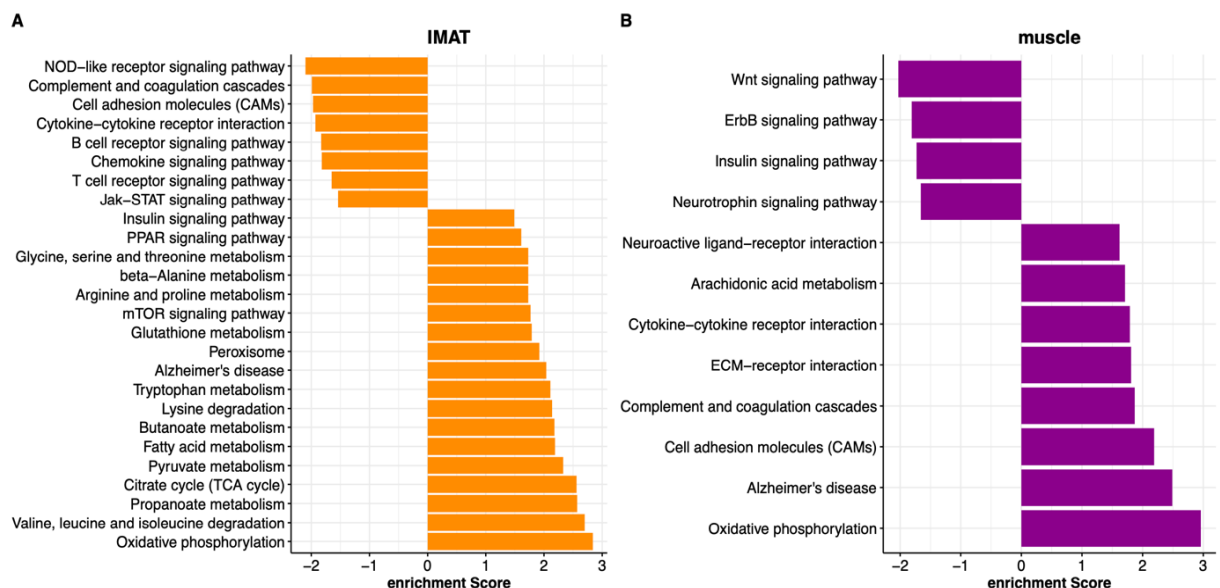
10. Supplement

10.1. Supplemental Figures

Supplemental Figure 1. Gene expression in the IMAT tissue identifies different subtypes of IMATs. Hierarchical clustering identifies four dissimilar IMAT subtypes(A), and the number of samples in each subtype is displayed in the bar graph (B). The number of DE gene for each subtype compared to subtype 3, the smallest sample group, are presented in the Ven-diagram (C).

Supplemental Figure 2.Gene expression in the muscle across different group. The number of DE genes for each study group compared to LC is presented in Ven-diagram (A). KEGG gene set enrichment analysis (GSEA) to identify pathways related to each condition are demonstrated in the bar graph (B:D).

Supplemental Figure 3. KEGG gene set enrichment KEGG for IMAT(A) and muscle(B). Genes in both tissues ranked by the correlation coefficients between gene expression and GIR.
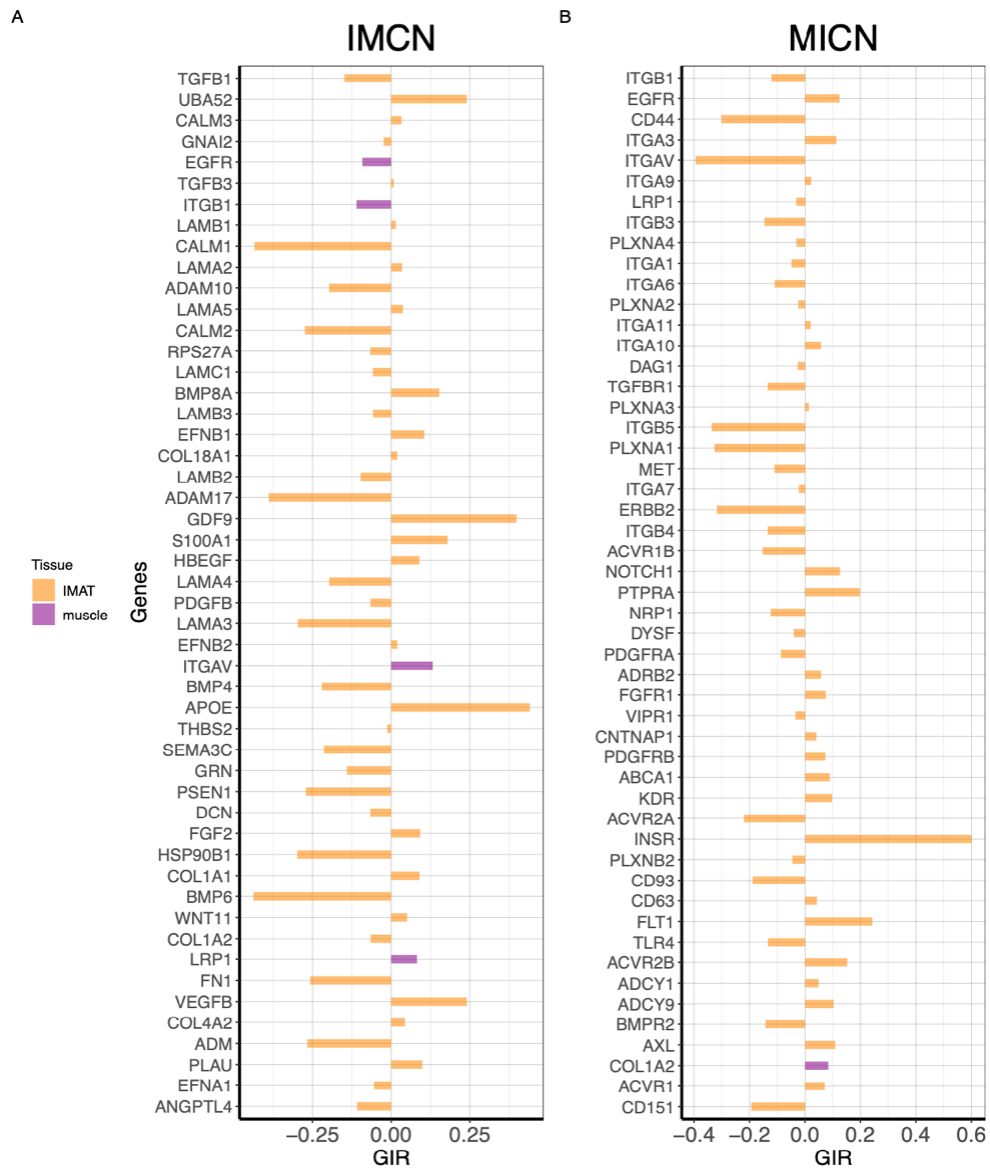
Supplemental Figure 4. List of top rewiring gene list in the IMCN(A) and MICN(B). The bar plot is to indicate the distribution of correlation between insulin sensitivity (GIR) and top gene expression. Majority of these genes have low correlation to GIR that make them to rewire during insulin sensitivity and resistance conditions.
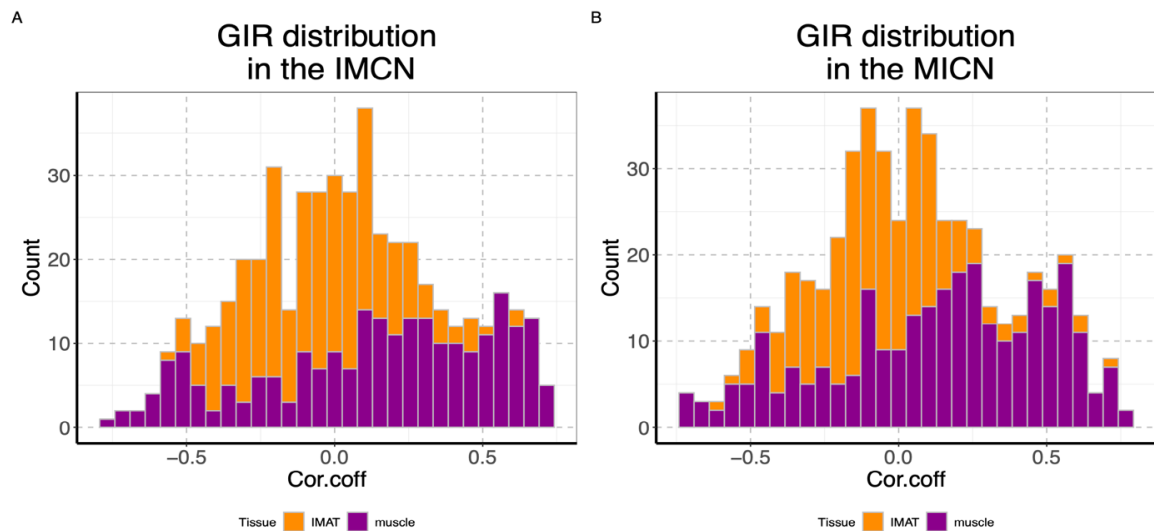
Supplemental Figure 5. Histogram for the distribution of correlation coefficients between all senders and receiver's genes with GIR in the IMCN(A) and MICN(B). Both histograms show muscle has a border range in insulin sensitivity regulation than IMAT.
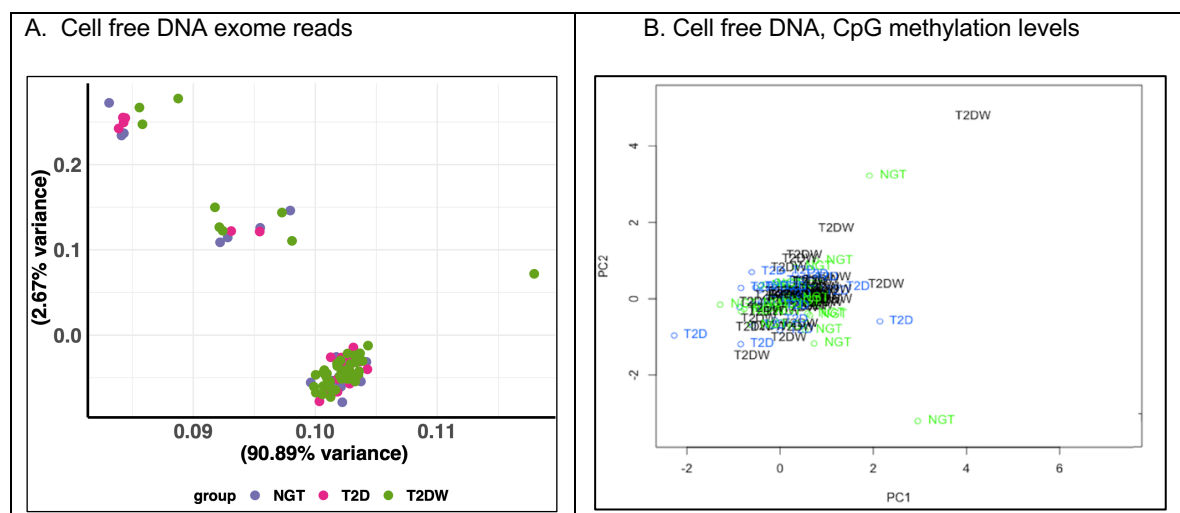
Supplemental Figure 6.Cell free DNA Whole exome sequence and methylation level among normal glucose tolerant (NGT), T2D, and T2D with complications. PCA analysis indicated in the scatter plots, cfDNA whole exome reads indicated in figure A and CpG methylation levels displayed in figure B.

10.2. Supplemental Tables

Supplemental Table 1: - KEGG pathways enriched for the genes in the insulin sensitivity networks of IMAT to muscle communication network (IMCN).

Pathway name	pvalue	p.adjust	qvalue	geneID	Count
ECM-receptor interaction	2.3811717 0790952e-12	9.28656966084714 e-11	8.2714385643 1729e-11	ITGA6/ITGA1/ITGA5/CD44/ITGB4/SDC3/ITGA10/TNXB/CD36/ITGA3/ITGAV/HSPG2/COL1A 1/COL6A3/COL4A2/LAMA5/LAMA2/LAMB1/VWF/AGRN	20
Complement and coagulation cascades	0.0001155 204816978 15	0.00225264939310 739	0.0020064083 6633046	F2R/CD46/F3/F10/F8/SERPING1/PLAU/A2M/PLAT/VWF	10
Notch signaling pathway	0.0001839 631466747 8	0.00239152090677 214	0.0021300995 930764	NOTCH1/NOTCH4/NOTCH3/JAG2/NOTCH2/DLL4/DLL1/JAG1	8
Cytokine-cytokine receptor interaction	0.0007061 642772590 51	0.00688510170327 574	0.0061324792 4988123	FLT1/FLT4/VEGFA/ACVRL1/TGFBR2/KDR/TNFRSF10D/PDGFRB/TNFRSF21/ACVR2A/LIF R/TNFRSF14/BMPR2/VEGFB/TNFRSF12A/TGFBR1/ACVR2B/TNFSF12/PDGFRA/TGFB3	20

Supplemental Table 2: - KEGG pathways enriched for the genes in the insulin resistance networks of IMAT to muscle communication network (IMCN).

Pathway name	pvalue	p.adjust	qvalue	geneID	Count
ECM-receptor interaction	1.0038702 5568973e-19	2.71044969036228 e-18	2.4304227243 0146e-18	THBS2/THBS4/ITGB5/LAMB3/LAMC1/COL1A2/COL4A1/ LAMB2/ITGA11/ITGB1/ITGB6/COL3A1/COL6A2/COL5A3/ COL6A1/THBS1/LAMA4/THBS3/FN1/COL5A1/LAMA3/COL5A2/DAG1/ITGA7	24
TGF-beta signaling pathway	2.6418923 1948385e-07	3.5665546313032e-06	3.1980801762 1729e-06	AMHR2/THBS2/THBS4/DCN/TGFB1/THBS1/ THBS3/BMP4/SMAD3/BMP6/BMPR1B/BMPR1A/ACVR1	13
Cytokine-cytokine receptor interaction	0.0005008 444265220 65	0.00450759983869 859	0.0040419023 8947631	AMHR2/TNFRSF19/CXCR4/CX3CL1/PDGFB/EGFR/ CXCL14/TGFB1/CXCL12/MET/BMPR1B/BMPR1A/ TNFRSF1A/CX3CR1/IL6R/ACVR1B/ACVR1	17

10.3. Abbreviations

1,2 DAG	1,2-diacylglycerol
2- h PG	2-hour plasma glucose (2-h PG)
ACs	Adipogenic cells
ADA	American Diabetes Association
ASCs	adipose stem cells
ATH	Athletes
ATM	Adipose Tissue Macrophages
ATP	Adenosine Triphosphate
ATP	Adenosine triphosphate
BAM	Binary Alignment Map
BCAA	Branched-chain Amino Acid
BMI	Body Mass Index
CAM	Cell adhesion molcules
CCK	Cholecystokinin
cfDNA	Cell free DNA
CG	Central Gene
CMR	Colorado Multiple Institution Review
CN	Central Node
CO	Computed Tomography
COPD	Chronic Obstructive Pulmonary Disease (COPD)
CT	Computed Tomography
ctDNA	Tumor DNA
CVAs	Cerebrovascular Accidents
CVS	Cardiovacular disorder
DAG	Diacylglycerol
DE	Differential Expression
DEA	Differential Expression Analysis
DESeq	Differential Expression Analysis Based on the Negative Binomial Distribution
DM	Diabetes mellitus
DO	Disease Ontology
ECM	Extracellular Matrix
ECM	Extracellular Matrix
EGFR	Epidermal Growth Factor Receptor
FA	Fatty acid
FABP	Fatty acid binding protein
FAPs	Fibro-Adipogenic Progenitor cells
FFA	Free fatty acid
FFM	Fat Free Mass
FPG	Fasting plasma glucose (FPG)
GEM	Genome Multitool
GFF	General Feature Format
GIR	Glucose Infusion Rate
GLM	Generalized Linear Model
GLUT	Glucose Transporter
GO	Gene ontology
GPCRs	Guanine nucleotide-coupled receptors
GSEA	Gene Set Enrichment Analysis
GTF	Gene Annotation Format
HbA1c	Glycated hemoglobin
HFD	High Fat Diet
IDF	International Diabetes Federation
IL-6	Interleukin-6

IM	IMAT to muscle
IMAT	Intermuscular adipose tissue
IMATA	Intramuscular Fat
IMCL	Intramyocellular Lipids
IMCN	IMAT to muscle network
ITGB3	Integrin beta 3
JNK	Jun N-terminal kinase
JSI	Jaccard similarity index
KEGG	Kyoto Encyclopedia of Genes and Genomes
kNN	K-Nearest Neighbors
KO	Knockout
LC	Lean Controls
MI	Muscle to IMAT
MICN	Muscle to IMAT Network
MPCs	Muscle Progenitor Cells
MRI	Magnetic Resonance Imaging
MRI	magnetic resonance imaging
mRNA	Messenger ribonucleic acid
MSCs	Muscle Satellite Stem Cells
MSigDB	Molecular Signatures Database
mtDNA	Mitochondrial DNA
mTOR	Mammalian target of rapamycin
mTORC	Mammalian target of rapamycin complex
NCBI	National Center for Biotechnology Information
NE	Negative Edges
NFκB	Nuclear factor kappa
NG	Neighbouring Gene
NN	Neighborhood Nodes
NNNs	Nearest Neighbour Networks
OGTT	Oral Glucose Tolerance Test
ORA	Over Representation Analysis
PAI-1	Plasminogen Activator Inhibitor 1
PAX7	Paired Box Proteins 7
PCA	Principal Component Analysis
PE	Posative Edges
PKC	Protein Kinase C
PPAR	Peroxisome Proliferator-Activated Receptor
PPY	Peptide YY
RBP4	Retinol binding protein 4
RINs	RNA integrity numbers
SAT	Subcutaneous Adipose Tissue
T2D	Type 2 Diabetes
TAG	Triacylglycerol
TMM	Trimmed Mean M Values
TNFα	Tumor necrosis factor α
TPM	Transcripts per kilobase Million
UCSC	University of California Santa Cruz
VAT	Visceral Adipose Tissue
WHO	World Health Organization
WNT5A	Wnt family member 5A
WT	Wild type

10.4. Glossary

Nodes: In biological networks nodes are connection points, for example, genes, proteins, or metabolites. Therefore, in this thesis Genes or nodes referred to the something.

Edges: Represents the physical interaction between nodes in a network. For example, physical interaction between two proteins. Thus, in this thesis Interacting pairs, physical interactions, or gene pairs implying the same thing.

Interaction networks: A network to represent the putative/physical interaction between two nodes.

Hub: A node in the network that has the highest connectivity.

Degree: The number of edges a node has.

Clusters: Group of genes, proteins or samples sharing identical futures.

Modules: A networks of genes or proteins that work together to preform specific functions.

Dynamic network: Network that changes over times or in response to disease conditions.

Static network: Network that does not change over the courses of time or disease conditions.

Rewiring: Node connective changes or restructuring of the interaction between nodes due to condition changes.

Differential networks: Network showing interaction or edge difference between two networks.

Bottleneck node: Node with high degree of betweenness (intersection point) that connects many sub-networks within the main network.

Group: Clinically identical study subjects

10.5. List of publications

Lutter D, Sachs S, Walter M, Kerege A, Perreault L, Kahn DE, Wolide AD, Kleinert M, Bergman BC, Hofmann SM. Skeletal muscle and intermuscular adipose tissue gene expression profiling identifies new biomarkers with prognostic significance for insulin resistance progression and intervention response. Diabetologia. 2023;66(5):873-883.

Alkhoury C, Henneman NF, Petrenko V, Shibayama Y, Segaloni A, Gadault A, Nemazanyy I, Le Guillou E, Wolide AD, Antoniadou K, Tong X, Tamaru T, Ozawa T, Girard M, Hnia K, Lutter D, Dibner C, Panasyuk G. Class 3 PI3K coactivates the circadian clock to promote rhythmic de novo purine synthesis. Nat Cell Biol. 2023;25(7):975-988.

Amare Desalegn Wolide, Susanna M Hofmann, Bryan C Bergman, Dominik Lutter. Molecular crosstalk communication between Intermuscular Adipose Tissue and Skeletal Muscle under progressing Insulin Resistance. **In preparation**

10.6. Conferences Participated

29/11/2021-01/12/2021	RNA Mechanisms and Therapeutics in Metabolic Disease, Copenhagen, Denmark.
	The workshop taught me the role of RNA biology and associated technologies in developing new strategies to combat obesity, type 2 diabetes, and other metabolic diseases.
25/09/2022–15/10/2022	21st European Conference on Computational Biology (ECCB2022), Sitges, Barcelona, Spain.
	Discussed current and upcoming issues with regards to human health and how systems biology and artificial intelligence could help
23/10/2022-25/10/2022	25th German Center for Diabetes Research (DZD) Workshop, Dresden, Germany.
	During the 25th DZD meeting, we discussed organ crosstalk in the pathophysiology of diabetes.

10.7. Curriculum vitae

Amare Desalegn Wolide

Date of birth:	08/01/1988
Place of birth:	Debre-tabor
Nationality:	Ethiopian
Family status:	Single

Education

11/2019 08/2023	–	PhD thesis (Dr. rer. nat.) at Technische Universität München, Division of Metabolic Diseases, Department of Medicine. Guest scientist at Helmholtz München, Institute for Diabetes and Obesity, Computational Discovery Research Thesis: "Molecular crosstalk communication between Intermuscular Adipose Tissue and Skeletal Muscle under progressing Insulin Resistance"
11/2017 08/2017	–	Mobility program on global health, University of Oslo, Norway
10/2011-11/2013		Medical Physiology at Jimma University, Jimma, Ethiopia, Master of Science, Grade Point Average: 3.4/4.00 Thesis: "Nutritional Iron Deficiency Anemia: Magnitude and Its Predictors among School Age Children, Southwest Ethiopia". Grade: A (excellent)
11/2006-09/2009		Applied Biology at Dilla University, Dilla, Ethiopia Bachelor of Science, Grade Point Average: 3.57/4.00 (very Good) Thesis: "Breeding disease and drought-resistant crops suitable for tropical climate at Adet Agricultural research institute". Grade: B+ (very good)
08/2004 - 08/2006		General qualification for university entrance at Tewodros II Secondary School, Natural sciences stream, Debre-tabor, Ethiopia.